THE PERFORMANCE OF COOPERATIVE-DIVERSITY WIRELESS NETWORKS USING ADAPTIVE MODULATION

HAO CHEN

The Performance of Cooperative-Diversity Wireless Networks using Adaptive Modulation

by

©Hao Chen
B. Eng., M.A.Sc.

A thesis submitted to
the School of Graduate Studies in
partial fulfillment of the requirement for the degree of
Master of Engineering.

Faculty of Engineering and Applied Science
Memorial University of Newfound

October 15, 2008

St. John's Newfoundland and Labrador

Abstract

This thesis analyzes the throughput performance of the cooperative diversity wireless network using adaptive modulation over Rayleigh fading channels. Cooperative diversity is achieved by utilizing neighboring terminals as relays. These relays can generate copies of the same signal, which can provide spatial diversity gain and high Signal-to-Noise Ratio (SNR). The main drawback of cooperative diversity is the throughput decrease due to the extra resources needed for relaying. Therefore, throughput is greatly reduced. In this thesis, the adaptive modulation is used to convert the obtained SNR gain to throughput gain to compensate for the throughput reduction. Results show that the cooperative diversity networks with adaptive modulation not only compensate for the throughput loss but also achieve considerable throughput gain compared with the classical system with direct transmission when the Channel State Information (CSI) is perfectly known in advance. Moreover, this thesis investigates the throughput gain of the cooperative diversity networks with adaptive modulation when the CSI is imperfect. Results show that a great throughput loss is caused by the imperfect CSI, but considerable throughput gain still exists. More importantly, this thesis sets up the mathematical models for the simulated systems. Hence, the analytical evaluation of the system performance is presented in both perfect CSI and imperfect CSI case to verify the simulation results. In addition, this thesis also analyzes the relationship between the throughput gain and the number of relays. The optimal number of relays that maximizes the throughput is found to be one, when simultaneous relaying is not considered. It is also

found that the throughput increases linearly with the number of relays, if simultaneous relaying is considered. Besides, the BER performance of the cooperative diversity network using fixed modulation is also investigated in simulation and analytical methods based on the analytical results from the cooperative diversity network using adaptive modulation. Results show that the BER performance of the cooperative diversity network under perfect CSI using fixed modulation is much better than that of the classical direct transmission system. In addition, there is significant BER performance degradation of the cooperative diversity network under imperfect CSI compared with that from the cooperative diversity network under perfect CSI. However, the cooperative diversity network under imperfect CSI is still better than the classical direct transmission system in BER performance.

Acknowledgement

I am very pleased to thank my supervisor, Dr. Mohamed Hossam Ahmed, for his great supervision in my MASCE project and MEng program. Thanks to his recognition, I can obtain this precious opportunity to study in the MEng program. During the past two years, Dr. Ahmed always gave me many meaningful suggestions, support and encouragement in my research. I also want to thank my co-supervisor, Dr. Ramachandran Venkatesan, for his generous help in teaching me to do the research.

I also want to thank the university and NSERC for the financial assistance through the funds for this research work.

Great thanks are also given to faculty members in Computer Engineering and all members in CERL for their generous support.

I am also very grateful to my parents and wife for their understanding and support in pursuing the study in Memorial University.

Table of Contents

List of Figures VIII

List of Tables XI

List of Abbreviations XIII

Chapter 1

Introduction 1

1.1 Wireless Communication 1

1.2 Cooperative Communication 4

1.3 Adaptive Modulation for Cooperative Diversity 7

1.4 Literature Review 8

1.5 Problem Statement 10

1.6 The Thesis Organization 11

Chapter 2

Performances of Fixed Modulation Systems 13

2.1 Classical Communication System over the AWGN Channel 13

2.1.1 AWGN Channel Model 13

2.1.2 Simulation Results 14

2.2 Classical Communication System over Rayleigh Fading Channel 15

2.2.1 Multi-path Fading Channel Model 15

2.2.2 Simulation Results 16

2.3 Cooperative Communication System over AWGN Channel 17

2.3.1 Simulation Model 17

2.3.2 Transmission Sequence in Cooperative Diversity Networks 18

2.3.3 The Mathematical Model 19

2.3.4 Simulation Results 19

2.4 Cooperative Communication Systems over Rayleigh Fading Channel 20

2.4.1 Maximal Ratio Combining (MRC) 21

2.4.2 Simulation Model 22

2.4.3 The Weights of MRC on Cooperative Communication 24

2.4.4 Simulation Results 27

Chapter 3

Cooperative Diversity Networks using Adaptive Modulation under Perfect CSI 27

3.1 Adaptive Modulation with Single Relay 27

3.1.1 The Principle of Adaptive Modulation 27

3.1.2 Calculation of Total SNR 28

3.1.3 Decision Metric of Modulation Scheme 28

3.1.4 Path Loss Effects 30

3.1.5 Relay Gain Classification 32

3.1.6 Relay Branch Analysis 33

3.2 Fixed Relay Gain Case 35

3.2.1 Simulation of Fixed Relay Gain Case 35

3.2.2 Analytical Evaluation of Fixed Relay Gain 39

3.2.3 Fixed Relay Gain Simulation with More Modulation Schemes 45

3.2.4 Fixed Relay Gain with Higher Target BER Simulation 50

3.3 Variable Relay Gain Case I 54

3.3.1 Simulation of Variable Gain Case I 54

3.3.2 Analytical Evaluation of Dynamic Gain Case I 59

3.4 Variable Relay Gain Case II 61

3.4.1 Simulation of Variable Gain Case II 61

3.4.1 Analytical Evaluation of Variable Gain case II 63

3.5 Adaptive Modulation for Multiple Relays 65

3.5.1 Multiple Relays Model 65

3.5.2 Multiple Relays with Simultaneous Reception Simulation 69

3.5.3 Multiple Relay Simulation with Sequential Reception Simulation 71

Chapter 4

Cooperative Diversity Networks using Adaptive Modulation under Imperfect CSI 73

4.1 Channel Estimation 74

4.2 Channel Estimators 75

4.2.1 Minimum Variance Unbiased (MVU) Estimator 75

4.2.2 Minimum Mean Square Error (MMSE) Estimator 76

4.2.3 Correlation Estimator 76

4.3 Channel Estimation in Cooperative Diversity Networks 77

4.3.1 Distribution of Channel Estimators 77

4.3.2 Estimation Algorithm 78

4.3.3 Adaptive Modulation Thresholds in Imperfect CSI 79

4.4 Fixed Relay Gain Case 80

4.4.1 Simulation of Fixed Relay Gain Case 80

4.4.2 General Model of Channel Estimator [14] 83

4.4.3 Simulation of Cooperative Diversity Networks using GM 84

4.4.4 Analytical Evaluation of Fixed Relay Gain 86

4.4.5 Simulation of Large Number Pilot Symbols 90

4.5 Variable Relay Gain 92

4.5.1 Variable Relay Gain Case I Simulation 92

4.5.2 Analytical Evaluation of Variable Relay Gain case I 94

4.5.3 Simulation of Variable Relay Gain Case II 95

4.5.4 Analytical Evaluation of Variable Relay Gain case II 98

Chapter 5

BER Analysis of Cooperative Diversity Networks using Fixed Modulation 101

5.1 BER Performance in Simulation 101

5.2 Analytical Evaluation of BER Performance 103

Chapter 6

Conclusions 107

References 110

List of Figures

Figure 1-1Principle of cooperative communication 5

Figure 2-1Model for AWGN channel 13

Figure 2-2 Performance of classical system using BPSK over AWGN channel 14

Figure 2-3 Performance of classical system using BPSK over Rayleigh fading channel 17

Figure 2-4 Cooperative diversity networks using BPSK over AWGN channel 18

Figure 2-5 Cooperating sequence 18

Figure 2-6 Performance of cooperative communication over AWGN channel 20

Figure 2-7 Maximal Ratio Combiner 21

Figure 2-8 Cooperative system over Rayleigh fading channel 23

Figure 2-9 MRC structure for cooperative system 24

Figure 2-10 Performance of cooperative communication over Rayleigh fading channel 27

Figure 3-1 BER curves for QAM modulations 29

Figure 3-2 Throughput comparisons of systems with fixed relay gain 36

Figure 3-3 Performance of simulation systems with fixed relay gain 37

Figure 3-4 Analytical throughput comparison with the simulation results 45

Figure 3-5 Throughput comparisons of simulation systems with eight modulation levels 46

Figure 3-6 Performance of simulation systems with eight modulation levels 47

Figure 3-7 Throughput comparisons of eight modulation choices 51

Figure 3-8 Performance of eight modulation choice 52

Figure 3-9 Throughput comparisons of simulation systems with variable relay gain I 55

Figure 3-10 Performance of simulation systems with variable relay gain I 56

Figure 3-11 Analytical results of cooperative networks with variable relay gain I 61

Figure 3-12 Throughput comparisons of simulation systems with variable relay gain II 62

Figure 3-13 BER performance of simulation system with variable relay gain II 63

Figure 3-14 Analytical throughput with variable relay gain II 65

Figure 3-15 Locations of multiple relays 66

Figure 3-16 Cooperative diversity network with multiple relays 67

Figure 3-17 Throughput comparisons with multiple relays and one slot loss 70

Figure 3-18 BER Performance of with multiple relays and one slot loss 71

Figure 3-19 Throughput comparisons with multiple relays and multiple time slot loss . 72

Figure 3-20 BER Performance with multiple relays and multiple time slot loss 73

Figure 4-1 The distribution of channel estimators 78

Figure 4-2 Throughput performance with imperfect CSI using MVUE, MMSE and CE 81

Figure 4-3 BER performance with imperfect CSI using MVUE, MMSE and CE 82

Figure 4-4 Throughput performance with imperfect CSI using GM 85

Figure 4-5 BER performance with imperfect CSI using GM 86

Figure 4-6 Analytical throughput with imperfect CSI 89

Figure 4-7 Throughput of cooperative diversity network using 8 pilot symbols 91

Figure 4-8 Throughput of cooperative diversity network using 8 pilot symbols 91

Figure 4-9 Throughput performance with variable relay gain I under imperfect CSI 93

Figure 4-10 BER performance with variable relay gain I under imperfect CSI 94

Figure 4-11 Analytical throughput with variable gain I under imperfect CSI 95

Figure 4-12 Throughput performance with variable relay gain II 97

Figure 4-13 BER performance with variable relay gain II 97

Figure 4-14 Analytical throughput with variable gain II under imperfect CSI..... 100

Figure 5-1 BER performance of fixed gain case in simulation 102

Figure 5-2 BER performance of variable gain case in simulation..... 103

Figure 5-3 Analytical BER performance of fixed gain case 105

Figure 5-4 Analytical BER performance of variable gain case 105

List of Tables

Table 3-1 Adaptive Threshold for BER (10^{-3}) under Perfect CSI 30

Table 3-2 SNR comparisons (fixed power per user) of two branches with fixed relay gain 37

Table 3-3 Throughput gain (fixed power per user) of adaptive modulation with fixed relay gain 38

Table 3-4 SNR comparisons (fixed total power) of two branches with fixed relay gain.. 38

Table 3-5 Throughput gain (fixed total power) of adaptive modulation (6 modulation choices) with fixed relay gain 38

Table 3-6 SNR comparison (fixed power per user) of two branches (8modulation choices) 47

Table 3-7 Throughput gain (fixed power per user) of adaptive modulation (8modulation choices) 48

Table 3-8 SNR comparison (fixed total power) of two branches (8modulation choices). 48

Table 3-9 Throughput gain (fixed total power) of adaptive modulation (8modulation choices) 49

Table 3-10 SNR comparison (fixed power per user) of two branches (8 modulation choices) (BER 10-6) 52

Table 3-11 Throughput gain (fixed power per user) with 8 modulation choices (BER 10-6) 53

Table 3-12 SNR comparison (fixed total power) of two branches (8 modulation choices) (BER 10-6) 53

Table 3-13 Throughput gain (fixed total power) with 8 modulation choices (BER 10-6) 54

Table 3-14 SNR comparisons (fixed power per user) of two branches (changeable gain)57

Table 3-15 Throughput gain (fixed power per user) of adaptive modulation (changeable gain) 58

Table 3-16 SNR comparisons (fixed total power) of two branches 58

Table 3-17 Throughput gain (fixed total power) of adaptive modulation (changeable relay gain) 59

Table 4-1 Adaptive Threshold for BER (10^{-3}) under imperfect CSI 80

List of Abbreviations

SNR ----Signal-to-Noise Ratio

CSI------Channel State Information

BER-----Bit Error Rate

MIMO---Multiple-Input Multiple-Output

QAM-----Quadrature Amplitude Modulation

CDMA---Code Division Multiple Access

FDMA----Frequency Division Multiple Access

PDF--------Probability Density Function

AWGN-----Additive White Gaussian Noise

MRC-------Maximal Ratio Combining

BPSK------Binary Phase Shift Keying

MVU-------Minimum Variance Unbiased

MMSE-----Minimum Mean Square Error

CE----------Correlation Estimator

GM---------General Model

Chapter 1

Introduction

1.1 Wireless Communication

Wireless communication was started by the Italian inventor Marchese Guglielmo Marconi through a public demonstration on 1901. Many great inventions soon emerged into the vision of mankind. From the earliest radio to recent cellular phones and wireless networks, wireless communication has experienced tremendous development in the past hundred years. Until today, it is still a very active area of research. Moreover, the benefits brought by its applications are continuously having the great impact on civilian life. An increasing amount of people are enjoying the services offered by wireless communication. From the popular cellular phone to the wireless home network, wireless communication is accelerating its pace to replace once prosperous wired infrastructures. Meanwhile, mobility is also becoming an implicit standard when customers are purchasing electronic devices such as the wireless keyboard and mouse.

To the consumers, the transition from wired products to wireless is merely the magic of wire removal. From the perspective of engineers, what kind of change do we need to make to have this magic and also what kind of new technique challenges are we going to face?

Wireless communication operates through the use of electromagnetic radiation in space.

The transmission medium between the transmitter and the receiver is called the radio channel. Unlike the wire channel in wired communication, radio channel has a distinct property called the multi-path fading, which is caused by the dispersive nature of the electromagnetic radiation. This means that the transmitted signal will be reflected or diffracted by objects between the transmitter and the receiver before arriving at the receiver. Therefore, a large number of possible propagation paths exist to carry the transmitted signal. As a result, multiple copies of the same transmitted signal will arrive at the receiver with distinct amplitudes, delays and phase shifts, since each copy is through unique propagation path.

These received copies of the transmitted signal sometimes interfere constructively at the receiver due to their similar phase shifts. In this case, a much stronger signal is generated. Sometimes, however, these multiple copies interfere destructively if the phase shift difference is large enough to cancel each other. Therefore, the receiver does not get any useful information about the transmitted signal.

In essence, all the phase shifts are triggered by the different run length, which is the time interval for signal to transmit from transmitter to receiver, reflection and deflection of the propagation paths. The small movement of either transmitter or receiver will result in the transition from the construction to destruction, or vice versa. This kind of phenomenon is named small-scale fading. On the contrary, if some dominant propagation paths are attenuated by the huge obstacles when the receiver is moving into the shadowing area, the received signal strength will decrease. This situation is defined as the large-scale fading. The solution is to move the receiver out of the shadowing region by a large distance.

Multi-path fading is playing a detrimental role in wireless communication. Small scale fading, in particular, degrades the performance to a large extent. Hence, combating multi-path fading is always the first thing to do in order to improve wireless communication performance.

The most effective technique to mitigate multi-path fading is the transmission and/or reception of multiple faded signals from independent fading paths. This is due to the fact that two independent fading paths may seldom experience deep fading simultaneously. With proper combining of these signals from independent paths, the resultant signal can be immune to multi-path fading. Naturally, the next question is how to create independent signal paths. Generally, there are three techniques to generate independent paths.

The common way is to use multiple antennas at the transmitter and/or the receiver. This technique tries to exploit the spatial diversity to create independent paths, as long as the separations among antennas are sufficiently large. Multiple-Input Multiple-Output (MIMO) antenna system is an implementation of this category.

The second technique, utilizing the frequency diversity, transmits the same information on multiple channels with different carrier frequencies. As long as the carrier separation is large enough, multiple independent fading signals can be obtained.

The third technique that makes use of time diversity by transmitting the same message for several times, as long as the separation time between two successive transmissions exceeds the coherence time [1].

In the previous discussion, the MIMO system is capable of combating multi-path fading based on its multiple antenna elements. However, this multiple antenna system will significantly increase the size, power consumption and hardware complexity of the

portable devices. All these factors impose the limitation on the implementation of a portable MIMO system. In fact, there is another way to utilize the spatial diversity without using multiple antennas in a multi-user environment. Cooperative communication is a technique that attempts to achieve the same benefits of spatial diversity without the need of multiple antennas at the terminals.

1.2 Cooperative Communication

Cooperative communication originates from the multi-user environment where not only does one user communicate but also do many other users. The key idea is that the user terminal can employ antennas from other terminals as additional antennas, since each terminal has at least one antenna. It is clear that these additional antennas, in conjunction with user's own antenna, can provide great spatial diversity. Hence, if the user device could exploit these additional antennas, a virtual antenna array is formed just like antenna array in the MIMO system.

This virtual antenna array could provide the same spatial diversity as a multiple antenna array in the MIMO system without using multiple antenna elements. Figure 1-1 below shows the principle of cooperative communication. In this figure, the multi-user environment is reduced to a three-user case for simplicity. The source represents the terminal which has messages to send out; similarly, the destination represents the terminal which requires these messages from the source. In classical communication, the communicating process involves only the source and destination terminals, but a new terminal represented by the relay is added in cooperative communication to generate an additional independent propagation path.

The whole cooperative diversity network can achieve spatial diversity as follows. At first, when the source is transmitting the message, the relay and the destination will receive this message due to the broadcasting nature of electromagnetic wave. Then, the received message at the relay terminal is forwarded to the destination terminal. As a result, the destination terminal has two copies of the same message through the independent propagation path. One copy is from the source and the other is from the relay terminal through the relaying process.

Generally, multiple relays can be imported to the cooperative diversity network. Therefore, multiple independent propagation paths can be generated so that the destination terminal has multiple copies of same message. In wireless communication, these multiple copies of same message can be used to generate a strong message. Thus, the multi-path fading problem can be solved.

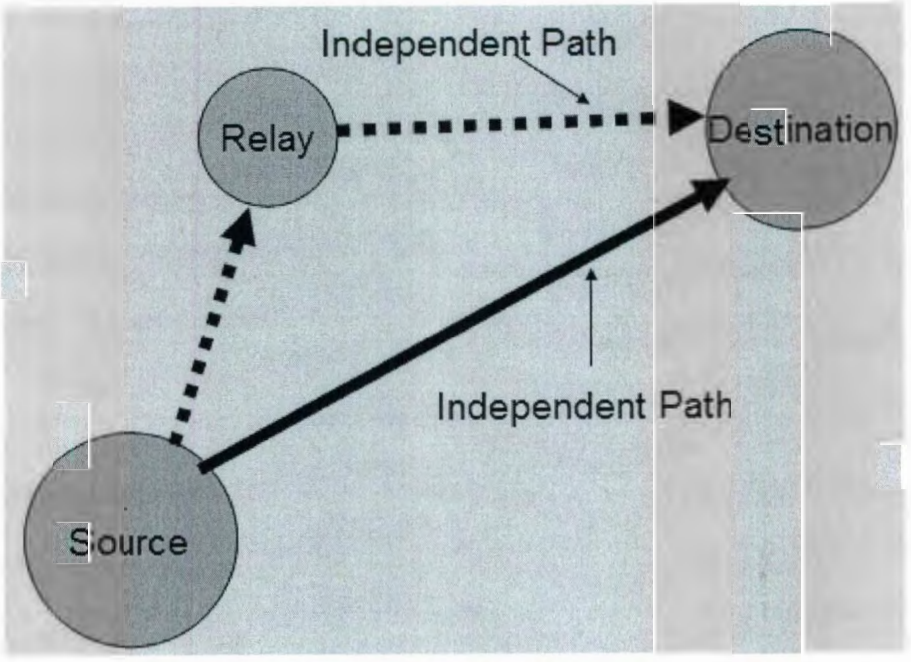

Figure 1-1Principle of cooperative communication

In cooperative communication, the cooperating process can be classified based on the different relaying techniques. The first technique is the Amplify-and-Forward. In this case, the relay receives a noisy copy of the message from the source terminal. The relay then amplifies and retransmits the noisy message to the destination. After that, the destination combines the two copies of messages using some combining techniques. The disadvantage of this technique is that the amplifying operation will amplify not only the signal but also the noise. [2]

The second technique, called Decode-and-Forward, is only different from the Amplify-and-Forward technique in that the relay is required to decode the received message from the source and then regenerates and transmits the message to the destination. This technique eliminates the noise amplification problem in the first technique since the relay must decode the received message first and regenerate the new message second. However, the incorrect decoding of received message in relay will result in the incorrect new message. [2]

For the third technique, the source only transmits part of the encoded message, but the relay needs to first calculate the remaining part in terms of the received part and transmit this derived part to the destination. This technique is called Coded Cooperation. [2]

There are other relaying techniques such as Incremental Relaying, which only use cooperative communication occasionally when the direct transmission cannot achieve the communication, and Best Relay Selection, where only the optimum relay is chosen to do the relay operation. [3]

As seen from the previous relaying techniques, extra resources are required to achieve the cooperative diversity since relay must forward the received message to the destination.

For instance, an extra time slot is used by the relay to forward the message in each message transmission between the source and the destination. As a result, half of the time resources are lost for relaying and the throughput of the system is greatly reduced. Hence, the cooperative diversity is derived at the expense of extra resources for the relaying process.

1.3 Adaptive Modulation for Cooperative Diversity [5]

In a classical communication system, the modulation scheme is usually fixed. For example, a system realizing 64 Quadrature Amplitude Modulation (QAM) will use this modulation scheme to transmit messages continuously. Obviously, systems utilizing fixed modulation are fit for wired communication since the wired channel is linear and time invariant.

In contrast, the radio channel is time variant. Therefore, the radio channel condition is sometimes in a good state. This means that a higher modulation level scheme can be used. At other times, however, the channel condition is in a bad state. In this case, only a lower modulation level scheme can realize the communication with certain quality. Consequently, if the system is able to change its modulation scheme according to the current channel state, the time variant property of the wireless channel is fully exploited. This changeable modulation scheme in terms of a channel state is called adaptive modulation.

Adaptive modulation has been applied to many wireless communication areas and has shown its excellent performance. Since it can adjust the modulation scheme according to the channel conditions, it always provides the best modulation choice.

Since cooperative diversity enhances the signal quality and overcomes the bad channel conditions such as deep fading, it is foreseeable that throughput gain can be achieved in cooperative diversity networks by using adaptive modulation.

1.4 Literature Review

The origin, evolution and main developments of the cooperative diversity network are discussed in [2], [3], [4]. Meanwhile, the block error rate performances of three relay schemes are also shown in order to compare with no cooperation scheme. More efficient relaying schemes related to cooperative diversity is well illustrated [7] [8]. In addition, the outage behavior is analyzed as well. Moreover, the model and outage behavior analysis to the multi-hop diversity network is given in [3].

The symbol error probability for the cooperative links is studied in paper [7], which gives the error probability formulas in high average SNR. The formula remains valid for a large class of fading channels. Moreover, the accurate results of symbol error probability for the cooperative diversity network over the Rayleigh fading channel is discussed in [7].

In the work discussed above, cooperative diversity is mainly used to reduce the BER, which provides a better signal quality. Although the SNR at the destination increases dramatically when utilizing cooperative diversity, this comes at the expense of the amount of required resources, since additional channels (time slots, carriers, etc.) are needed for the relays. Therefore, the throughput of the cooperative diversity networks is reduced.

In [6], the throughput performance of the cooperative ad-hoc networks over Rayleigh

fading channels is examined. To achieve high throughput, the relay is set to transmit and receive simultaneously, which is impractical in the real situation.

A novel scheme, presented by [8], uses two relays and multiple receiving antennas at the destination terminal to avoid the throughput loss in cooperative diversity networks. In this scheme, the source terminal will first send a message to the destination and any one of the relay terminals. Then, the source terminal will send out the next message to the other unselected relay and the destination while the first selected relay is forwarding the previous message to the destination terminal. Therefore, multiple antennas are needed in destination to receive two messages from the relay and source terminal simultaneously. Although there is no throughput loss in this scheme, the multiple antennas for the destination terminal is not practical in some cases.

A more practical scheme is given in [7], which is similar to the scheme in [6] except that only a single antenna is used at the destination. In this scheme, orthogonal channels are assigned to each terminal. For example, orthogonal channels can be a set of orthogonal codes in Code Division Multiple Access (CDMA) or a set of orthogonal carriers in Frequency Division Multiple Access (FDMA). In some environments such as the downlink of a cellular system, this scheme saves time-slots at the expense of frequency or code channels. Hence, there is no saving of the resources anyway.

Most of the discussions related to cooperative diversity networks are based on the assumption that all terminals in the networks have perfect knowledge of current channel state information. However, this assumption cannot be realized in real world due to the estimation error.

The imperfect CSI case has been studied extensively for the MIMO system. However,

these results cannot be applied to cooperative diversity networks. The main reason for this is that the channel distributions are not identical in direct and indirect branch since the indirect branch goes through two independent paths while the direct branch experiences only one. The other reason is that the noise power is unequal in the direct and indirect branch. Hence, the available results [9] of the imperfect CSI analysis for the MIMO system cannot be used in the cooperative diversity network. From the analytical perspective, this non-identical channel distribution and unequal noise power are more difficult to model.

In [10], the Probability Density Function (PDF) of normalized SNR with imperfect CSI conditioned on ideal SNR in MIMO system is given regardless of noise power. Therefore, this PDF can be modified to cooperative diversity networks under imperfect CIS as shown in Chapter 4.

1.5 Problem Statement

Form the previous literature review, the research status of the cooperative diversity network is mainly focused on the improvement of received signal quality. However, the issue of throughput loss is ignored. In this thesis, the primary efforts are on the throughput enhancement of cooperative diversity networks.

Adaptive modulation is devised to convert additional SNR gain to the extra throughput increase in wireless communication. In general, the system is designed to meet the worst case of the channel. But the wireless channel has wide variations, which means sometimes the channel is in good condition and sometimes it is in bad condition. If the system could keep track of channel condition, then it can use a larger constellation size to

transmit when the channel is in good conditions, which means high SNR [11]. Therefore, the throughput of the system will be greatly increased.

This motivates us to use adaptive modulation in cooperative diversity network in order to make use of additional SNR gain provided by cooperative diversity networks. We hope this cooperative diversity network, using adaptive modulation, could provide enough throughput gain so that not only the throughput loss in using cooperative diversity can be compensated but the extra throughput gain can be obtained.

Current research in the cooperative diversity networks, whether it is about the SNR improvement or the throughput enhancement, is based on the perfect channel state information assumption. Actually, the perfect channel state information assumption is not realistic in the real world. There must be some kind of estimation techniques to measure the channel state information. Hence, estimation error exists. It is certain that the estimation error will affect the performance of cooperative diversity.

In this thesis, first, the throughput of the cooperative diversity networks over the Rayleigh fading channel under perfect channel state information is investigated using simulation and analytical methods. Then, the throughput of the cooperative diversity networks over the Rayleigh fading channel under imperfect channel state information is also investigated using simulation and analytical methods.

1.6 The Thesis Organization

This thesis is organized in six chapters. The introduction of the cooperative diversity network, adaptive modulation and literature review are included in Chapter 1. In Chapter 2, the performance of fixed modulation in the cooperative diversity network is studied

briefly to set up a basis for later work. A basic classical direct system is built first to provide the performance for later comparisons. Then, the cooperative system is set up based on the classical direct system. The throughput of the cooperative diversity network using adaptive modulation under perfect CSI is analyzed in both simulation and analytical methods in Chapter 3. The different relay gain schemes are studied by given the simulation first and analytical verification second. Similarly, Chapter 4 analyzes the throughput of the cooperative diversity network using adaptive modulation under imperfect CSI in both simulation and analytical methods. The corresponding relay gain schemes are investigated. Chapter 5 analyzes the BER performance of cooperative diversity networks using fixed modulation in both simulation and analytical methods. The analytical results are based on the results from the previous chapters. Chapter 6 covers the conclusions and future work.

Chapter 2

Performances of Fixed Modulation Systems

This Chapter will study the BER performance of the classical communication system using the Binary Phase Shift Keying (BPSK) modulation over Rayleigh fading channel with Additive White Gaussian Noise (AWGN). The cooperative communication system using the BPSK modulation is also investigated. In addition, the cooperative communication system derived in this chapter will be used as a reference for the later cooperative system using adaptive modulation.

2.1 Classical Communication System over the AWGN Channel

2.1.1 AWGN Channel Model

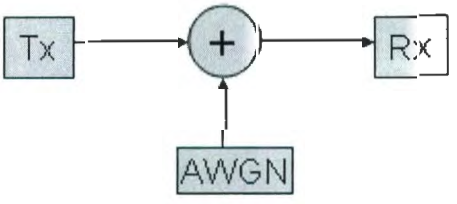

Figure 2-1Model for AWGN channel

The AWGN channel model is shown in Figure 2-1. Tx is the transmitter and the Rx is the receiver. The transmitted signal is corrupted by the addition of white Gaussian noise, which is caused by electronic components and amplifiers at the receiver.

2.1.2 Simulation Results

Figure 2-2 below shows the BER performance of the classical communication system using the BPSK modulation scheme under the AWGN channel. The figure shows the BER results versus SNR for AWGN channel. Besides, the theoretical result is also provided to check the correctness of the simulation system [MATLAB]. The objective of building this simulation system is to set up the basic classical communication system so that the advanced cooperative simulation system can be derived based on this simple system. Besides, the classical system can provide results for future comparisons with cooperative system.

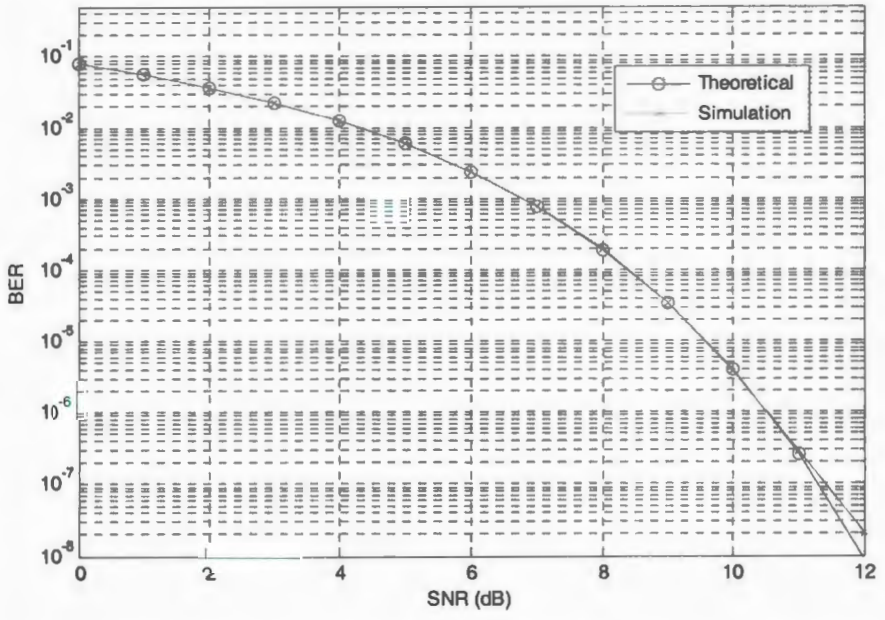

Figure 2-2 Performance of classical system using BPSK over AWGN channel

From this figure, it can be shown that the simulation result conforms to the theoretical results of BPSK in the AWGN channel very well below 10 dB. Since only (10^9 bits) samples are used in this simulation, the precision can only reach 10^{-7} since the precision can be approximated by formula (100/ total samples).

2.2 Classical Communication System over Rayleigh Fading Channel

2.2.1 Multi-path Fading Channel Model

The multi-path fading effect is briefly illustrated in the introduction chapter. The mathematical description given here is used to simulate the multi-path fading channel in this thesis.

The unmodulated carrier is given by

$$c(t) = A\cos 2\pi f_c t. \tag{2.1}$$

where A is the amplitude of the sinusoid, *cos* is the cosine function, f_c is the carrier frequency and t is the time.

The received signal without the noise can be expressed as

$$R(t) = A\sum_n \alpha_n(t)\cos[2\pi f_c(t-\tau_n(t))] = A\,\mathrm{Re}[\sum_n \alpha_n(t)\exp[-2\pi f_c\tau_n(t)]\exp[2\pi f_c t]] \\ = A\,\mathrm{Re}[z(t)\exp[-2\pi f_c t]], \tag{2.2}$$

where $\alpha_n(t)$ is the time-variant attenuation factor on the nth path, and $\tau_n(t)$ is the corresponding delay on the n_{th} path. From the perspective of formula, $z(t) = \sum_n \alpha_n(t)\exp[-2\pi f_c\tau_n(t)]$ can be any value since f_c is fairly large. A small delay

$\tau_n(t)$ can make the product $2\pi f_c \times \tau_n(t)$ several times larger than basic period 2π . [12]

In fact, the delay $\tau_n(t)$ associated with each path changes in its own way which is independent of other paths. Therefore, the addition of large amount of signal paths, *Z(t)*, can be modeled by a complex Gaussian random variable according to the Central Limit theorem. Furthermore, *Z(t)* in rectangular notation can also be transformed to polar notation. The distribution of the magnitude and the phase are presented as follows.

The PDF of the magnitude of *Z(t)* in polar notation is given by

$$f_v(v) = \frac{v}{\sigma^2}\exp(-\frac{v^2}{2\sigma^2}), \tag{2.3}$$

where *v* is the magnitude of *Z(t)* and σ^2 is the variance of the Gaussian random variable.

The PDF of the phase of *Z(t)* in polar notation is given by

$$f_\theta(\theta) = \frac{1}{2\pi} \quad 0 \le \theta \le 2\pi, \tag{2.4}$$

where θ is the phase of the phase of *Z(t)*.

2.2.2 Simulation Results

Figure 2-3 shows the BER performance of the classical communication system using BPSK modulation under the Rayleigh fading channel. The figure shows the BER results versus SNR over the Rayleigh fading channel. The theoretical result is also provided by MATLAB to show the correctness of simulation result [12]. The purpose is to set up a correct simulation system for classical communication and then revise this correct classical system to the cooperative system.

In Figure 2-3, it can be verified that the simulation of BPSK over the Rayleigh fading channel is accurate. The simulation result agrees with the theoretical result. This lays a

good foundation for later simulation of cooperative communication.

2.3 Cooperative Communication System over AWGN Channel

2.3.1 Simulation Model

The simulation model of the cooperative communication system over AWGN channel is shown in Figure 2-4. One relay terminal is added in order to implement cooperative communication. The plus symbol is used to represent AWGN noise; the amplifier gain is denoted by α. The AWGN noise for each channel is represented by n_i and $i = 1, 2, 3$. The dashed line represents the indirect link and the solid line corresponds to the direct link.

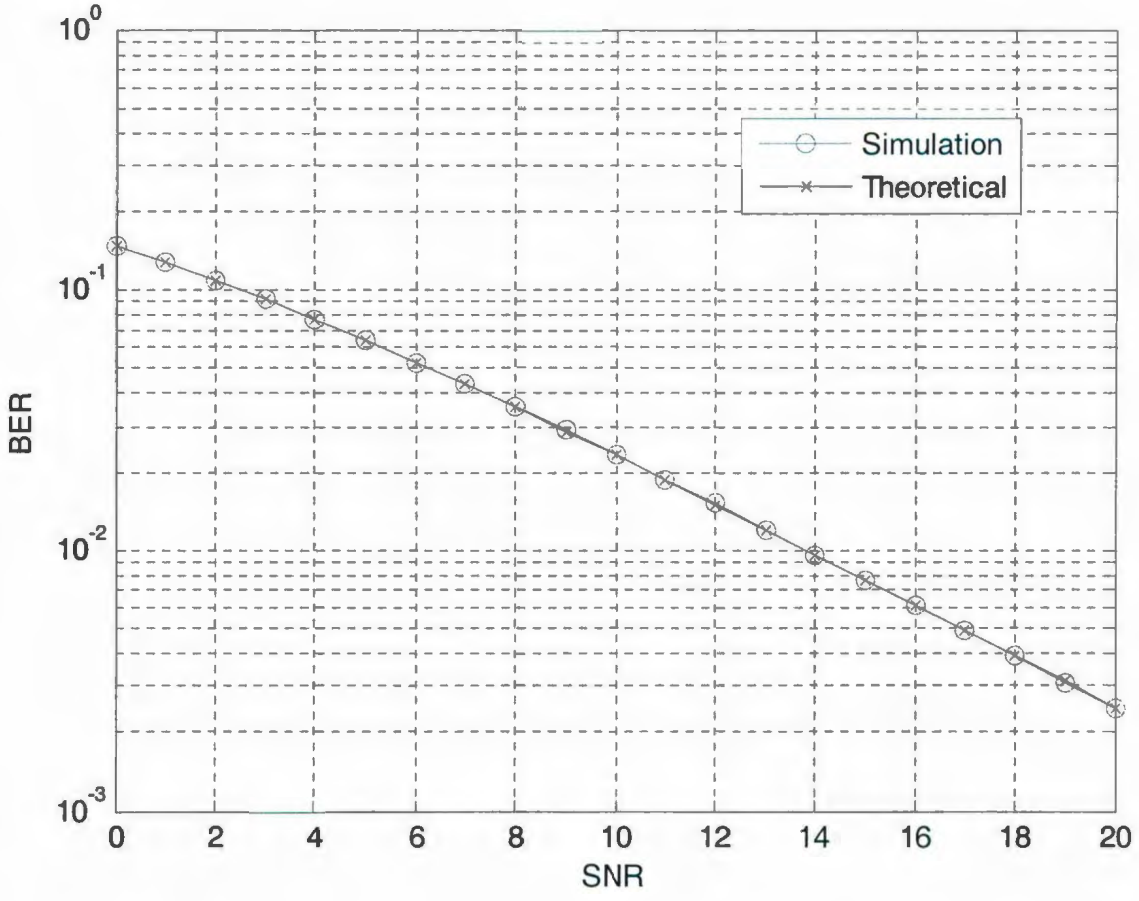

Figure 2-3 Performance of classical system using BPSK over Rayleigh fading channel

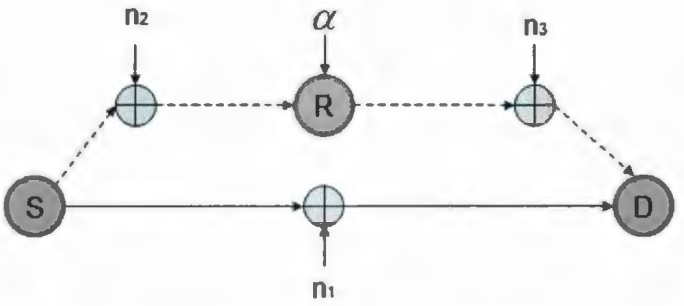

Figure 2-4 Cooperative diversity networks using BPSK over AWGN channel

2.3.2 Transmission Sequence in Cooperative Diversity Networks

For each transmitting frame

a. The source terminal sends out the signal, which is received by both the relay terminal and destination terminal because of the broadcasting nature of electromagnetic wave;

b. The relay terminal amplifies the received signal and retransmits it to the destination;

c. The destination terminal combines these two signals. The combined signal will be used to decide what information is transmitted by the source terminal. The following diagram describes the process.

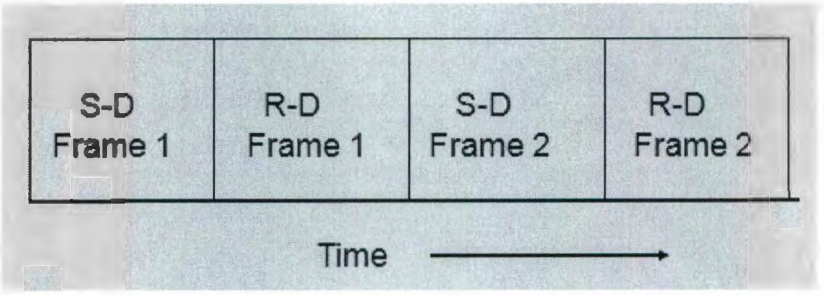

Figure 2-5 Cooperating sequence

2.3.3 The Mathematical Model

If the transmitted signal in source terminal is represented by s and α is denoted as the amplifier gain in the relay terminal. Then, the received signals in each terminal of cooperative diversity networks can be expressed as follows:

-Received signal at the relay node:

$$R_{RelayFromSource} = s + n_1, \tag{2.5}$$

-Received signal at the destination node from the source terminal:

$$R_{DesFromSource} = s + n_2, \tag{2.6}$$

-Received signal at the destination terminal from the relay terminal:

$$R_{DesFromRelay} = \alpha[s + n_2] + n_3, \tag{2.7}$$

-The total received signal:

$$\begin{aligned} R_{total} &= R_{DesFromRelay} + R_{DesFromSource} \\ &= \alpha[s + n_2] + n_3 + s + n_1 \\ &= (1+\alpha)s + n_1 + \alpha n_2 + n_3. \end{aligned} \tag{2.8}$$

2.3.4 Simulation Results

Figure 2-6 below shows the BER results versus SNR for a cooperative system using BPSK modulation over the AWGN channel, where the relay gain is 1. The BER of the classical system using BPSK is also given for comparison.

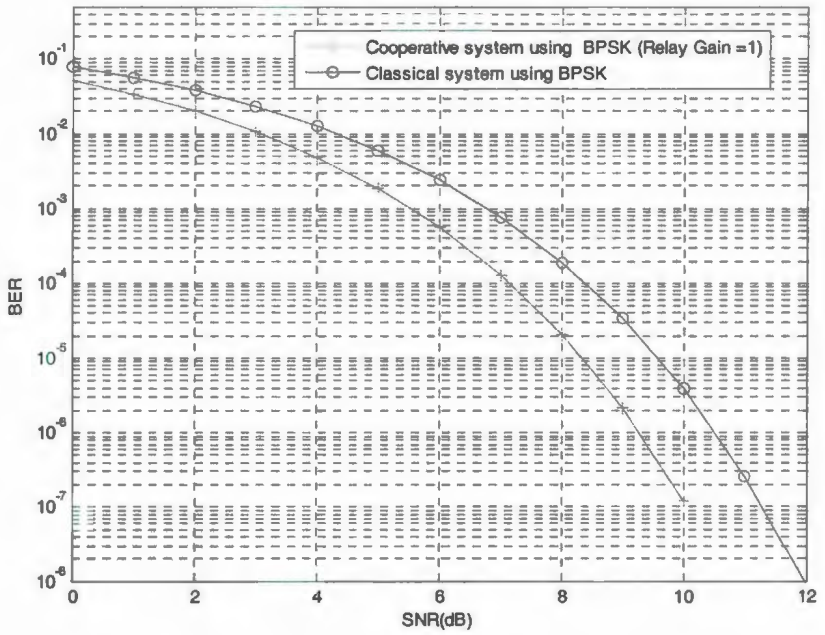

Figure 2-6 Performance of cooperative communication over AWGN channel

The above figure shows that the BER curve of cooperative system is obviously below the BER curve of classical direct system. For the same BER, the gain is approximately 1dB. Since two copies of transmitted signals and three copies of noise are received at the receiver, the received SNR is 1dB larger than system without cooperative simulation. Hence, the simulation result conforms to the theory. However, the BER gain is small in this simulation because the network is symmetric; therefore, the path loss effects is not taken into account. Moreover, this simulation does not consider the fading effect. Therefore, the diversity gain is not included. The only gain here is the virtual antenna array gain, which increased the received SNR.

2.4 Cooperative Communication Systems over Rayleigh Fading Channel

2.4.1 Maximal Ratio Combining (MRC) [1]

In Chapter 1, it is said that the independent fading paths can effectively eliminate the fading. A new problem is how to mitigate the fading by using the independent fading paths. This question is solved by combining independent signals using some combining techniques such as the MRC technique. The MRC can maximize the SNR when independent signals are combined. The MRC can be modeled as shown in Figure 2-7. In this model, the fading effect in each input to MRC is represented by $r_i e^{j\theta_i}$ where r_i and θ_i are the effects of amplitude and phase from the channel to the transmitted signal $s(t)$. Besides, the weight on each branch is expressed by α_i.

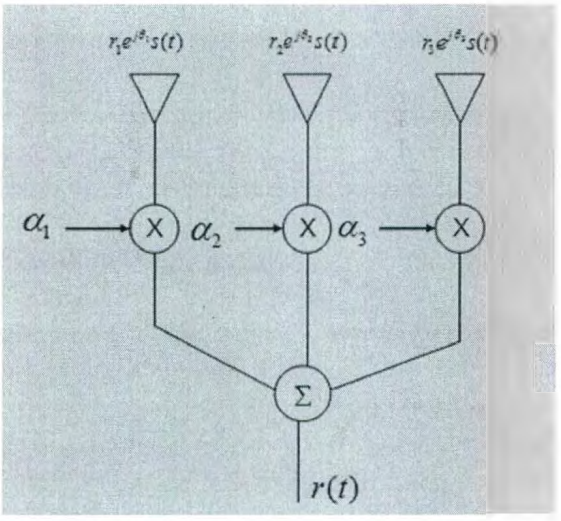

Figure 2-7 Maximal Ratio Combiner

In order to realize the MRC, the first condition is the coherent detection of each branch so that the phase θ_i in branch i can be removed by multiplying the signal at that path by $\alpha_i = a_i e^{-j\theta_i}$. The other condition is that the noise power spectral density (PSD) is the same in each branch. With these two constraints, the combined signal $r(t)$ is given by

$$
\begin{aligned}
r(t) &= \alpha_1 r_1 e^{j\theta_1} s(t) + \alpha_2 r_2 e^{j\theta_2} s(t) + \alpha_3 r_3 e^{j\theta_3} s(t) \\
&= (a_1 r_1 + a_2 r_2 + a_3 r_3) s(t) \\
&= \left(\sum_{i=1}^{3} a_i r_i \right) s(t),
\end{aligned}
\tag{2.9}
$$

The total noise power can be expressed as follows:

$$
N_{total} = \left(\sum_{i=1}^{3} a_i^{\,2} \right) N_o, \tag{2.10}
$$

where N_0 is the noise power density on each branch.

Thus, the SNR at the output of MRC

$$
SNR = \frac{\left(\sum_{i=1}^{3} a_i r_i \right)^2 E_s}{\left(\sum_{i=1}^{3} a_i^{\,2} \right) N_o}, \tag{2.11}
$$

The maximal value of SNR can be obtained by

$$
SNR_{\max} = \gamma_1 + \gamma_2 + \gamma_3 \text{ where } a_i = \frac{r_i}{\sqrt{N_0}}. \tag{2.12}
$$

2.4.2 Simulation Model

Figure 2-8 below shows the simulation model for the cooperative communication system over Rayleigh fading channel. In this model, the Rayleigh fading is represented by h_i and AWGN noise is denoted by n_i where i indicates the channel index. Both the Rayleigh fading effect and the AWGN are considered in this model. The solid line indicates the direct link and the dashed line indicates the indirect link.

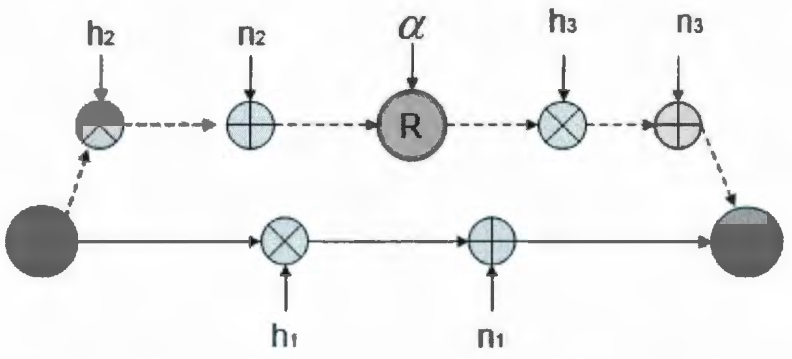

Figure 2-8 Cooperative system over Rayleigh fading channel

Compared with the previous cooperative communication over the AWGN case, the only difference here is the inclusion of fading. Hence the cooperative sequence will be the same as previous simulation except that the fading effect will be taken into consideration. Therefore, the mathematical description needs to have some modifications.

Assuming the transmitted signal is s , the Rayleigh fading coefficients (Complex Gaussian Random Variables) in the three links are h_1, h_2 and h_3.

-Received signal in the destination terminal from the source terminal:

$$R_{DesFromSource} = h_1 s + n_1, \tag{2.13}$$

-Received signal in the relay terminal:

$$R_{RelayFromSource} = h_2 s + n_2, \tag{2.14}$$

-Received signal in the destination terminal from the relay terminal:

$$\begin{aligned} R_{DesFromRelay} &= \alpha h_3 [h_2 s + n_2] + n_3 \\ &= \alpha h_3 h_2 s + \alpha h_3 n_2 + n_3, \end{aligned} \tag{2.15}$$

With the above knowledge of MRC, the MRC model used in the cooperative diversity networks can be constructed as shown in Figure 2-8. The branch weights of the direct and indirect branches are represented by the β_D and β_I, respectively.

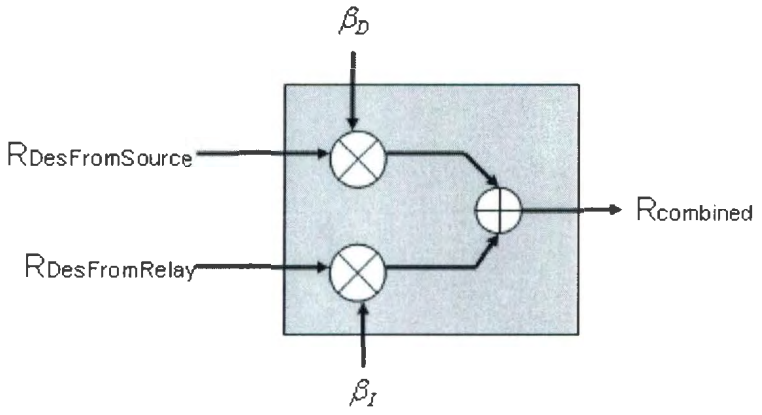

Figure 2-9 MRC structure for cooperative system

-Combined signal $R_{combined}$ at the output of the MRC:

$$R_{combined} = \beta_D R_{DesFromsource} + \beta_I R_{DesFrom\,Relay}. \tag{2.16}$$

2.4.3 The Weights of MRC on Cooperative Communication

It is obvious that the combining of signals in cooperative communication is different from the normal signal combining (discussed in the Literature Review) in that the received noise power is different in each branch. Therefore, the branch weights must be recalculated for cooperative communication.

As mentioned before, the combined SNR after MRC should be the sum of SNR on the individual branches. Hereafter, we will verify the correctness of β_D, β_I, which make the total SNR be the sum of each SNR. The power of signal s is assumed to be E, and noise power on three individual channels n_1, n_2, n_3 have the same power N.

If the noise power between the direct branch and the indirect branch are not equal, the optimum weights should be given by

$$\beta_D = \frac{h_1^*}{N}, \beta_I = \frac{\alpha h_2^* h_3^*}{\left(1+\alpha^2|h_3|^2\right)N}. \tag{2.17}$$

The two inputs of MRC can be written as

$$R_{desFromSource} = h_1 S + n_1, \tag{2.18}$$

$$R_{desFromRelay} = \alpha h_3 h_2 S + \alpha h_3 n_2 + n_3, \tag{2.19}$$

The SNR of each branch can be represented as

$$\begin{aligned} SNR_{desFromSource} &= \frac{|h_1|^2 E}{N}, \\ SNR_{desFromRelay} &= \frac{\alpha^2 |h_3|^2 |h_2|^2 E}{\left(\alpha^2 |h_3|^2 + 1\right) N}, \end{aligned} \tag{2.20}$$

The signal at the output of MRC can be represented as following equation.

$$\begin{aligned} R_{combined} &= \beta_D R_{DesFromsource} + \beta_I R_{DesFromRelayNormalize} \\ &= \frac{|h_1|^2}{N} S + \frac{h_1}{N} n_1 + \frac{\alpha^2 |h_2|^2 |h_3|^2}{\left(1 + \alpha^2 |h_3|^2\right) N} S + \frac{\alpha h_2^* h_3^* (\alpha h_3 n_2 + n_3)}{\left(1 + \alpha^2 |h_3|^2\right) N} \\ &= \left(|h_1|^2 + \frac{\alpha^2 |h_2|^2 |h_3|^2}{\left(1 + \alpha^2 |h_3|^2\right)} \right) \frac{S}{N} + \left[\frac{h_1}{N} n_1 + \frac{\alpha h_2^* h_3^* (\alpha h_3 n_2 + n_3)}{\left(1 + \alpha^2 |h_3|^2\right) N} \right]. \end{aligned} \tag{2.21}$$

The SNR of MRC output

$$\begin{aligned} SNR_{combined} &= \frac{\left(|h_1|^2 + \frac{\alpha^2 |h_2|^2 |h_3|^2}{\left(1 + \alpha^2 h_3^2\right)} \right)^2 \frac{E}{N^2}}{\frac{|h_1|^2}{N^2} N + \frac{\left(\alpha |h_3| |h_2|\right)^2 (\alpha^2 |h_3|^2 + 1) N}{\left(1 + \alpha^2 |h_3|^2\right)^2 N^2}} \\ &= \frac{\left(|h_1|^2 + \frac{\alpha^2 |h_2|^2 |h_3|^2}{\left(1 + \alpha^2 |h_3|^2\right)} \right)^2 \frac{E}{N^2}}{\frac{|h_1|^2}{N^2} N + \frac{\left(\alpha |h_3| |h_2|\right)^2 N}{\left(1 + \alpha^2 |h_3|^2\right) N^2}} = \frac{\left(h_1^2 + \frac{\alpha^2 |h_2|^2 |h_3|^2}{\left(1 + \alpha^2 |h_3|^2\right)} \right)^2 \frac{E}{N^2}}{\frac{|h_1|^2 \left(1 + \alpha^2 |h_3|^2\right) + \left(\alpha |h_3| |h_2|\right)^2}{\left(1 + \alpha^2 |h_3|^2\right) N}} \end{aligned} \tag{2.22}$$

$$
\begin{aligned}
&= \frac{\left(|h_1|^2 + \frac{\alpha^2|h_2|^2|h_3|^2}{(1+\alpha^2 h_3^2)}\right)^2 \frac{E}{N^2}}{\frac{|h_1|^2 + \alpha^2|h_3|^2(|h_1|^2+|h_2|^2)}{(1+\alpha^2|h_3|^2)N}} \\
&= \left(|h_1|^2 + \frac{\alpha^2|h_2|^2|h_3|^2}{(1+\alpha^2|h_3|^2)}\right)^2 \frac{E}{N^2} \times \frac{(1+\alpha^2|h_3|^2)N}{|h_1|^2 + \alpha^2|h_3|^2(|h_1|^2+|h_2|^2)} \\
&= \left(|h_1|^4 + \frac{\alpha^4|h_2|^4|h_3|^4}{(1+\alpha^2|h_3|^2)^2} + \frac{2\alpha^2|h_1|^2|h_2|^2|h_3|^2}{(1+\alpha^2|h_3|^2)}\right) \frac{E}{N^2} \times \frac{(1+\alpha^2|h_3|^2)N}{|h_1|^2 + \alpha^2|h_3|^2(|h_1|^2+|h_2|^2)} \\
&= \left(\frac{|h_1|^4(1+\alpha^2|h_3|^2)^2 + \alpha^4|h_2|^4|h_3|^4 + 2\alpha^2|h_1|^2|h_2|^2|h_3|^2(1+\alpha^2|h_3|^2)}{(1+\alpha^2|h_3|^2)^2}\right) \frac{E}{N^2} \times \frac{(1+\alpha^2|h_3|^2)N}{|h_1|^2 + \alpha^2|h_3|^2(|h_1|^2+|h_2|^2)} \\
&= \left(\frac{|h_1|^4 + \alpha^4|h_1|^4|h_3|^4 + 2\alpha^2|h_1|^4|h_3|^2 + \alpha^4|h_2|^4|h_3|^4 + 2\alpha^2|h_1|^2|h_2|^2|h_3|^2 + 2\alpha^4|h_1|^2|h_2|^2|h_3|^4}{(1+\alpha^2|h_3|^2)^2}\right) \frac{E}{N^2} \times \frac{(1+\alpha^2|h_3|^2)N}{|h_1|^2 + \alpha^2|h_3|^2(|h_1|^2+|h_2|^2)} \\
&= \left(\frac{|h_1|^4 + \alpha^4|h_1|^4|h_3|^4 + 2\alpha^2|h_1|^4|h_3|^2 + \alpha^4|h_2|^4|h_3|^4 + 2\alpha^2|h_1|^2|h_2|^2|h_3|^2 + 2\alpha^4|h_1|^2|h_2|^2|h_3|^4}{(1+\alpha^2|h_3|^2)\times(|h_1|^2 + \alpha^2|h_3|^2(|h_1|^2+|h_2|^2))}\right) \frac{E}{N}
\end{aligned}
$$

The sum of the SNR on each individual branch

$$
\begin{aligned}
SNR_{sum} &= SNR_{desFromSource} + SNR_{desFrom\,Relay} \\
&= \frac{|h_1|^2 E}{N} + \frac{\alpha^2|h_3|^2|h_2|^2 E}{(\alpha^2|h_3|^2+1)N} = \left(\frac{|h_1|^2(\alpha^2|h_3|^2+1) + \alpha^2|h_3|^2|h_2|^2}{(\alpha^2|h_3|^2+1)}\right)\frac{E}{N}
\end{aligned} \tag{2.23}
$$

We want to show that equation (2.22) is equal to equation (2.23). By multiplying equation (2.23) by $\frac{(|h_1|^2 + \alpha^2|h_3|^2(|h_1|^2+|h_2|^2))}{(|h_1|^2 + \alpha^2|h_3|^2(|h_1|^2+|h_2|^2))}$. Then the denominators are the same in equation (2.22) and (2.23).

Then the numerator of equation (2.23) becomes

$$
\begin{aligned}
&(|h_1|^2 + \alpha^2|h_3|^2(|h_1|^2+|h_2|^2)) \times (|h_1|^2(\alpha^2|h_3|^2+1) + \alpha^2|h_3|^2|h_2|^2) \\
&= (|h_1|^2 + \alpha^2|h_3|^2|h_1|^2 + \alpha^2|h_3|^2|h_2|^2) \times (\alpha^2|h_1|^2|h_3|^2 + \alpha^2|h_3|^2|h_2|^2 + |h_1|^2) \\
&= (|h_1|^4 + \alpha^4|h_1|^4|h_3|^4 + 2\alpha^2|h_1|^4|h_3|^2 + \alpha^4|h_2|^4|h_3|^4 + 2\alpha^2|h_1|^2|h_2|^2|h_3|^2 + 2\alpha^4|h_1|^2|h_2|^2|h_3|^4)
\end{aligned} \tag{2.24}
$$

Since the numerators are also equal, this proves the correctness of MRC weights given by (2.17) for the case of non-equal noise power.

2.4.4 Simulation Results

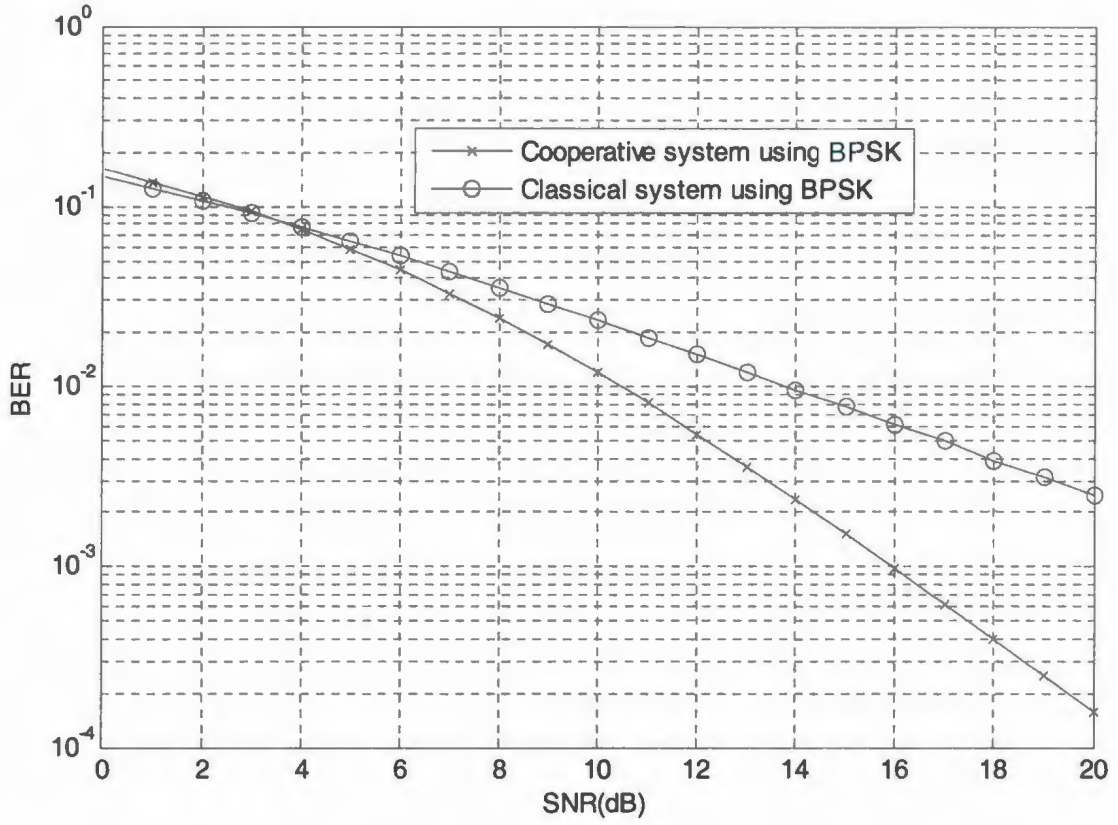

Figure 2-10 Performance of cooperative communication over Rayleigh fading channel

Figure 2-10 shows the BER results versus SNR of the cooperative communication system over the Rayleigh fading channel using BPSK modulation scheme. The same result published by [23] is also given to check the accuracy of the results. Besides, the BER results of the classical system over Rayleigh fading channel using BPSK is also provided to show the superiority of cooperative system.

Chapter 3

Cooperative Diversity Networks using Adaptive Modulation under Perfect CSI

This chapter studies the performance of the cooperative communication system using adaptive modulation scheme over the Rayleigh fading channel under perfect CSI. In the first part, one relay case is analyzed. The multi-relay case is then investigated in the second section. Some important simulation results will be given for both cases.

3.1 Adaptive Modulation with Single Relay

3.1.1 The Principle of Adaptive Modulation

As mentioned in Chapter 1, the basic idea of the adaptive modulation is to adjust the modulation scheme based on the current channel state. When the channel is in good state, a higher modulation scheme is chosen to communicate. Otherwise, a lower modulation scheme will be employed. The modulation scheme is selected such that the signal quality in terms of the average bit error rate is guaranteed to fulfill the desired requirement. To implement this mechanism in the real situation, the following question needs to be answered: what kind of metric should be used to indicate the channel quality? In this project, the total SNR at the output of MRC is used as the metric since it directly

determines the performance of communication system.

Since the exact SNR at the receiver side is impossible to know in advance, the only way to do this is to estimate the total SNR before each transmission and then select the modulation scheme based on the estimated total SNR. However, the estimation of the total SNR requires the knowledge of current CSI, which can be obtained by sending a pilot sequence through the channel. In this Chapter, we assume that all terminals have perfect knowledge of the current channel state information.

3.1.2 Calculation of Total SNR

The total SNR at the output of the MRC can be calculated based on the individual received SNR on each branch. As shown in Chapter 2, two received signals are expressed in Equation (2.18) and (2.19).

Assuming the average power of the transmitted signal S is E and the noise power is N, the SNR of the two branches are given by

$$\left(\frac{S}{N}\right)_{SD} = \frac{|h_1|^2 E}{N}, \tag{3.1}$$

$$\left(\frac{S}{N}\right)_{RD} = \frac{\alpha^2 |h_2|^2 |h_3|^2 E}{N(1+\alpha^2 |h_3|^2)}, \tag{3.2}$$

Since the MRC is employed and the perfect channel state information is known, the aggregated SNR at the output of MRC should be the sum of two individual SNRs.

$$\left(\frac{S}{N}\right)_{Total} = \left(\frac{S}{N}\right)_{RD} + \left(\frac{S}{N}\right)_{SD} = \frac{\alpha^2 |h_2|^2 |h_3|^2 E}{N(1+\alpha^2 |h_3|^2)} + \frac{|h_1|^2 E}{N}. \tag{3.3}$$

3.1.3 Decision Metric of Modulation Scheme

Since each frame transmission has a single fixed fading value, the BER of that frame depends on the instantaneous SNR at the destination terminal, which is affected by the fading and noise parameters. Therefore, the decision metric of each frame transmission should be obtained from the BER curve over the AWGN channel in classical communication. Figure 3-1 plots BER curves of most Quadrature Amplitude Modulation (QAM) schemes under the AWGN channel. The x axis is the bit energy-to-noise ratio in all plots; this should be converted to symbol energy-to-noise ratio for convenience. The conversion formula is as follows:

$$\left(\frac{E_s}{N_0}\right)_{dB} = 10\log\left(\frac{E_b}{N_0}\right) + 10\log(k), \tag{3.4}$$

where k is the number of information bits per symbol.

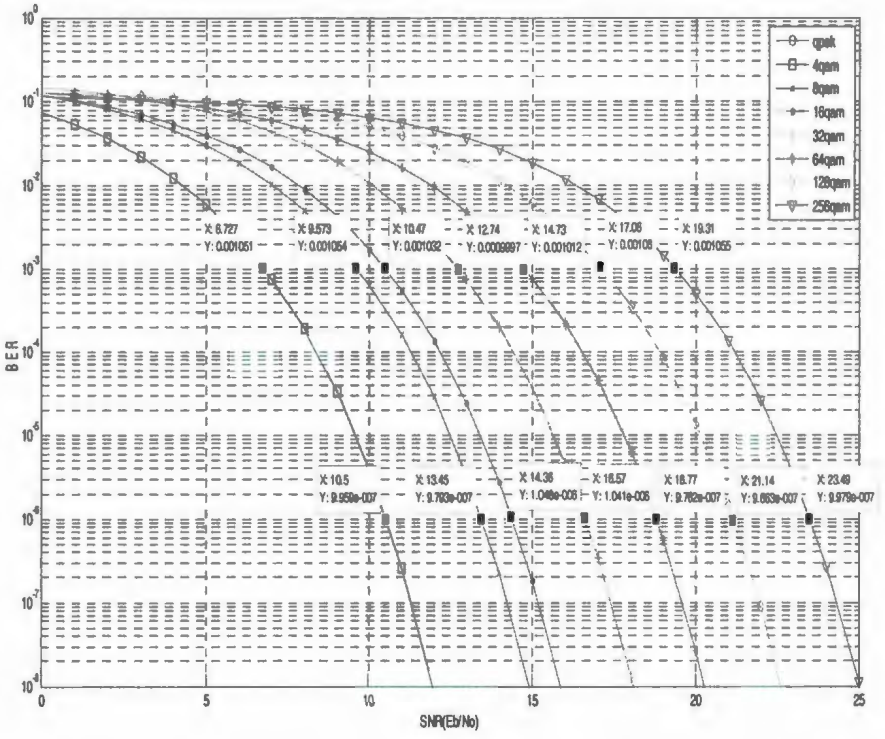

Figure 3-1 BER curves for QAM modulations

Table 3-1 shows the minimum SNR for all kinds of modulation levels for BER of 10^{-3}.

Table 3-1 Adaptive Threshold for BER (10^{-3}) under Perfect CSI

Modulation Scheme	Minimal(E_b/N_o)(dB)	Spectral Efficiency(bit/s/Hz)	Minimal(Es/No)(dB)
BPSK	6.781	1	6.781
4QAM	6.78	2	9.79
8QAM	9.6	3	14.37
16QAM	10.5	4	16.52
32QAM	12.74	5	19.73
64QAM	14.75	6	22.53
128QAM	17.12	7	25.57
256QAM	19.34	8	28.37

3.1.4 Path Loss Effects

So far, the system model did not take into account the path-loss. In order to model the real situation precisely, this property should be incorporated into the system model as follows. The received signal power, including path-loss, can be expressed as [1]

$$r^2 = |h|^2 \cdot P_t \cdot G \cdot PL, \tag{3.5}$$

where h is channel coefficient, P_t is transmission power, G is antenna gain, PL is the path loss. The PL can also be represented by [1]

$$PL = PL_0 (\frac{d}{d_0})^{-a}, \tag{3.6}$$

where PL_0 is a reference path-loss at a distance d_0, a is the path-loss exponent. a can have values from 2 to 6, where 2 is for free space, 4 for the relatively scattering environment (such as urban areas) and 6 for indoor environment. Substituting PL into the above

equation,

$$r^2 = |h|^2 \cdot P_t \cdot G \cdot PL_0 (\frac{d}{d_0})^{-a}, \tag{3.7}$$

The expectation of the received signal power on two receiving branches of the cooperative diversity network can be described by this equation separately:

$$\begin{aligned} \overline{R_{DesFromSource}}^2 &= \overline{|h_1|^2} \cdot P_t \cdot G \cdot PL_0 (\frac{d_{sd}}{d_0})^{-a} = 2\sigma^2_1, \\ \overline{R_{RelayFromSource}}^2 &= \overline{|h_1|^2} \cdot P_t \cdot G \cdot PL_0 (\frac{d_{sr}}{d_0})^{-a} = 2\sigma^2_2, \end{aligned} \tag{3.8}$$

According to the variance relationship between Rayleigh distribution and Gaussian distribution

$$\begin{aligned} \sigma_{f1}^2 &= 0.429\sigma_1^2, \\ \sigma_{f2}^2 &= 0.429\sigma_2^2, \end{aligned} \tag{3.9}$$

where σ^2_{f1} and σ^2_{f2} are the variances of the Rayleigh fading from the source to destination (s-d) link and from source to relay (s-r) link respectively, σ^2_1 and σ^2_2 are the variances of the Gaussian Random variables which generate the Rayleigh fading parameters on the s-d link and s-r link, respectively. The ratio of the received power of the s-d link to that of s-r link is given by

$$\frac{\overline{R_{DesFromSource}}^2}{\overline{R_{RelayFromSource}}^2} = \frac{\sigma_{f1}^2}{\sigma_{f2}^2} = \frac{2\sigma^2_1}{2\sigma^2_2} = \frac{\overline{|h_1|^2} \cdot P_t \cdot G \cdot PL_0 (\frac{d_{sd}}{d_0})^{-a}}{\overline{|h_2|^2} \cdot P_t \cdot G \cdot PL_0 (\frac{d_{sr}}{d_0})^{-a}} = \frac{(\frac{d_{sd}}{d_0})^{-a}}{(\frac{d_{sr}}{d_0})^{-a}} = (\frac{d_{sd}}{d_{sr}})^{-a} \tag{3.10}$$

Since the expectation of $|h_1|^2$ and $|h_2|^2$ are equal. Therefore,

$$\sigma_2^2 = \sigma_1^2 \cdot (\frac{d_{sd}}{d_{sr}})^{a} \tag{3.11}$$

The above equation incorporates the path loss into the variance of the Rayleigh fading.

If the path loss is different over s-d, s-r and r-d link, the network is called the asymmetric network; otherwise, the network with same distance and exponent in all links is called the symmetric network, which is easy to analyze compared to asymmetric case.

3.1.5 Relay Gain Classification

The cooperative diversity network can be classified based on the different amplifying gains in the relay terminal. In general, they are all falling into two categories. One is the fixed relay gain category, the other one is the variable relay gain category. In the former case, the relay gain is always a constant, which means whatever receives at the relay terminal is sent to the destination terminal without any change. In this thesis, all fixed gain simulations of cooperative diversity networks are set to 1.

In the latter case, the relay gain is a variable, which can be set in two different ways. To eliminate the fading effects to the signal transmitted on the channel between the source and the relay link, the relay gain is set $1/|h_2|$, which is called as Variable Gain I. To maintain the constant average power output, the gain is called as Variable Gain II, which is given by $\sqrt{\frac{E}{N+E|h_2|^2}}$. Since the fading coefficient is changing all the time, so is the amplifying gain.

In the following part, the fixed gain case is first studied. After that, the Variable Gain I case in the variable gain scenario is investigated. Finally, the Variable Gain II case in the changeable gain group is examined.

Two different power schemes, the fixed-power-per-user scheme and the fixed-total-power scheme, are presented. The former scheme lets the source and the relay terminals

use the same transmission power P as that of the source of the classical system with no indirect links, whereas the latter scheme fixes the total transmission power of the whole network to P. This means that for each complete message transmission in the cooperative diversity network, the energy consumed in the fixed-total-power scheme is equal to that of the direct transmission scheme with transmission power P. Therefore, the fixed total power scheme provides a fair comparison platform for the cooperative diversity network and the classical direct transmission system.

3.1.6 Relay Branch Analysis

One of the reasons that the throughput gain is achieved is that the indirect branch provides the sufficient increase of SNR to support the larger modulation scheme to compensate for the time-slot loss due to relaying process. As discussed in the previous section, the amplifying gain can be either fixed or changeable. Hence, the different choice of amplifying gain may result in different SNR increase on the indirect branch. However, the amplifying gain, which can generate maximum SNR increase, is able to provide maximum throughput gain. In this part, the SNR from the indirect branch will be investigated under both fixed gain and changeable gain situation. The SNR on this indirect branch can be written as follows.

$$\left(\frac{S}{N}\right)_{RD} = \frac{\alpha^2 |h_2|^2 |h_3|^2 E}{N(1+\alpha^2 |h_3|^2)} \tag{3.12}$$

The relay gain α is first set to the Variable Gain I in the variable gain case, which is the reciprocal of the Rayleigh fading on the s-r link. Then, equation (3.12) can be transformed to the following form.

$$\left(\frac{S}{N}\right)_{RD} = \frac{\alpha^2|h_2|^2|h_3|^2 E}{N(1+\alpha^2|h_3|^2)} = \frac{(1/|h_2|)^2|h_2|^2|h_3|^2 E}{N(1+(1/|h_2|)^2|h_3|^2)} \approx \frac{|h_3|^2 E}{N(1+1)} = \frac{1}{2}\frac{|h_3|^2 E}{N} \tag{3.13}$$

where $|h_3|^2/|h_2|^2$ is approximated by 1, which means h_2 and h_3 is likely to have values with same magnitude due to the equal variance of h_2 and h_3. Compared with $\left(\frac{S}{N}\right)_{SD} = \frac{|h_1|^2 E}{N}$ since $\overline{|h_2|^2} = \overline{|h_3|^2} = 16\overline{|h_1|^2}$ (Equation (3.11)), if $d_{sr} = d_{rd} = 0.5d_{sd}$ and path loss exponent is equal to 4. Hence, the ratio of average SNR is as follows:

$$\overline{\left(\frac{S}{N}\right)_{RD}} \Big/ \overline{\left(\frac{S}{N}\right)_{SD}} = 8 \tag{3.14}$$

When the relay gain α is set to a constant such as 1 in the fixed gain case, equation (3.13) can be transformed to another form as follows.

$$\left(\frac{S}{N}\right)_{RD} = \frac{\alpha^2|h_2|^2|h_3|^2 E}{N_0(1+\alpha^2|h_3|^2)} = \frac{|h_2|^2|h_3|^2 E}{N_0(1+|h_3|^2)} \approx \frac{|h_2|^2|h_3|^2 E}{N_0|h_3|^2} = \frac{|h_2|^2 E}{N_0} \tag{3.15}$$

In this case, the ratio of average SNR is as follows:

$$\overline{\left(\frac{S}{N}\right)_{RD}} \Big/ \overline{\left(\frac{S}{N}\right)_{SD}} = 16 \tag{3.16}$$

From equations (3.14), (3.16), the fixed relay gain can provide much higher SNR on the indirect branch than the changeable relay gain. Therefore, the maximum throughput gain can be generated when the fixed relay gain is adopted.

3.2 Fixed Relay Gain Case

3.2.1 Simulation of Fixed Relay Gain Case

In this case, the fixed relay gain ($\alpha = 1$) is used to simulate the performance of cooperative system. The relay is assumed to locate in the middle of the source and destination terminals, which means the distance between the source and relay, relay and destination is only half of the distance between source and relay. Hence, the links are asymmetric by using the equation (3.11) to model the path loss effects. We will use the following set of parameters in this simulation.

Channel bandwidth: 5 MHZ

Bit Error Rate: 10^{-3}

Relay gain: 1

Modulation levels: BPSK, 4QAM, 8QAM, 16QAM, 32QAM and 64QAM

Number of samples: 600000

Transmission power: fixed total power and fixed power per user

Link property: asymmetric network

Path-loss exponent: 4

Simulation Results

Figure 3-2 shows the throughput results of the classical system and two cooperative systems with the unit relay gain but different power schemes. It is clear that both power schemes in cooperative system outperform the classical system. Moreover, fixed-power-per-user case is much better than fixed-total-power case since more energy is consumed for each transmission. Figure 3-3 shows the BER results over the SNR in these systems. As we can see, the target 10^{-3} BER is satisfied in all cases.

Table 3-2 shows the average SNR on each link for the cooperative system with fixed-power-per-user. The purpose is to check whether the average SNR on indirect link is approximately 16 times the average SNR on the direct link in the previous theoretical analysis. Table 3-3 shows the throughput gain between the classical and the cooperative system with fixed-power-per-user in percentage.

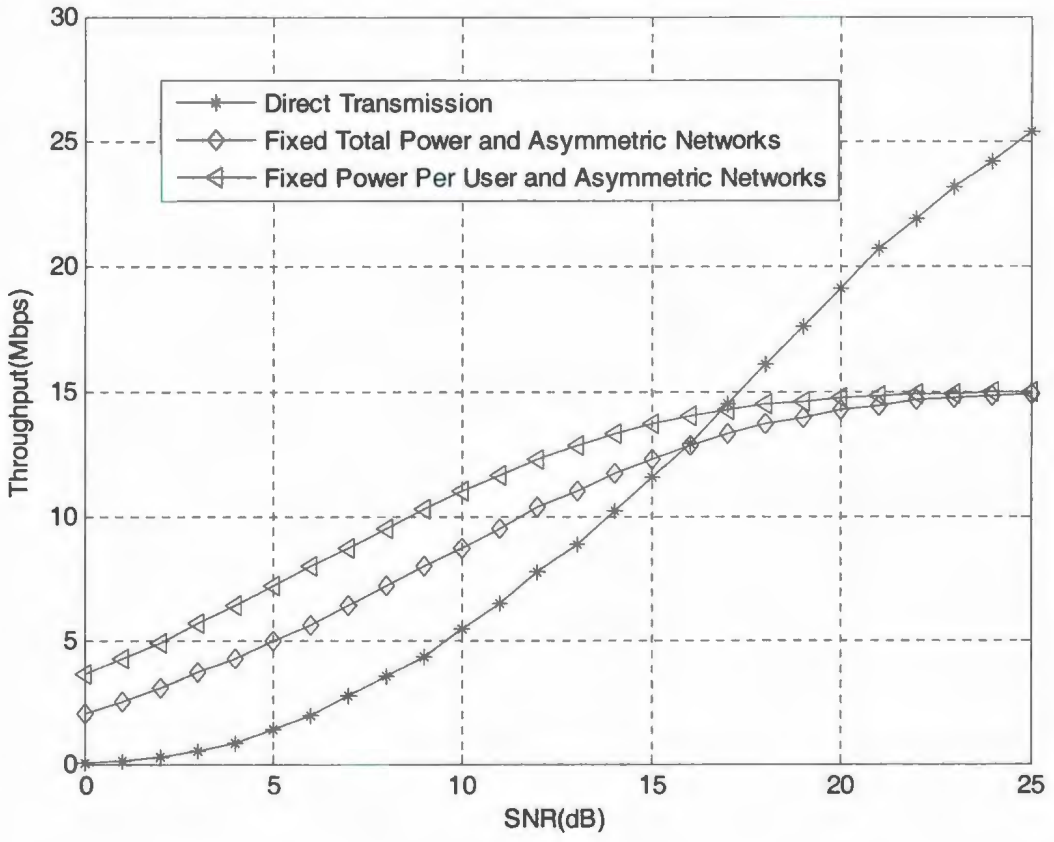

Figure 3-2 Throughput comparisons of systems with fixed relay gain

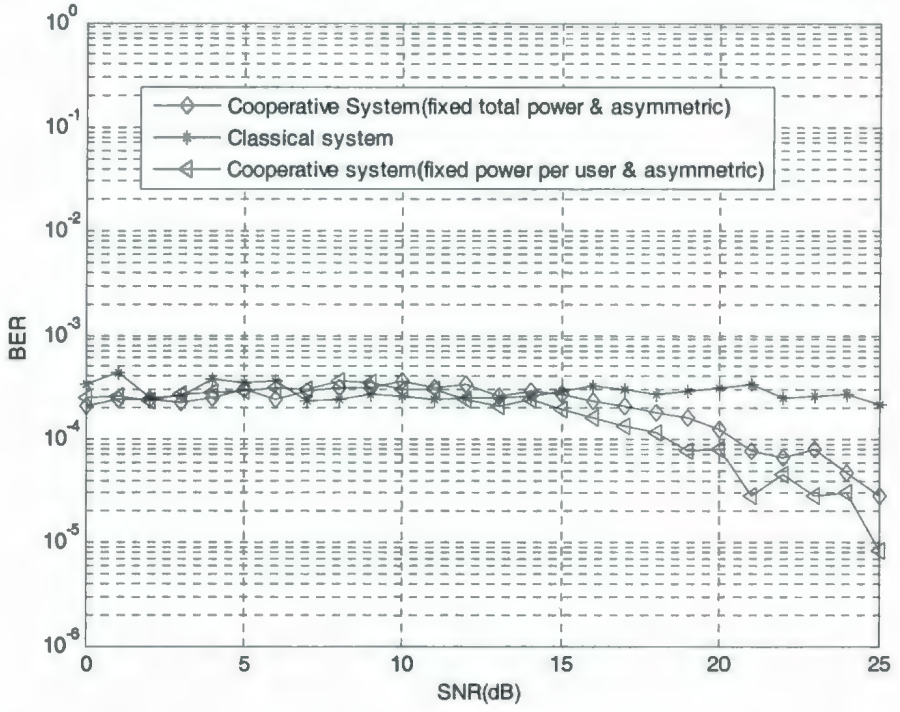

Figure 3-3 Performance of simulation systems with fixed relay gain

Table 3-2 SNR comparisons (fixed power per user) of two branches with fixed relay gain

Fixed power per user and asymmetric networks									
E/N(dB)	**0**	**1**	**2**	**3**	**4**	**5**	**6**	**7**	**8**
$(E_s/N_o)_{rd}$	13.48	17.086	21.484	27.763	33.928	42.723	55.021	67.748	84.492
$(E_s/N_o)_{sd}$	0.994	1.2776	1.587	1.9915	2.5293	3.124	3.9022	4.9003	6.236
$(E_s/N_o)_{sr}$	15.86	20.103	25.295	32.473	40.272	50.036	64.921	79.928	99.384
$(E_s/N_o)_{rd}/(E_s/N_o)_{sd}$	13.55	13.374	13.538	13.941	13.414	13.676	14.1	13.825	13.547
$(E_s/N_o)_{sr}/(E_s/N_o)_{sd}$	15.94	15.735	15.939	16.306	15.922	16.017	16.637	16.311	15.935
E/N(dB)	**9**	**10**	**11**	**12**	**13**	**14**	**15**	**16**	**17**
$(E_s/N_o)_{rd}$	107.8	135.51	169.94	213.05	269.81	341.01	436.07	542.27	674.59
$(E_s/N_o)_{sd}$	8.020	10.066	12.655	16.186	20.044	25.177	31.569	38.822	49.802
$(E_s/N_o)_{sr}$	127.2	160.13	199.7	251.78	319.08	400.7	513.59	636.69	798.48
$(E_s/N_o)_{rd}/(E_s/N_o)_{sd}$	13.44	13.463	13.429	13.163	13.461	13.545	13.813	13.968	13.545
$(E_s/N_o)_{sr}/(E_s/N_o)_{sd}$	15.862	15.908	15.78	15.555	15.919	15.916	16.269	16.4	16.033
E/N(dB)	**18**	**19**	**20**	**21**	**22**	**23**	**24**	**25**	
$(E_s/N_o)_{rd}$	876.5	1070.8	1362.8	1737	2152.9	2703.5	3396.2	4307.6	
$(E_s/N_o)_{sd}$	63.14	79.244	100.46	127.74	157.69	199.86	254.11	320.6	
$(E_s/N_o)_{sr}$	1027.	1259.5	1607.3	2040.1	2529.6	3174.5	3995.6	5066	
$(E_s/N_o)_{rd}/(E_s/N_o)_{sd}$	13.882	13.513	13.567	13.598	13.653	13.527	13.365	13.436	
$(E_s/N_o)_{sr}/(E_s/N_o)_{sd}$	16.271	15.894	16	15.971	16.042	15.884	15.724	15.801	

Table 3-3 Throughput gain (fixed power per user) of adaptive modulation with fixed relay gain

Throughput gain for fixed power per user and asymmetric networks									
E/N(dB)	**0**	**1**	**2**	**3**	**4**	**5**	**6**	**7**	**8**
Cooperative	3.629	4.2635	4.917	5.7022	6.3535	7.1542	7.9688	8.7293	9.4505
Classical	0.050	0.116	0.248	0.5225	0.866	1.387	1.914	2.7355	3.517
Thr_gain	7087.	3575.4	1882.7	991.34	633.66	415.81	316.34	219.11	168.71
E/N(dB)	**9**	**10**	**11**	**12**	**13**	**14**	**15**	**16**	**17**
Cooperative	10.25	10.991	11.611	12.294	12.843	13.296	13.694	13.983	14.235
Classical	4.357	5.4535	6.484	7.755	8.845	10.233	11.537	12.93	14.492
Thr_gain	135.3	101.54	79.075	58.53	45.198	29.921	18.704	8.1419	-1.7751
E/N(dB)	**18**	**19**	**20**	**21**	**22**	**23**	**24**	**25**	
Cooperative	14.46	14.583	14.702	14.806	14.861	14.904	14.946	14.965	
Classical	16.04	17.57	19.086	20.682	21.894	23.116	24.176	25.343	
Thr_gain	-9.84	-16.998	-22.969	-28.411	-32.123	-35.524	-38.179	-40.953	

Similarly, Table 3-4 and 3-5 show the average SNR on each link and the throughput gain respectively for the fixed total power case.

Table 3-4 SNR comparisons (fixed total power) of two branches with fixed relay gain

Fixed total power and asymmetric networks									
E/N(dB)	**0**	**1**	**2**	**3**	**4**	**5**	**6**	**7**	**8**
$(E_s/N_o)_{rd}$	6.8431	8.4757	10.651	13.78	16.94	21.613	26.99	33.747	42.959
$(E_s/N_o)_{sd}$	0.4991	0.62683	0.77759	1.0247	1.2686	1.591	1.9649	2.4815	3.1588
$(E_s/N_o)_{rd}/(E_s/N_o)_{sd}$	13.711	13.521	13.697	13.448	13.353	13.585	13.736	13.599	13.6
E/N(dB)	**9**	**10**	**11**	**12**	**13**	**14**	**15**	**16**	**17**
$(E_s/N_o)_{rd}$	54.61	67.457	86.264	109.93	135.47	170.9	212.61	270.3	340.01
$(E_s/N_o)_{sd}$	4.0342	5.0064	6.2654	7.8903	10.155	12.606	15.767	19.826	25.03
$(E_s/N_o)_{rd}/(E_s/N_o)_{sd}$	13.537	13.474	13.768	13.933	13.34	13.557	13.484	13.634	13.584
E/N(dB)	**18**	**19**	**20**	**21**	**22**	**23**	**24**	**25**	
$(E_s/N_o)_{rd}$	435.98	535.58	685.35	850.18	1081.8	1344.8	1674.2	2193.5	
$(E_s/N_o)_{sd}$	31.536	38.845	50.176	62.862	79.358	99.166	124.87	155.01	
$(E_s/N_o)_{rd}/(E_s/N_o)_{sd}$	13.825	13.788	13.659	13.525	13.632	13.561	13.408	14.15	

Table 3-5 Throughput gain (fixed total power) of adaptive modulation (6 modulation choices) with fixed relay gain

Throughput gain for fixed total power and asymmetric networks									
E/N(dB)	**0**	**1**	**2**	**3**	**4**	**5**	**6**	**7**	**8**
Cooperative	2.0538	2.508	3.024	3.6715	4.2452	4.959	5.6215	6.372	7.1565

Classical	0.0505	0.116	0.248	0.5225	0.866	1.387	1.914	2.7355	3.517
Thr_gain	3966.8	2062.1	1119.4	602.68	390.21	257.53	193.7	132.94	103.48
E/N(dB)	**9**	**10**	**11**	**12**	**13**	**14**	**15**	**16**	**17**
Cooperative	7.9845	8.6977	9.4955	10.347	11.022	11.703	12.243	12.813	13.285
Classical	4.3575	5.4535	6.484	7.755	8.845	10.233	11.537	12.93	14.492
Thr_gain	83.236	59.489	46.445	33.417	24.607	14.362	6.1219	-0.90487	-8.3305
E/N(dB)	**18**	**19**	**20**	**21**	**22**	**23**	**24**	**25**	
Cooperative	13.674	13.968	14.21	14.421	14.618	14.703	14.782	14.856	
Classical	16.046	17.57	19.086	20.682	21.894	23.116	24.176	25.343	
Thr_gain	-14.784	-20.5	-25.546	-30.273	-33.232	-36.395	-38.858	-41.382	

In this simulation, two scenarios, fixed-total-power and fixed-power-per-user, are considered. The fixed-total-power case shows a fair comparison with the classical communication system such that both systems consume the same transmitting power for one bit of information transmission. The fixed power of each mobile case is more practical. The power of each terminal does not depend on whether it is using cooperative communication or not. As shown in Tables 3-2 and 3-4, the ratio of average SNR in the indirect link to the SNR in the direct link is almost 13.5 in both cases. That means that this ratio is independent of the power level. For the throughput gain range, fixed total power case starts from 0 dB and ends at 15 dB, the maximum gain is 40 times the direct counterpart. Moreover, the fixed power per user extends this range to 16 dB and the maximum gain increases to 71 times. All this data definitely confirms the appealing advantage of cooperative communication over traditional direct communication. Next, more modulation levels are added into the choice list. This will make extensive use of cooperative communication.

3.2.2 Analytical Evaluation of Fixed Relay Gain

The throughput of the cooperative diversity network is determined by the average

spectral efficiency at each average SNR. The average spectral efficiency of a particular average SNR can be calculated as following formula.

$$\overline{SE} = \sum_{i=1}^{I} SE(i) \bullet p(i) \tag{3.17}$$

where i is the ith modulation scheme, $SE(i)$ is the spectral efficiency of the ith modulation scheme, $p(i)$ is the probability of choosing the ith modulation scheme at this particular average SNR, I is the modulation scheme with highest levels and $\overline{SE}$ is the average spectral efficiency.

Once the average spectral efficiency is derived, the average throughput of the cooperative diversity network at a particular average SNR can be obtain as follows.

$$\overline{Throughput} = \overline{SE} \bullet BW \tag{3.18}$$

Where $\overline{Throughput}$ represents the average throughput of a specific average SNR and BW is the channel bandwidth.

As seen in above formula, the probability of choosing each particular modulation scheme at a specific SNR is necessary to calculate the average throughput at this specific SNR. To find this probability, the probability density function of the total SNR at the destination terminal is required. Then, this probability of choosing each modulation scheme can be obtained by using following formula,

$$p(i) = \int_{\min SNR(i)}^{\max SNR(i)} f(\gamma) d\gamma, \tag{3.19}$$

where $f(\gamma)$ is the PDF of the SNR, γ is the instantaneous SNR and the integral limits decides the SNR range of the ith modulation scheme.

To verify the simulation results in this case, the key purpose is on finding the PDF of the total SNR at the destination terminal. Then, the average throughput can be calculated

using the Equations (3.17) and (3.18).

Next, the distribution of the total SNR at the destination terminal will be derived by analyzing the following model.

The received signal in the direct branch:

$$R_{DesFromSource} = h_1 s + n_1, \tag{3.20}$$

The received signal-to-noise ratio from the direct branch:

$$\gamma_1 = \frac{|h_1|^2 E}{N}, \tag{3.21}$$

The probability density function of γ_1:

$|h_1|$ follows the Rayleigh distribution $f_{|h_1|}(|h_1|) = \frac{|h_1|}{\sigma^2}\exp(-\frac{|h_1|^2}{2\sigma^2})$,

By calculating the PDF of a function with respect to PDF of $|h_1|$

$$f_{\gamma_1}(\gamma_1) = \frac{N}{2\sigma_1^2 E}\exp(-\frac{\gamma_1 N}{2\sigma_1^2 E}), \tag{3.22}$$

If $\frac{N}{2\sigma_1^2 E}$ is substituted by a constant b_1, the PDF will be simplified as a standard exponential distribution.

$$f_{\gamma_1}(\gamma_1) = b_1 \exp(-b_1\gamma_1), \tag{3.23}$$

The received signal in the indirect branch

$$R_{DesFromRelay} = \alpha h_3 h_2 S + \alpha h_3 n_2 + n_3, \tag{3.24}$$

The received signal-to-noise ratio from the indirect branch

$$\gamma_{indirect} = \frac{\alpha^2 |h_3|^2 |h_2|^2 E}{\left(\alpha^2 |h_3|^2 + 1\right) N} = \frac{\frac{|h_2|^2 E}{N} \frac{|h_3|^2 E}{N}}{\frac{|h_3|^2 E}{N} + \frac{E}{\alpha^2 N}}, \tag{3.25}$$

Substituting $\gamma_2 = \frac{|h_2|^2 E}{N}$ and $\gamma_3 = \frac{|h_3|^2 E}{N}$ into above equation. Similarly, γ_2 and γ_3 follow the exponential distribution as follows.

$$f_{\gamma_2}(\gamma_2) = b_2 \exp(-b_2 \gamma_2), \; f_{\gamma_3}(\gamma_3) = b_3 \exp(-b_3 \gamma_3), \tag{3.26}$$

where $b_2 = \frac{N}{2\sigma_2^2 E}$ and $b_3 = \frac{N}{2\sigma_3^2 E}$.

Equation (3.26) is simplified in the following form,

$$\gamma_{indirect} = \frac{\frac{|h_2|^2 E}{N} \bullet \frac{|h_3|^2 E}{N}}{\frac{|h_3|^2 E}{N} + \frac{E}{\alpha^2 N}} = \frac{\gamma_2 \gamma_3}{C + \gamma_3}, \tag{3.27}$$

The total SNR under perfect CSI can be represented by the summation of the SNRs on direct and indirect branches.

$$\gamma = \frac{\gamma_2 \gamma_3}{\gamma_3 + C} + \gamma_1, \tag{3.28}$$

where the first term is the SNR on the indirect branch, the second term is the SNR on the direct branch and C is $E/(\alpha^2 N)$.

In the fixed relay gain case, α is a constant. Hence, C is a constant when the average SNR is a constant. The PDF of the total SNR conditioned on γ_3 can be found by following method.

$$\gamma = \frac{\gamma_2\gamma_3}{\gamma_3 + C} + \gamma_1 = \left(\frac{\gamma_3}{\gamma_3 + C}\right)\gamma_2 + \gamma_1 = C_1\gamma_2 + \gamma_1 = \gamma_2' + \gamma_1, \tag{3.29}$$

where C_1 is equal to $\gamma_3/(\gamma_3 + C)$ and γ_2' is equal to $C_1\gamma_2$.

The PDF of γ_2' can be derived after simple random variable transformation

$$f_{\gamma_2'}(\gamma_2') = \frac{1}{C_1} f_{\gamma_2}(\frac{\gamma_2'}{C_1}) = \frac{b_2}{C_1} e^{-\frac{b_2\gamma_2'}{C_1}}, \tag{3.30}$$

The PDF of γ should be the convolution of random variable γ_2' and γ_1 like following.

$$\begin{aligned} f(\gamma \mid \gamma_3 = \gamma') &= \int_0^{\gamma} f_{\gamma_2}(\tau) f_{\gamma_1}(\gamma - \tau) d\tau \\ &= \int_0^{\gamma} f_{\gamma_2'}(\tau) f_{\gamma_1}(\gamma - \tau) d\tau \\ &= \int_0^{\gamma} \frac{b_2}{C_1} e^{-\frac{b_2\tau}{C_1}} \times b_1 e^{-b_1(\gamma-\tau)} d\tau \\ &= \frac{b_1 b_2}{C_1} e^{-b_1\gamma} \int_0^{\gamma} e^{-\frac{b_2\tau}{C_1}} e^{b_1\tau} d\tau \end{aligned} \tag{3.31}$$

$$\begin{aligned} &= \frac{b_1 b_2}{C_1} e^{-b_1\gamma} \int_0^{\gamma} e^{-(\frac{b_2}{C_1} - b_1)\tau} d\tau \\ &= \frac{b_1 b_2}{b_2 - b_1 C_1} \left[1 - e^{-(\frac{b_2}{C_1} - b_1)\gamma}\right] e^{-b_1\gamma}, \end{aligned}$$

The PDF of the total SNR under perfect CSI

$$\begin{aligned} f_{\gamma}(\gamma) &= \int_0^{\infty} f(\gamma \mid \gamma_3) f_{\gamma_3}(\gamma_3) d\gamma_3 \\ &= \int_0^{\infty} \frac{b_1 b_2}{b_2 - b_1 C_1} \left[1 - e^{-(\frac{b_2}{C_1} - b_1)\gamma}\right] e^{-b_1\gamma} \times b_3 e^{-b_3\gamma_3} d\gamma_3 \end{aligned} \tag{3.32}$$

$$= e^{-b_1\gamma}\int_0^\infty \frac{b_1b_2b_3}{b_2-b_1C_1}e^{-b_3\gamma_3}d\gamma_3 - \int_0^\infty \frac{b_1b_2b_3}{b_2-b_1C_1}e^{-b_3\gamma_3}e^{-\frac{b_2}{C_1}\gamma}d\gamma_3, C_1 = \frac{\gamma_3}{\gamma_3 + C}$$

$$\frac{b_1b_2b_3}{b_2-b_1C_1} = \frac{b_1b_2b_3\gamma_3 + b_1b_2b_3C}{(b_2-b_1)\gamma_3 + b_2C} = \frac{A\gamma_3+B}{D\gamma_3+E}, F = b_3, G = b_2\gamma C$$

$$= e^{-b_1\gamma}\int_0^\infty \frac{A\gamma_3+B}{D\gamma_3+E}e^{-F\gamma_3}d\gamma_3 - e^{-b_2\gamma}\int_0^\infty \frac{A\gamma_3+B}{D\gamma_3+E}e^{-G/\gamma_3}e^{-F\gamma_3}d\gamma_3$$

$$\int_0^\infty \frac{A\gamma_3+B}{D\gamma_3+E}e^{-F\gamma_3}d\gamma_3 = \frac{e^{-F\gamma_3}\left[(BD-AE)e^{F(\frac{E}{D}+\gamma_3)}F \bullet Ei(-\frac{F(E+D\gamma_3)}{D}) - AD\right]}{D^2F}$$

$$\int_0^\infty \frac{A\gamma_3+B}{D\gamma_3+E}e^{-G/\gamma_3}e^{-F\gamma_3}d\gamma_3$$

To solve the above integration, the fraction part is first represented by the series. Then, the following integral can be used.

$$\int_0^\infty x^{\nu-1}\exp(-\beta x^p - \gamma x^{-p})dx = \frac{2}{p}\left(\frac{\gamma}{\beta}\right)^{\frac{\nu}{2p}}K_{\frac{\nu}{p}}(2\sqrt{\beta\gamma}) \qquad (3.33)$$

However, the negative value of D will result in an infinite discontinuity point inside the integration. As a result, there is no way to express this fraction in series. Therefore, there is no closed form solution for this integral. An alternative way to find the solution of this integral is using the numerical method. Therefore, the numerical PDF of the received SNR can be obtained after using the numerical integration. Similarly, this PDF is used to calculate the analytical throughput by using the formulas in the changeable gain proof.

Analytical results

As seen from Figure 3-4, the analytical throughput of cooperative diversity networks with unit relay gain is plotted in the crossed curve. The triangle curve shows the results from the simulation. It is obvious that two curves overlap to each other very well in the whole range of SNR. Therefore, the analytical results verify the simulation results.

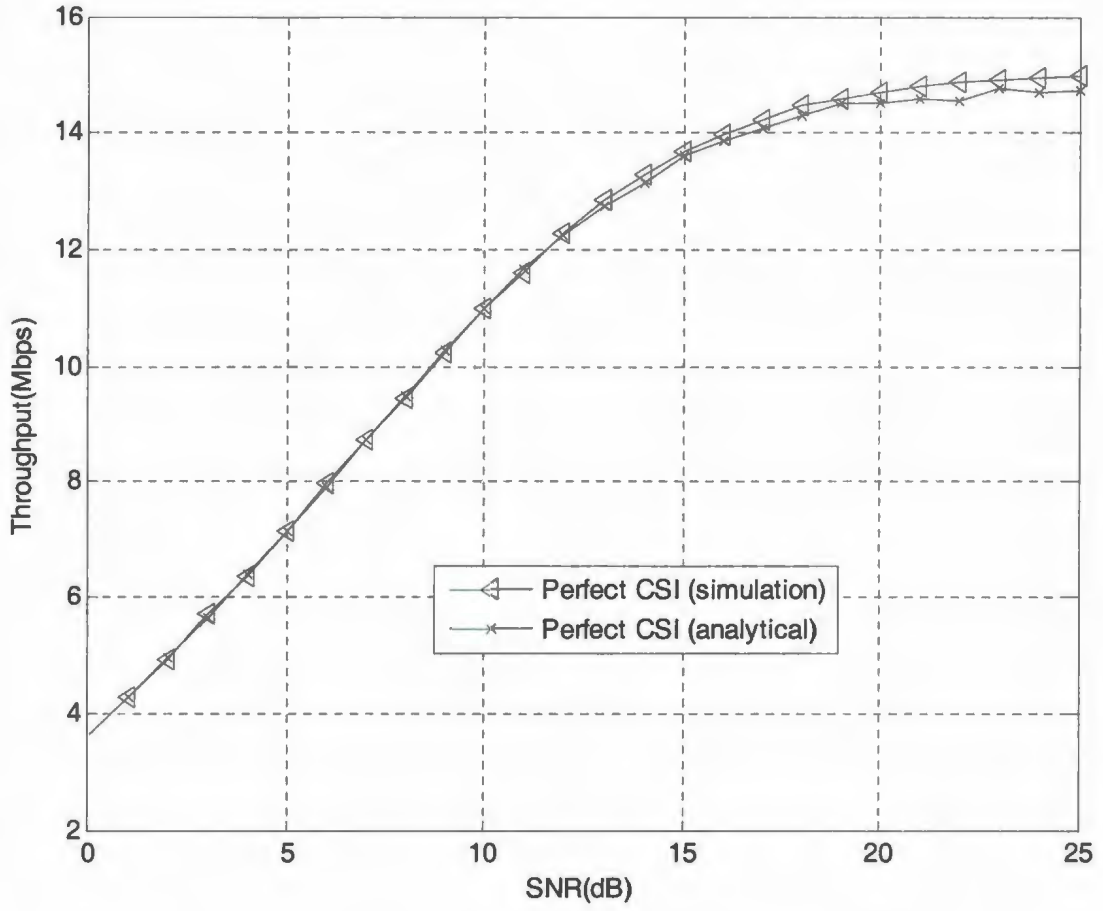

Figure 3-4 Analytical throughput comparison with the simulation results

3.2.3 Fixed Relay Gain Simulation with More Modulation Schemes

In this case, we use eight modulation levels while the other conditions are the same. The following set of parameters will be used in this simulation.

Channel bandwidth: 5 MHZ

Bit Error Rate: 10^{-3}

Modulation levels: BPSK, 4QAM, 8QAM, 16QAM, 32QAM, 64QAM, 128QAM and 256QAM

Relay gain: 1

Number of samples: 8400000 (More Modulation Schemes Included and different block size is chosen to make the block size dividable by the spectral efficiency of all modulation schemes)

Transmission Power: total fixed power and fixed power per user

Link property: asymmetric network

Path-loss exponent: 4

Simulation Results

Figure 3-5 below shows the throughput of the classical communication system and two cooperative communication systems with different power schemes. These two cooperative systems correspond to the fixed-power-per-user and fixed-total-power cases. The BER result versus SNR in this simulation is given in Figure 3-6.

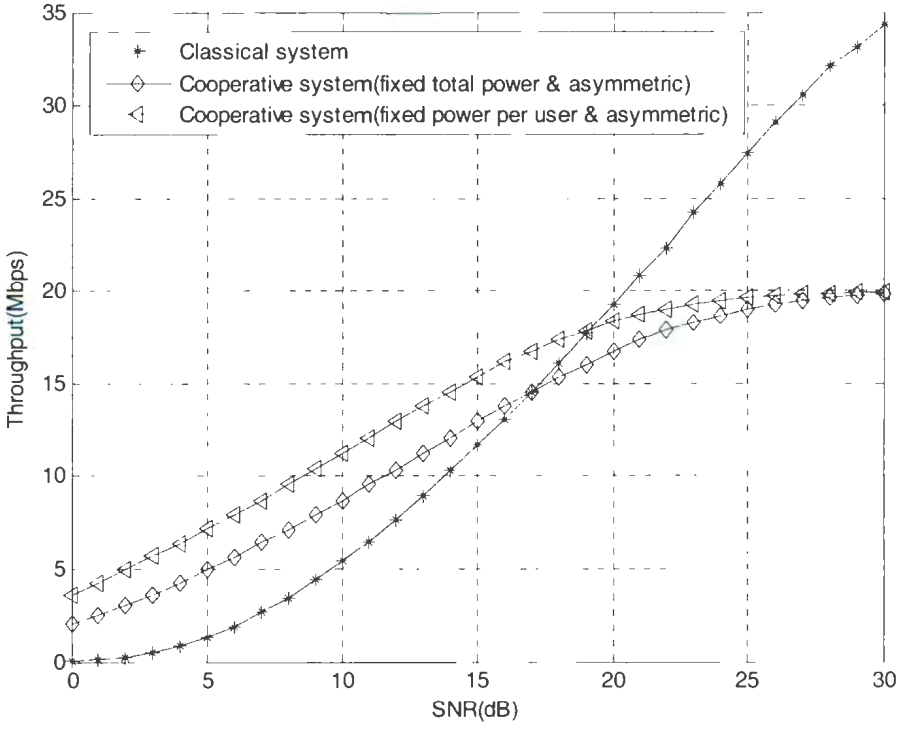

Figure 3-5 Throughput comparisons of simulation systems with eight modulation levels

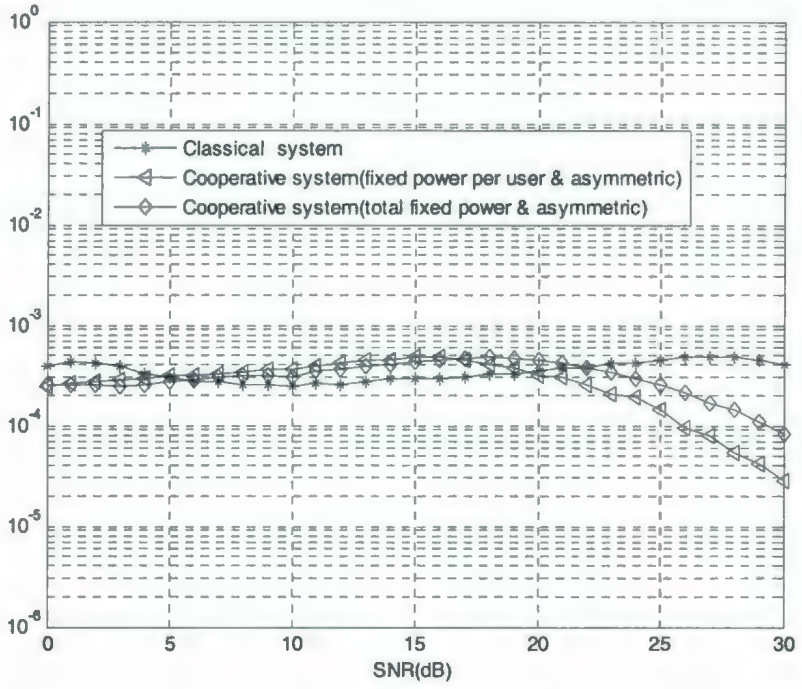

Figure 3-6 Performance of simulation systems with eight modulation levels

Table 3-6 lists the average SNR in each link for the fixed-power-per-user case. The ratio of the average SNR in the indirect link to the average SNR in the direct link is given to further prove the theoretical result. Table 3-7 shows the throughput gain numerically.

Table 3-6 SNR comparison (fixed power per user) of two branches (8modulation choices)

Fixed power per user and asymmetric networks									
E/N(dB)	**0**	**1**	**2**	**3**	**4**	**5**	**6**	**7**	**8**
$(E_s/N_o)_{rd}$	13.61	16.816	21.8	27.664	34.446	42.989	53.561	67.265	85.471
$(E_s/N_o)_{sd}$	1.0113	1.2561	1.6244	2.0042	2.4756	3.1191	4.0158	4.9451	6.3676
$(E_s/N_o)_{sr}$	15.95	19.931	25.679	32.442	40.453	50.592	63.089	78.863	100.8
$(E_s/N_o)_{rd}/(E_s/N_o)_{sd}$	13.46	13.388	13.42	13.803	13.914	13.783	13.338	13.602	13.423
$(E_s/N_o)_{sr}/(E_s/N_o)_{sd}$	15.78	15.867	15.808	16.187	16.34	16.22	15.71	15.948	15.83
E/N(dB)	**9**	**10**	**11**	**12**	**13**	**14**	**15**	**16**	**17**
$(E_s/N_o)_{rd}$	108.4	136.69	172.09	220.82	272.91	338.22	425.13	536.43	682.02
$(E_s/N_o)_{sd}$	7.861	9.894	12.96	15.968	20.104	25.084	31.338	40.338	49.583
$(E_s/N_o)_{sr}$	127.9	161.2	202.93	259.3	321.89	398.94	503.18	628.73	802.69
$(E_s/N_o)_{rd}/(E_s/N_o)_{sd}$	13.79	13.815	13.279	13.829	13.575	13.484	13.566	13.298	13.755
$(E_s/N_o)_{sr}/(E_s/N_o)_{sd}$	16.281	16.292	15.658	16.239	16.011	15.904	16.056	15.587	16.189

E/N(dB)	18	19	20	21	22	23	24	25	26
$(E_s/N_o)_{rd}$	874.4	1071.1	1368.2	1708.8	2121.2	2745.3	3408.1	4312.8	5395.1
$(E_s/N_o)_{sd}$	62.61	78.97	101.38	125.07	157.62	201.66	254.06	316.28	394.9
$(E_s/N_o)_{sr}$	1030.	1256.3	1603.4	2024.8	2508	3214	4015.2	5055.9	6381.7
$(E_s/N_o)_{rd}/(E_s/N_o)_{sd}$	13.966	13.563	13.495	13.663	13.457	13.613	13.415	13.636	13.662
$(E_s/N_o)_{sr}/(E_s/N_o)_{sd}$	16.456	15.909	15.815	16.189	15.911	15.937	15.804	15.986	16.16
E/N(dB)	**27**	**28**	**29**	**30**					
$(E_s/N_o)_{rd}$	6899.	8394.8	10930	13489					
$(E_s/N_o)_{sd}$	506.0	627.75	790.14	980.7					
$(E_s/N_o)_{sr}$	8113.5	9924.3	12862	15895					
$(E_s/N_o)_{rd}/(E_s/N_o)_{sd}$	13.635	13.373	13.834	13.754					
$(E_s/N_o)_{sr}/(E_s/N_o)_{sd}$	16.034	15.809	16.278	16.208					

Table 3-7 Throughput gain (fixed power per user) of adaptive modulation (8modulation choices)

Throughput gain for fixed power per user and asymmetric networks									
E/N(dB)	**0**	**1**	**2**	**3**	**4**	**5**	**6**	**7**	**8**
Cooperative	3.658	4.242	4.9845	5.7108	6.3805	7.1528	7.93	8.6855	9.5787
Classical	0.039	0.113	0.2555	0.4945	0.865	1.3615	1.898	2.723	3.4615
Thr_gain	9281.4	3654	1850.9	1054.9	637.63	425.36	317.81	218.97	176.72
E/N(dB)	**9**	**10**	**11**	**12**	**13**	**14**	**15**	**16**	**17**
Cooperative	10.388	11.251	12.091	12.974	13.744	14.544	15.355	16.127	16.76
Classical	4.45	5.4585	6.4245	7.619	8.96	10.325	11.639	13.06	14.537
Thr_gain	133.44	106.11	88.205	70.288	53.393	40.862	31.931	23.482	15.292
E/N(dB)	**18**	**19**	**20**	**21**	**22**	**23**	**24**	**25**	**26**
Cooperative	17.381	17.811	18.352	18.695	18.992	19.292	19.473	19.625	19.728
Classical	16.069	17.695	19.294	20.843	22.34	24.213	25.763	27.422	29.059
Thr_gain	8.165	0.6541	-4.8822	-10.306	-14.988	-20.323	-24.417	-28.432	-32.11
E/N(dB)	**27**	**28**	**29**	**30**					
Cooperative	19.825	19.869	19.913	19.945					
Classical	30.541	32.069	33.118	34.329					
Thr_gain	-35.088	-38.043	-39.872	-41.901					

Similarly, Tables 3-8 and 3-9 show the SNR on each link and the throughput gain, respectively, for the fixed-total-power-case.

Table 3-8 SNR comparison (fixed total power) of two branches (8modulation choices)

Fixed total power and asymmetric networks									
E/N(dB)	**0**	**1**	**2**	**3**	**4**	**5**	**6**	**7**	**8**
$(E_s/N_o)_{rd}$	6.8938	8.6204	10.757	13.699	17.096	21.811	26.748	34.436	42.239
$(E_s/N_o)_{sd}$	0.49897	0.61595	0.79239	1.0003	1.2651	1.589	2.0181	2.5001	3.0978
$(E_s/N_o)_{rd}/(E_s/N_o)_{sd}$	13.816	13.995	13.576	13.695	13.513	13.727	13.254	13.774	13.635

E/N(dB)	9	10	11	12	13	14	15	16	17
$(E_s/N_o)_{rd}$	53.064	67.162	85.831	106.53	136	170.38	215.87	270.96	337.86
$(E_s/N_o)_{sd}$	3.9257	4.9881	6.2328	7.8284	9.9838	12.412	15.793	19.914	24.681
$(E_s/N_o)_{rd}/(E_s/N_o)_{sd}$	13.517	13.465	13.771	13.607	13.622	13.727	13.669	13.607	13.689
E/N(dB)	**18**	**19**	**20**	**21**	**22**	**23**	**24**	**25**	**26**
$(E_s/N_o)_{rd}$	434.97	537.54	660.14	849.19	1105.7	1348.3	1704.3	2101.2	2749.1
$(E_s/N_o)_{sd}$	31.29	39.806	49.776	62.007	78.295	99.002	125.98	156.09	197.65
$(E_s/N_o)_{rd}/(E_s/N_o)_{sd}$	13.901	13.504	13.262	13.695	14.123	13.619	13.528	13.461	13.909
E/N(dB)	**27**	**28**	**29**	**30**					
$(E_s/N_o)_{rd}$	3480.6	4222.3	5557.9	6742.1					
$(E_s/N_o)_{sd}$	246.86	317.63	401.08	502.06					
$(E_s/N_o)_{rd}/(E_s/N_o)_{sd}$	14.1	13.293	13.857	13.429					

Table 3-9 Throughput gain (fixed total power) of adaptive modulation (8modulation choices)

Throughput gain for fixed total power and asymmetric networks									
E/N(dB)	**0**	**1**	**2**	**3**	**4**	**5**	**6**	**7**	**8**
Cooperative	2.0667	2.5313	3.0707	3.661	4.277	4.9678	5.614	6.4345	7.1395
Classical	0.039	0.113	0.2555	0.4945	0.865	1.3615	1.898	2.723	3.4615
Thr_gain	5199.4	2140	1101.9	640.34	394.45	264.87	195.79	136.3	106.25
E/N(dB)	**9**	**10**	**11**	**12**	**13**	**14**	**15**	**16**	**17**
Cooperative	7.8857	8.6578	9.5695	10.327	11.249	12.047	12.949	13.762	14.523
Classical	4.45	5.4585	6.4245	7.619	8.96	10.325	11.639	13.06	14.537
Thr_gain	77.208	58.61	48.953	35.536	25.547	16.68	11.253	5.3733	-0.09803
E/N(dB)	**18**	**19**	**20**	**21**	**22**	**23**	**24**	**25**	**26**
Cooperative	15.352	16.032	16.707	17.354	17.933	18.293	18.681	19.007	19.267
Classical	16.069	17.695	19.294	20.843	22.34	24.213	25.763	27.422	29.059
Thr_gain	-4.4575	-9.4035	-13.411	-16.737	-19.73	-24.45	-27.49	-30.686	-33.697
E/N(dB)	**27**	**28**	**29**	**30**					
Cooperative	19.493	19.612	19.736	19.802					
Classical	30.541	32.069	33.118	34.329					
Thr_gain	-36.176	-38.846	-40.407	-42.319					

Compared with the previous case, this simulation adds two more modulation schemes. It is clear from the throughput curves in Figure 3-11 that the SNR of the fixed-total-power and the fixed-power-per-user cases are improved by 1 dB and 2 dB, respectively. Moreover, the maximum throughput gain increases to 93 in the fixed-power–per-user case and approximately 77 in the fixed-total-power case. The proof of simulation in this part is very close to the previous one using 6 modulation levels. Hence, it is not repeated

here.

3.2.4 Fixed Relay Gain with Higher Target BER Simulation

In this case, the BER is increased from the previous 10^{-3} to 10^{-6} while the modulation levels are the same as previous case. We will use the following set of parameters in this simulation:

Channel bandwidth: 5 MHZ

Bit Error Rate: 10^{-6}

Modulation levels: BPSK, 4QAM, 8QAM, 16QAM, 32QAM, 64QAM, 128QAM and 256QAM

Relay gain: 1

Number of samples: 840000000

Transmission power: fixed total power and fixed power per user

Link property: asymmetric network

Path-loss exponent: 4

Simulation Results

Figure 3-7 shows the throughput of the classical system and cooperative systems. In this case, the BER is set to 10^{-6}. Therefore, larger sample size is required to generate more accurate simulation results. Figure 3-8 shows the BER results versus SNR for these communication systems.

Table 3-10 shows the SNR in each link of cooperative communication system with the fixed-power-per-user scheme. Moreover, the ratio of the average SNR in the indirect link to the average SNR in the direct link is also given. Table 3-11 shows the throughput gain

numerically.

Cooperative communication is continuously showing its superiority to the classical communication system in this case, where the target BER is equal to 10^{-6}. Both the fixed-power-per-user curve and the fixed-total-power curve intersect with the classical curve at 23 dB and 21 dB respectively. Compared with Figure 3-5, the throughput of classical system in this case is less than that of classical system in 10^{-3} case since the BER in this case is increased to 10^{-6}. This means that each transmission is less likely to succeed in 10^{-6} case than in 10^{-3} case under same average SNR. These two intersection points are higher than those of the previous case (target BER=10^{-3}), because the higher target BER value increases the SNR threshold of each modulation level. Therefore, it is less likely for the classical communication to use high modulation levels.

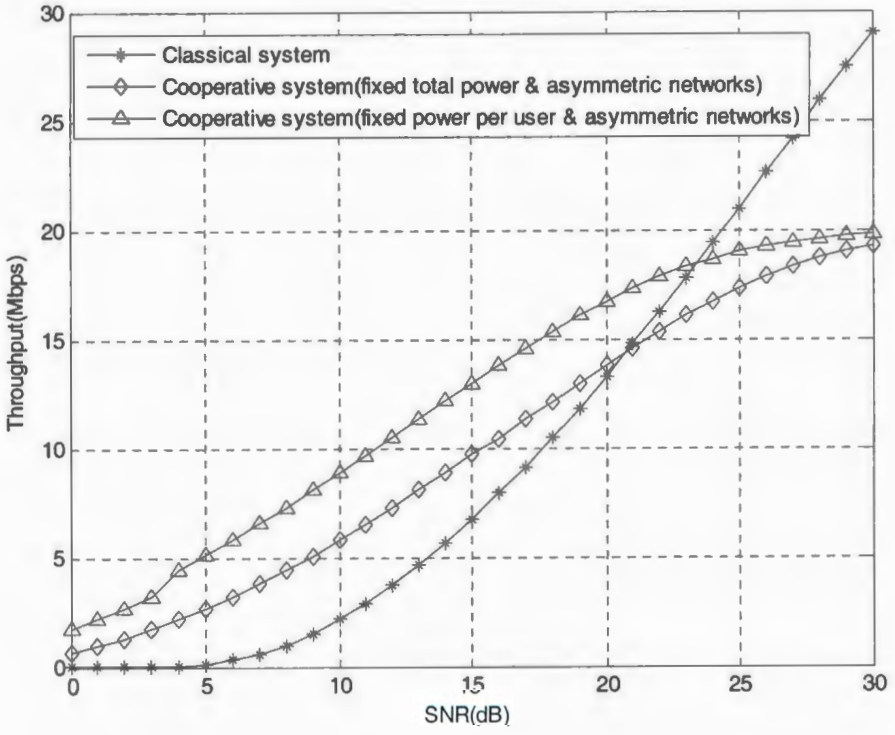

Figure 3-7 Throughput comparisons of eight modulation choices

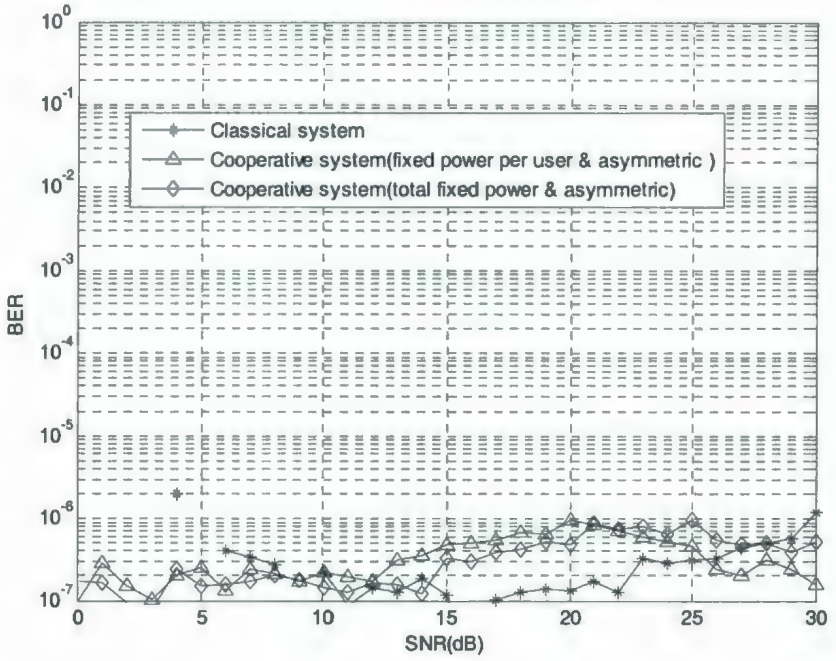

Figure 3-8 Performance of eight modulation choice

Table 3-10 SNR comparison (fixed power per user) of two branches (8 modulation choices) (BER 10-6)

Fixed power per user and asymmetric networks									
E/N(dB)	**0**	**1**	**2**	**3**	**4**	**5**	**6**	**7**	**8**
$(E_s/N_o)_{rd}$	13.635	17.113	21.563	27.004	43.041	54.017	68.345	86.237	108.48
$(E_s/N_o)_{sd}$	1.0008	1.2558	1.5752	2.0084	3.1498	3.9655	5.0202	6.2988	7.896
$(E_s/N_o)_{sr}$	16.031	20.157	25.38	31.746	50.689	63.619	80.38	101.53	127.51
$(E_s/N_o)_{rd}/(E_s/N_o)_{sd}$	13.624	13.627	13.689	13.445	13.665	13.621	13.614	13.691	13.739
$(E_s/N_o)_{sr}/(E_s/N_o)_{sd}$	16.018	16.051	16.112	15.806	16.093	16.043	16.011	16.119	16.148
E/N(dB)	**9**	**10**	**11**	**12**	**13**	**14**	**15**	**16**	**17**
$(E_s/N_o)_{rd}$	136.33	170.31	214.74	271.74	342.14	431	539.86	679.31	858.7
$(E_s/N_o)_{sd}$	10.017	12.58	15.915	19.88	25.028	31.6	39.579	50.126	62.898
$(E_s/N_o)_{sr}$	160.33	200.13	252.85	319.9	402.97	507.15	634.45	800.81	1010.1
$(E_s/N_o)_{rd}/(E_s/N_o)_{sd}$	13.61	13.538	13.493	13.669	13.67	13.639	13.64	13.552	13.652
$(E_s/N_o)_{sr}/(E_s/N_o)_{sd}$	16.006	15.909	15.887	16.092	16.101	16.049	16.03	15.976	16.059
E/N(dB)	**18**	**19**	**20**	**21**	**22**	**23**	**24**	**25**	**26**
$(E_s/N_o)_{rd}$	1082.3	1360.9	1705	2157.8	2718	3425	4280.7	5427.8	6826.4
$(E_s/N_o)_{sd}$	79.493	99.848	125.97	158.31	199.71	251.95	317.03	396.22	497.98
$(E_s/N_o)_{sr}$	1273.1	1601.7	2005.2	2541.3	3194.1	4027.2	5032.3	6379.6	8020.4
$(E_s/N_o)_{rd}/(E_s/N_o)_{sd}$	13.615	13.63	13.536	13.63	13.61	13.594	13.503	13.699	13.708
$(E_s/N_o)_{sr}/(E_s/N_o)_{sd}$	16.015	16.042	15.919	16.052	15.994	15.984	15.873	16.101	16.106

E/N(dB)	27	28	29	30					
$(E_s/N_o)_{rd}$	8590	10780	13666	17135					
$(E_s/N_o)_{sd}$	629.81	793.83	997.81	1262.1					
$(E_s/N_o)_{sr}$	10108	12703	16073	20166					
$(E_s/N_o)_{rd}/(E_s/N_o)_{sd}$	13.639	13.58	13.696	13.577					
$(E_s/N_o)_{sr}/(E_s/N_o)_{sd}$	16.05	16.003	16.109	15.979					

Table 3-11 Throughput gain (fixed power per user) with 8 modulation choices (BER 10-6)

Throughput gain for fixed power per user and asymmetric networks									
E/N(dB)	**0**	**1**	**2**	**3**	**4**	**5**	**6**	**7**	**8**
Cooperative	1.712	2.164	2.663	3.1973	4.421	5.083	5.811	6.554	7.297
Classical	5.0E-5	0.0007	0.004	0.0176	0.06005	0.145	0.3143	0.5873	0.98585
Thr_gain	34241	2884.5	664.74	180.66	72.622	34.055	17.489	10.16	6.4004
E/N(dB)	**9**	**10**	**11**	**12**	**13**	**14**	**15**	**16**	**17**
Cooperative	8.0847	8.856	9.659	10.488	11.333	12.156	12.967	13.78	14.584
Classical	1.5116	2.1773	2.9219	3.7475	4.7176	5.6671	6.7595	7.9019	9.1816
Thr_gain	4.3486	3.067	2.3057	1.7987	1.4022	1.145	0.91839	0.74381	0.58843
E/N(dB)	**18**	**19**	**20**	**21**	**22**	**23**	**24**	**25**	**26**
Cooperative	15.368	16.08	16.745	17.352	17.872	18.316	18.684	19.006	19.255
Classical	10.486	11.859	13.236	14.786	16.297	17.87	19.422	21.028	22.598
Thr_gain	0.4654	0.355	0.265	0.1735	0.0966	0.02495	-0.0380	-0.096	-0.1479
E/N(dB)	**27**	**28**	**29**	**30**					
Cooperative	19.459	19.60	19.722	19.812					
Classical	24.25	25.88	27.502	29.045					
Thr_gain	-0.197	-0.242	-0.282	-0.3178					

Similarly, Tables 3-12 and 3-13 show the average SNR on each link and the throughput gain, respectively, for the fixed-total-power case.

Table 3-12 SNR comparison (fixed total power) of two branches (8 modulation choices) (BER 10-6)

Fixed total power and asymmetric networks									
E/N (dB)	**0**	**1**	**2**	**3**	**4**	**5**	**6**	**7**	**8**
$(E_s/N_o)_{rd}$	6.8447	8.5034	10.756	13.543	17.241	21.554	26.948	34.198	42.87
$(E_s/N_o)_{sd}$	0.49926	0.62968	0.79698	0.99614	1.2573	1.5826	1.9782	2.513	3.1372
$(E_s/N_o)_{rd}/(E_s/N_o)_{sd}$	13.71	13.504	13.496	13.596	13.712	13.619	13.623	13.608	13.665
E/N (dB)	**9**	**10**	**11**	**12**	**13**	**14**	**15**	**16**	**17**
$(E_s/N_o)_{rd}$	53.774	67.959	85.335	107.83	136.31	169.83	216.83	268.5	342.07
$(E_s/N_o)_{sd}$	3.9866	5.0001	6.2862	7.9206	9.9487	12.546	15.841	19.871	25.079
$(E_s/N_o)_{rd}/(E_s/N_o)_{sd}$	13.489	13.591	13.575	13.614	13.701	13.536	13.688	13.512	13.639
E/N (dB)	**18**	**19**	**20**	**21**	**22**	**23**	**24**	**25**	**26**

$(E_s/N_o)_{rd}$	430.83	541.14	682.71	855.19	1076.8	1360	1706.6	2160.1	2682.8
$(E_s/N_o)_{sd}$	31.633	39.842	50.436	62.694	79.735	100.2	125.46	157.93	198.21
$(E_s/N_o)_{rd}/(E_s/N_o)_{sd}$	13.619	13.582	13.536	13.641	13.505	13.573	13.603	13.677	13.535
E/N (dB)	**27**	**28**	**29**	**30**					
$(E_s/N_o)_{rd}$	3428.2	4302.7	5439.4	6788.6					
$(E_s/N_o)_{sd}$	249.93	315.81	397.98	499.47					
$(E_s/N_o)_{rd}/(E_s/N_o)_{sd}$	13.717	13.624	13.668	13.592					

Table 3-13 Throughput gain (fixed total power) with 8 modulation choices (BER 10-6)

Throughput gain for fixed total power and asymmetric networks									
E/N(dB)	**0**	**1**	**2**	**3**	**4**	**5**	**6**	**7**	**8**
Cooperative	0.6373	0.9307	1.305	1.6991	2.152	2.6644	3.1925	3.7978	4.4215
Classical	5.E-5	0.0007	0.004	0.0176	0.06005	0.145	0.3143	0.5873	0.98585
Thr_gain	12741	1240	325.4	95.54	34.836	17.375	9.1576	5.4666	3.485
E/N(dB)	**9**	**10**	**11**	**12**	**13**	**14**	**15**	**16**	**17**
Cooperative	5.0973	5.8023	6.524	7.282	8.0641	8.8748	9.6662	10.469	11.294
Classical	1.5116	2.1773	2.921	3.7475	4.7176	5.6671	6.7595	7.9019	9.1816
Thr_gain	2.3722	1.6649	1.233	0.94315	0.70939	0.56602	0.43001	0.3249	0.23004
E/N(dB)	**18**	**19**	**20**	**21**	**22**	**23**	**24**	**25**	**26**
Cooperative	12.142	12.954	13.77	14.586	15.352	16.073	16.743	17.348	17.866
Classical	10.486	11.859	13.23	14.786	16.297	17.87	19.422	21.028	22.598
Thr_gain	0.1578	0.0922	0.040	-0.0135	-0.0580	-0.1005	-0.1379	-0.175	-0.2093
E/N(dB)	**27**	**28**	**29**	**30**					
Cooperative	18.31	18.695	19.00	19.26					
Classical	24.25	25.886	27.50	29.045					
Thr_gain	-0.24	-0.277	-0.30	-0.336					

3.3 Variable Relay Gain Case I

3.3.1 Simulation of Variable Gain Case I

The following simulation will simulate the cooperative diversity networks using the Amplify-and-Forward method. The relay gain in this case is adjustable and it is equal to the reciprocal of the fading coefficient of the s-r link. Therefore, this changeable relay gain tries to eliminate the fading effect from the source to the relay link. We will use the

following set of parameters in this simulation.

Channel bandwidth: 5 MHZ

Bit Error Rate: 10^{-3}

Relay gain: $1/|h_2|$

Modulation scheme: BPSK, QPSK, 8QAM, 16QAM, 32QAM and 64QAM

Number of samples: 600000

Transmission power: total fixed power, fixed power per user

Link property: asymmetric network

Path-loss exponent: 4

Simulation Results

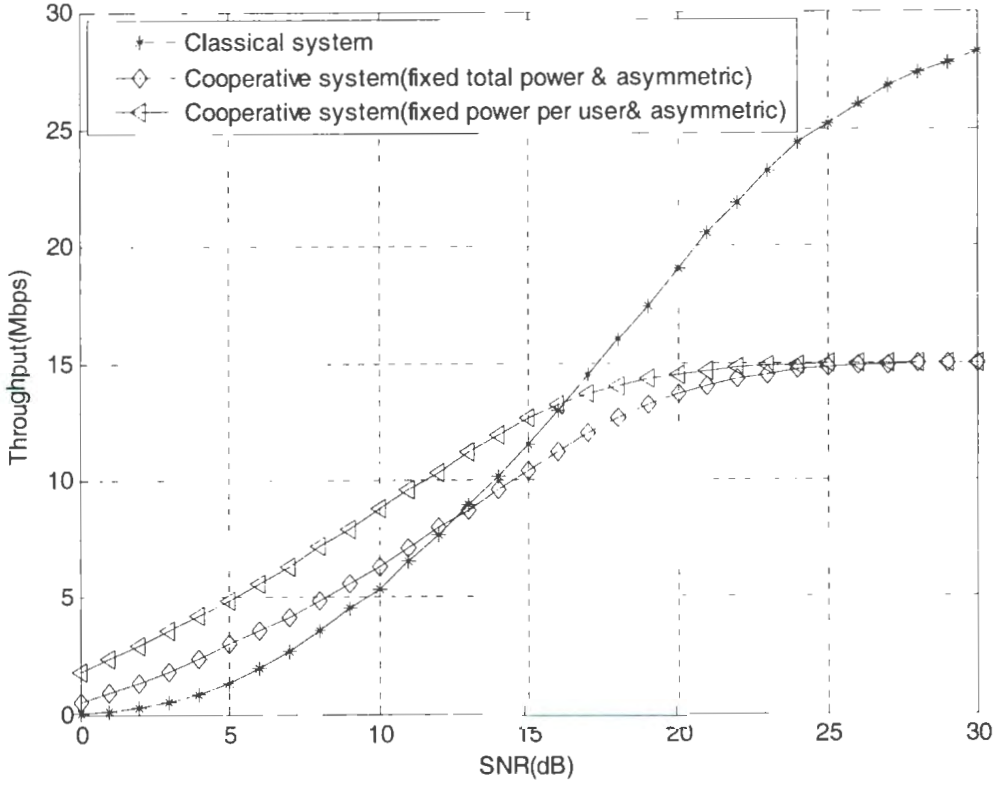

Figure 3-9 Throughput comparisons of simulation systems with variable relay gain I

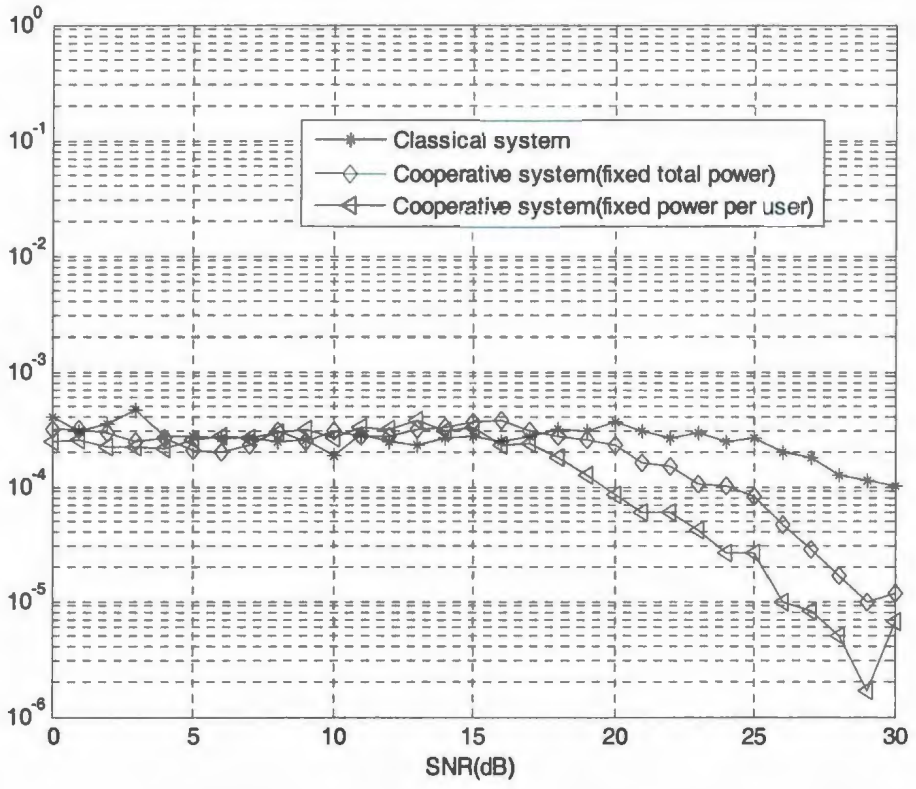

Figure 3-10 Performance of simulation systems with variable relay gain I

Figure 3-9 shows the throughput of three different cases, one for the classical communication system and the other two for the cooperative communication system. Figure 3-10 shows the BER results versus SNR for the classical communication system and the cooperative communication system with changeable relay gain. Based on the decision metric presented before, regardless of which modulation scheme is chosen in each frame transmission, the BER should be under threshold 10^{-3}.

From the above results, we can see that the BER curves of the three different systems are all under the target BER (10^{-3}). The throughput gain can be seen in the range from 0 dB to 13 dB for fixed total power case and from 0 dB to 16 dB for fixed-power-per-user case. The simulation results are exciting.

Table 3-14 shows the ratio of the average SNR in the indirect link to the average SNR in the direct link (E/N). Table 3-15 gives the accurate throughput gain in this simulation by giving the throughput of cooperative communication system and classical communication system. The throughput gain is calculated by following equation

$$Thr\_gain = \frac{ThroughputOfCooperativeSystem - ThroughputOfClassicalSystem}{ThroughputOfClassicalSystem} \times 100\% \quad (3.34)$$

Table 3-14 SNR comparisons (fixed power per user) of two branches (changeable gain)

Fixed power per user and asymmetric networks									
E/N(dB)	**0**	**1**	**2**	**3**	**4**	**5**	**6**	**7**	**8**
$(E_s/N_o)_{rd}$	4.99	5.0321	5.4768	5.5269	5.3973	5.2096	5.4682	4.9798	5.626
$(E_s/N_o)_{sd}$	0.98	1.0565	0.9875	0.9384	1.0751	1	1.0087	1.0067	1.0432
$(E_s/N_o)_{sr}$	15.7	15.119	16.436	16.034	15.288	15.842	16.088	15.306	17.241
$(E_s/N_o)_{rd}/(E_s/N_o)_{sd}$	5.08	4.7631	5.5461	5.8896	5.0203	5.2095	5.421	4.9466	5.3931
$(E_s/N_o)_{sr}/(E_s/N_o)_{sd}$	16.0	14.311	16.644	17.086	14.22	15.841	15.949	15.204	16.527
E/N(dB)	**9**	**10**	**11**	**12**	**13**	**14**	**15**	**16**	**17**
$(E_s/N_o)_{rd}$	5.11	6.458	6.7308	6.6817	6.7507	6.7496	6.6426	6.9486	6.4956
$(E_s/N_o)_{sd}$	0.93	1.2689	1.3341	1.3088	1.2913	1.2813	1.2332	1.2403	1.257
$(E_s/N_o)_{sr}$	16.3	19.763	20.798	19.925	20.623	20.231	19.958	20.661	20.17
$(E_s/N_o)_{rd}/(E_s/N_o)_{sd}$	5.48	5.0895	5.045	5.1051	5.2278	5.2676	5.3864	5.6023	5.1676
$(E_s/N_o)_{sr}/(E_s/N_o)_{sd}$	17.5	15.575	15.589	15.224	15.971	15.789	16.184	16.658	16.046
E/N(dB)	**18**	**19**	**20**	**21**	**22**	**23**	**24**	**25**	**26**
$(E_s/N_o)_{rd}$	7.06	6.9222	8.6433	8.1645	8.5607	8.072	8.8061	8.634	8.0993
$(E_s/N_o)_{sd}$	1.27	1.2742	1.6344	1.5418	1.5827	1.6161	1.6132	1.5619	1.6256
$(E_s/N_o)_{sr}$	20.6	20.76	25.366	23.632	24.968	24.148	26.101	26.135	24.307
$(E_s/N_o)_{rd}/(E_s/N_o)_{sd}$	5.53	5.4327	5.2885	5.2954	5.4089	4.9947	5.4587	5.5279	4.9824
$(E_s/N_o)_{sr}/(E_s/N_o)_{sd}$	16.1	16.293	15.521	15.327	15.776	14.942	16.179	16.733	14.953
E/N(dB)	**27**	**28**	**30**	**31**					
$(E_s/N_o)_{rd}$	8.38	8.119	8.5862	10.304					
$(E_s/N_o)_{sd}$	1.56	1.5354	1.5501	2.0096					
$(E_s/N_o)_{sr}$	23.9	26.171	24.645	31.147					
$(E_s/N_o)_{rd}/(E_s/N_o)_{sd}$	5.36	5.2879	5.539	5.1277					
$(E_s/N_o)_{sr}/(E_s/N_o)_{sd}$	15.3	17.045	15.899	15.499					

Table 3-15 Throughput gain (fixed power per user) of adaptive modulation (changeable gain)

Throughput gain for fixed power per user and asymmetric networks									
E/N(dB)	**0**	**1**	**2**	**3**	**4**	**5**	**6**	**7**	**8**
Cooper	1.820	2.405	2.947	3.5718	4.1857	4.891	5.5883	6.3368	7.1448
Classical	0.040	0.1125	0.27	0.5425	0.8675	1.3145	1.9685	2.6795	3.532
Thr(%)	4395	2037.8	991.48	558.39	382.51	272.08	183.88	136.49	102.29
E/N(dB)	**9**	**10**	**11**	**12**	**13**	**14**	**15**	**16**	**17**
Cooper	7.927	8.7585	9.6105	10.332	11.165	11.947	12.628	13.2	13.665
Classical	4.518	5.344	6.5055	7.628	8.911	10.165	11.481	12.989	14.515
Thr(%)	75.45	63.894	47.729	35.452	25.292	17.532	9.9904	1.6264	-5.856
E/N(dB)	**18**	**19**	**20**	**21**	**22**	**23**	**24**	**25**	**26**
Cooper	14.01	14.313	14.506	14.678	14.782	14.84	14.898	14.938	14.959
Classical	16	17.425	19.023	20.535	21.822	23.252	24.415	25.249	25.995
Thr(%)	-12.3	-17.857	-23.744	-28.526	-32.262	-36.176	-38.98	-40.838	-42.451
E/N(dB)	**27**	**28**	**29**	**30**					
Cooper	14.97	14.985	14.991	14.992					
Classical	26.79	27.401	27.829	28.297					
Thr(%)	-44.0	-45.312	-46.133	-47.018					

Similarly, Table 3-16 and 3-17 show the average SNR on each link and the throughput gain, respectively, for the fixed total power case.

Table 3-16 SNR comparisons (fixed total power) of two branches (changeable relay gain)

Fixed total power and asymmetric networks									
E/N(dB)	**0**	**1**	**2**	**3**	**4**	**5**	**6**	**7**	**8**
$(E_s/N_o)_{rd}$	2.7116	2.615	2.7393	2.6619	2.5972	2.5563	2.4793	2.5955	2.6291
$(E_s/N_o)_{sd}$	0.49168	0.47706	0.49648	0.48088	0.51731	0.47452	0.49187	0.51184	0.47876
$(E_s/N_o)_{rd}$ $/(E_s/N_o)_{sd}$	5.515	5.4814	5.5176	5.5356	5.0206	5.3871	5.0405	5.071	5.4915
E/N(dB)	**9**	**10**	**11**	**12**	**13**	**14**	**15**	**16**	**17**
$(E_s/N_o)_{rd}$	2.5834	3.4297	3.2425	3.3246	3.2794	3.4696	3.3461	3.5232	3.4456
$(E_s/N_o)_{sd}$	0.5171	0.62989	0.59695	0.60982	0.63823	0.63005	0.62997	0.63253	0.60766
$(E_s/N_o)_{rd}$ $/(E_s/N_o)_{sd}$	4.996	5.4449	5.4317	5.4518	5.1382	5.5069	5.3115	5.57	5.6703
E/N(dB)	**18**	**19**	**20**	**21**	**22**	**23**	**24**	**25**	**26**
$(E_s/N_o)_{rd}$	3.1417	3.3917	4.2737	4.2522	4.3021	4.0956	4.1453	4.0009	4.2077
$(E_s/N_o)_{sd}$	0.63812	0.61277	0.84247	0.83853	0.76433	0.78051	0.78609	0.79875	0.83102
$(E_s/N_o)_{rd}$ $/(E_s/N_o)_{sd}$	4.9235	5.535	5.0728	5.071	5.6286	5.2473	5.2734	5.009	5.0633
E/N(dB)	**27**	**28**	**29**	**30**					
$(E_s/N_o)_{rd}$	4.2604	3.932	4.0684	5.1944					
$(E_s/N_o)_{sd}$	0.79719	0.771	0.73473	0.98633					
$(E_s/N_o)_{rd}$ $/(E_s/N_o)_{sd}$	5.3442	5.0998	5.5373	5.2664					

Table 3-17 Throughput gain (fixed total power) of adaptive modulation (changeable relay gain)

Throughput gain for fixed total power and asymmetric networks									
E/N(dB)	**0**	**1**	**2**	**3**	**4**	**5**	**6**	**7**	**8**
Cooperative	0.5465	0.9055	1.3018	1.8413	2.365	2.9807	3.5365	4.1668	4.8578
Classical	0.0405	0.1125	0.27	0.5425	0.8675	1.3145	1.9685	2.6795	3.532
Diff(%)	1249.4	704.89	382.13	239.4	172.62	126.76	79.655	55.505	37.535
E/N(dB)	**9**	**10**	**11**	**12**	**13**	**14**	**15**	**16**	**17**
Cooperative	5.5535	6.2913	7.138	7.9675	8.7402	9.6155	10.422	11.177	11.957
Classical	4.5185	5.344	6.5055	7.628	8.911	10.165	11.481	12.989	14.515
Diff(%)	22.906	17.725	9.7225	4.4507	-1.9162	-5.4012	-9.2261	-13.945	-17.627
E/N(dB)	**18**	**19**	**20**	**21**	**22**	**23**	**24**	**25**	**26**
Cooperative	12.599	13.191	13.654	14.023	14.306	14.506	14.683	14.783	14.84
Classical	16	17.425	19.023	20.535	21.822	23.252	24.415	25.249	25.995
Diff(%)	-21.256	-24.297	-28.226	-31.712	-34.443	-37.616	-39.863	-41.449	-42.911
E/N(dB)	**27**	**28**	**29**	**30**					
Cooperative	14.913	14.946	14.957	14.97					
Classical	26.791	27.401	27.829	28.297					
Diff(%)	-44.338	-45.456	-46.253	-47.097					

3.3.2 Analytical Evaluation of Dynamic Gain Case I

In the previous simulation process, the throughput of the cooperative network with one relay node is derived in the variable gain I case. This part verifies the correctness of preceding simulation results through analytical approach.

Let relay gain α be $1/|h_2|$ in variable gain I case, then Equation (3.26) is transformed to the following equation.

$$\gamma_{indirect} = \frac{\frac{|h_2|^2 E}{N}\frac{|h_3|^2 E}{N}}{\frac{|h_3|^2 E}{N}+\frac{|h_2|^2 E}{N}} = \frac{\gamma_2\gamma_3}{\gamma_2+\gamma_3}, \tag{3.35}$$

According to [13], the indirect PDF with changeable gain has the following form.

$$f_{Indirect}(\gamma) = \frac{2\gamma e^{-\gamma\left(\frac{1}{\gamma_2+\gamma_3}\right)}}{\overline{\gamma_2\gamma_3}}\left[\left(\frac{\overline{\gamma_2}+\overline{\gamma_3}}{\sqrt{\overline{\gamma_2\gamma_3}}}\right)K_1\left(\frac{2\gamma}{\sqrt{\overline{\gamma_2\gamma_3}}}\right)+2K_0\left(\frac{2\gamma}{\sqrt{\overline{\gamma_2\gamma_3}}}\right)\right]U(\gamma), \tag{3.36}$$

where $\overline{\gamma_2} = 2\sigma_2^2(E/N)$, $\overline{\gamma_3} = 2\sigma_3^2(E/N)$, $K_0()$ and $K_1()$ are the zero-order modified Bessel function and first-order modified Bessel function of second kind.

Up to this point, the PDF of direct branch and indirect branch are derived, next we will combine them together and find the PDF of the combined SNR. As we know, the received SNR after the maximal ratio combining is the sum of two individual SNR from two branches.

$$\gamma_{combined} = \gamma_1 + \gamma_{indirect} \tag{3.37}$$

According to the probability theory, the distribution of a sum of two independent random variables is the convolution of these two distributions. Hence, the PDF of the total SNR can be derived by numerical convolution.

$$f_{\gamma_{combined}}(\gamma) = f_{\gamma_1}(\gamma) * f_{\gamma_{indirect}}(\gamma) \tag{3.38}$$

where $*$ is the convolution operation

Once the PDF of the total SNR is found, the previous throughput calculation Equations (3.17) and (3.18) based on the PDF of the total SNR can be applied to derive the theoretical throughput of such system.

Analytical results

As seen from the Figure 3-11, the analytical results derived from the above analysis completely overlap with the simulation results. Therefore, the simulation results are proved to be correct. Also, the cooperative diversity network using adaptive modulation with changeable relay gain can provide great throughput gain compared with the classical system.

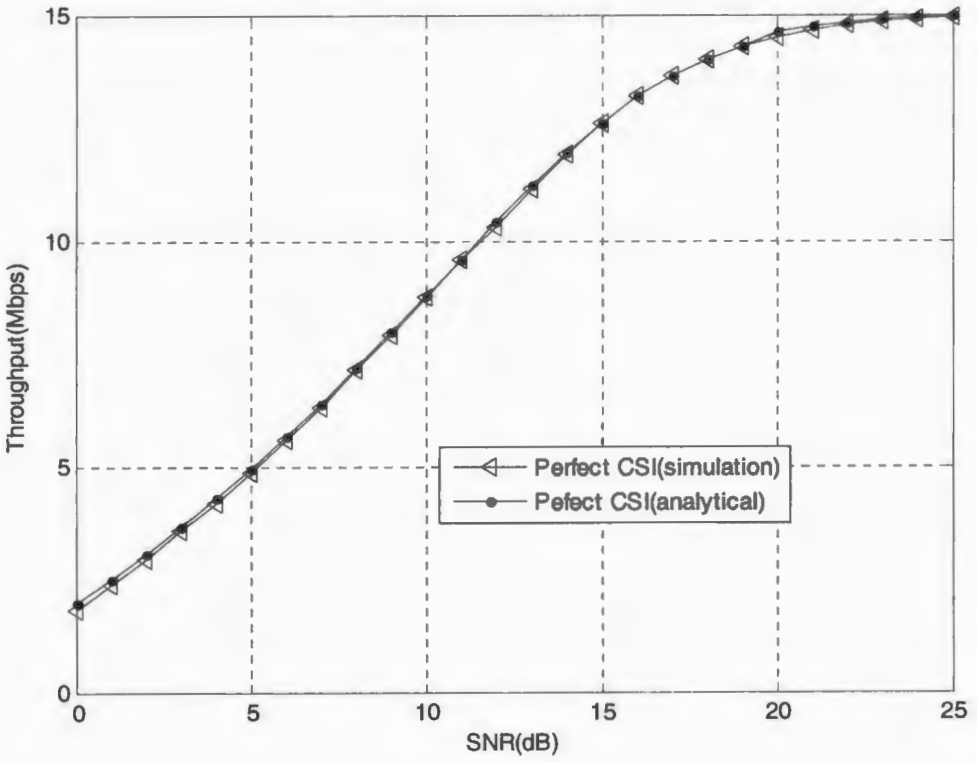

Figure 3-11 Analytical results of cooperative networks with variable relay gain I

3.4 Variable Relay Gain Case II

3.4.1 Simulation of Variable Gain Case II

The objective of this part is to simulate the cooperative diversity network using the variable relay gain II in the relay terminal. The relay gain in this case is still dynamic, but with different value from the previous section. The purpose of this new relay gain is to maintain the constant average power output, which is equal to the transmitting power [10]. The following set of parameters is used in this simulation.

Channel bandwidth: 5 MHZ

Bit Error Rate: 10^{-3}

Relay gain: $\sqrt{\frac{E}{N + E|h_2|^2}}$

Modulation scheme: BPSK, QPSK, 8QAM, 16QAM, 32QAM and 64QAM

Number of samples: 600000

Transmission power: total fixed power, fixed power per user

Link property: asymmetric network

Path-loss exponent: 4

Simulation Results

In Figure 3-12, the fixed-power-per-user case of cooperative diversity network is able to provide as much throughput gain as the previous reciprocal gain case. In addition, the BER performance is always below the preset target BER 10^{-3} in Figure 3-13.

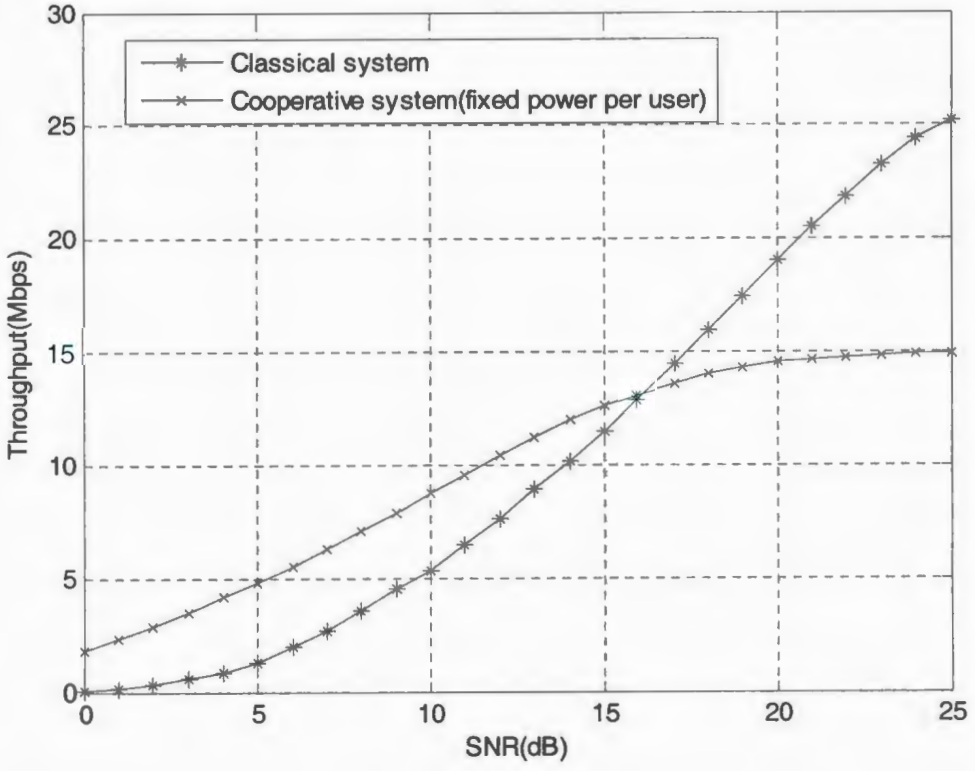

Figure 3-12 Throughput comparisons of simulation systems with variable relay gain II

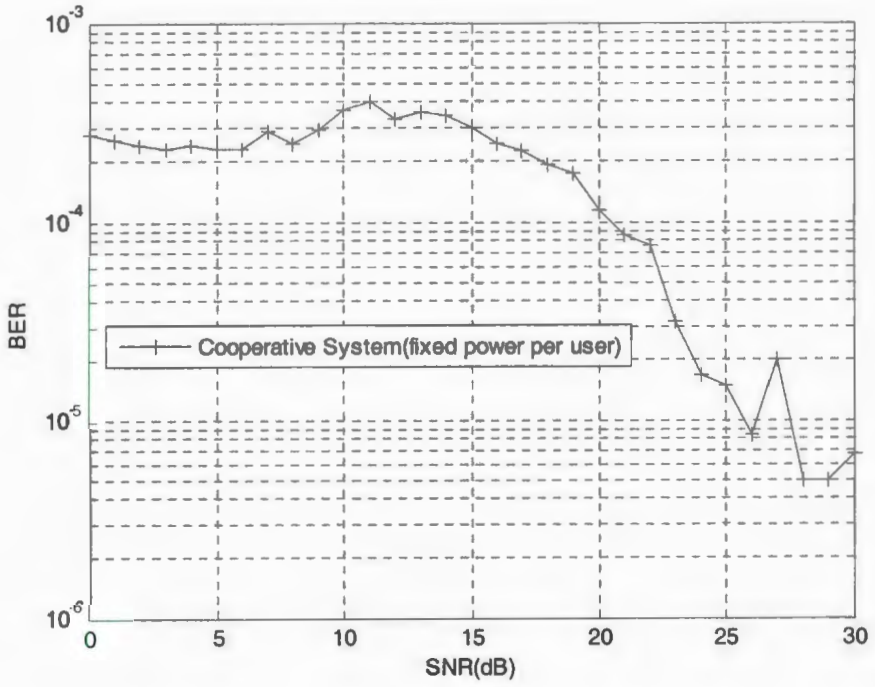

Figure 3-13 BER performance of simulation system with variable relay gain II

3.4.1 Analytical Evaluation of Variable Gain case II

The proof of this part is the same as the previous one in the spectral calculation and throughput calculation. But the probability density function of the received SNR is different due to the different gain. Therefore, the major work in this part is to find the new PDF and then use the same method to find the average throughput. The new gain can be represented as follows:

$$A = \sqrt{\frac{E}{N + E|h_2|^2}}, \tag{3.39}$$

For the indirect branch, the SNR can be represented as

$$\gamma_{Indirect} = \frac{\gamma_2 \gamma_3}{\gamma_2 + \gamma_3 + 1}, \tag{3.40}$$

A very tight upper bound of $\gamma_{Indirect}$ is given by [15]

$$\gamma_{IndirectApproximate} = \min(\gamma_{SR}, \gamma_{RD}), \tag{3.41}$$

The PDF of the $\gamma_{IndirectApproximate}$ can be given by

$$f_{\gamma}(\gamma_{in}) = \frac{1}{\bar{\gamma}}\exp(-\frac{\gamma_{in}}{\bar{\gamma}}) \text{ where } \bar{\gamma} = (\bar{\gamma}_2\bar{\gamma}_3)/(\bar{\gamma}_2 + \bar{\gamma}_3) \text{ and } \bar{\gamma}_2 = \frac{2\sigma_2^2 E}{N}, \bar{\gamma}_3 = \frac{2\sigma_3^2 E}{N} \tag{3.42}$$

For the direct branch, the exponential PDF is used as in the previous section

$$f_{\gamma_1}(\gamma_1) = \frac{1}{\bar{\gamma}_1}\exp(-\frac{\gamma_1}{\bar{\gamma}_1}) \text{ where } \bar{\gamma}_1 = \frac{2\sigma_1^2 E}{N} \tag{3.43}$$

Similarly, the combined total SNR can be calculated as the following equation.

$$\gamma_t = \gamma_{IndirectApproximate} + \gamma_1 \tag{3.44}$$

The PDF of the combined total SNR

$$f(\gamma_t) = f(\gamma_{IndirectApproximate}) * f(\gamma_1) \tag{3.45}$$

This convolution can be solved by using the following integral

$$\begin{aligned}
f(\gamma_t) &= \int_0^{\gamma_t} f_{\gamma_{in}}(\tau) f_{\gamma_1}(\gamma_t - \tau) d\tau \\
&= \int_0^{\gamma_t} \frac{1}{\bar{\gamma}}\exp(-\frac{\tau}{\bar{\gamma}})\frac{1}{\bar{\gamma}_1}\exp(-\frac{\gamma_t - \tau}{\bar{\gamma}_1}) d\tau \\
&= \frac{1}{\bar{\gamma}\bar{\gamma}_1}\exp(-\frac{\gamma_t}{\bar{\gamma}_1})\int_0^{\gamma_t}\exp(-\tau(1/\bar{\gamma} - 1/\bar{\gamma}_1)) d\tau \\
&= \frac{1}{\bar{\gamma}\bar{\gamma}_1}\exp(-\frac{\gamma_t}{\bar{\gamma}_1})\left[\frac{-\exp(-\tau(1/\bar{\gamma} - 1/\bar{\gamma}_1))}{(1/\bar{\gamma} - 1/\bar{\gamma}_1)}\right]_0^{\gamma_t} \\
&= \frac{1}{\bar{\gamma}\bar{\gamma}_1}\exp(-\frac{\gamma_t}{\bar{\gamma}_1})\left[\frac{1 - \exp(-\gamma_t(1/\bar{\gamma} - 1/\bar{\gamma}_1))}{(1/\bar{\gamma} - 1/\bar{\gamma}_1)}\right]
\end{aligned} \tag{3.46}$$

Similar to the previous case, the PDF derived here can be used to find the analytical throughput.

Analytical Results

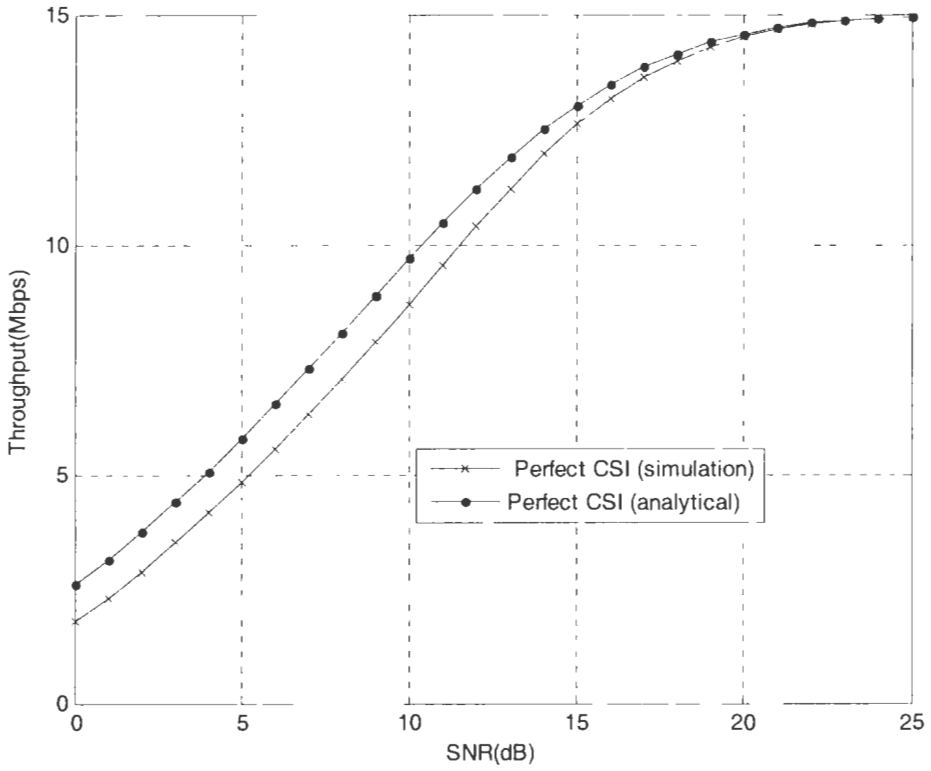

Figure 3-14 Analytical throughput with variable relay gain II

As seen in Figure 3-14, there is a gap between analytical results and the simulation result between 0 and 15dB. But the gap closes as the SNR increases. Actually, this difference is caused by the approximate PDF of the indirect branch since this approximation is accurate only when the SNR is fairly large.

3.5 Adaptive Modulation for Multiple Relays

3.5.1 Multiple Relays Model

As shown in the single-relay case, the results of the cooperative network are impressive. In this section, the number of relays will be changed from one to two or even more. As

shown in Figure 3-15, the locations of all relays are distributed along the dashed central line and the distance between two adjacent relays is one tenth of the distance between source and destination terminals. Therefore, the path loss on each relay link can be determined based on the distance between the relay and the source or the destination terminal.

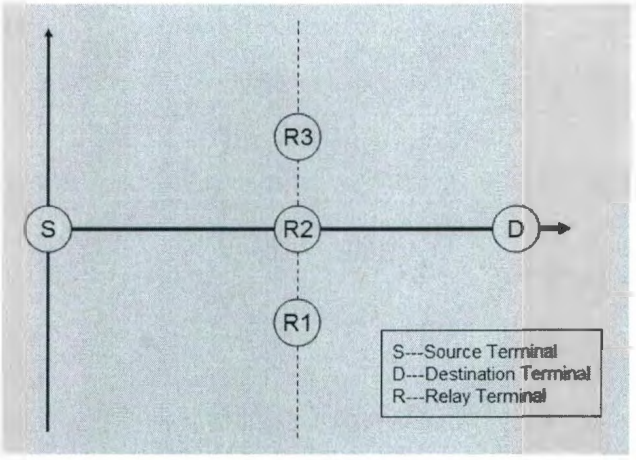

Figure 3-15 Locations of multiple relays

The model of multiple relays is more complicated than the one-relay case, which is shown in Figure 3-16. But it is very easy to interpret with the knowledge of the previous one- relay model. The only difference is that extra relay branches are added due to the extra relays. By doing this, we can see that each relay terminal corresponds to an independent message transmission.

Figure 3-16 shows the detailed multiple-relay cooperative diversity networks. In this model, $h_{i,j}$ is the Rayleigh fading coefficient on the ith branch and index j can choose either the channel from the source to relay the relay to destination, $n_{i,j}$ is the AWGN noise on the corresponding channel, and R_n represents the relay index to show a particular relay. The Rayleigh fading coefficient and AWGN noise of the direct branch are denoted

by h_1 and n_1.

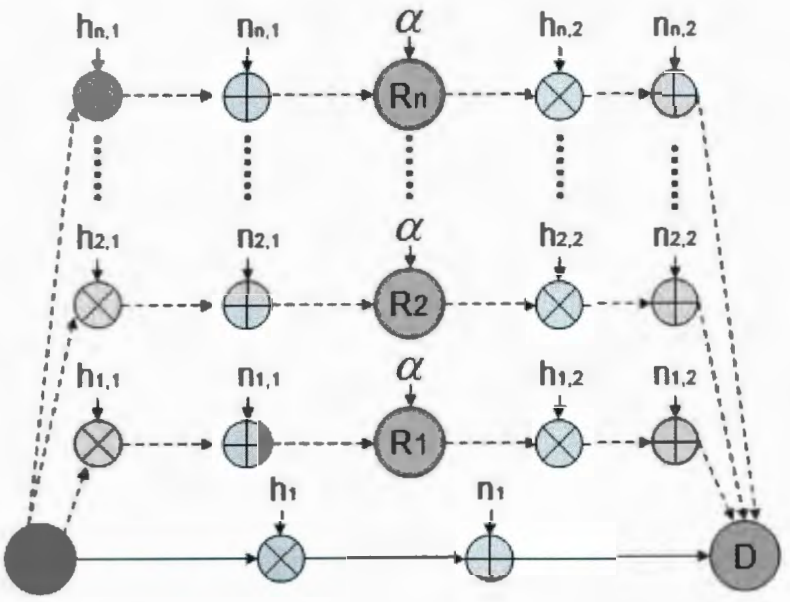

Figure 3-16 Cooperative diversity network with multiple relays

In cooperative diversity networks with multiple relays, the destination terminal will have multiple copies of the same signal from independent paths. To properly combine these copies of signal into a single one, the same MRC technique as in the single relay case is used. As a result, the total SNR at the destination is the sum of SNR of each link. Since the direct and the indirect branches in multiple relay case is the same as these in single relay case, the combining weights are set in the similar way. The combining weight for the direct branch is

$$\beta = \frac{h_1^*}{N} \tag{3.47}$$

where h_1^* is the conjugate of h_1 , N is the noise power, while the weight for the nth indirect branch is

$$\beta_n = \frac{\alpha h_{n,1}^{*} h_{n,2}^{*}}{\left(1+\alpha^2 \left|h_{n,2}\right|^2\right) N} \tag{3.48}$$

where $h^*_{n,1}$ and $h^*_{n,2}$ are the conjugates of $h_{n,1}$ and $h_{n,2}$. The received signal at the output of MRC should be

$$R(t) = \beta R_{sd} + \sum_{k=1}^{n} \beta_k R_{srd}(k) \tag{3.49}$$

The weight calculation in Equation (3.47) and (3.48) requires the channel state information, which can be provided by using channel estimation.

We assume that all terminals have perfect knowledge of the channels state. Hence, the source terminal can easily predict the total received SNR at the destination terminal as follows.

$$SNR_{total} = SNR_{sd} + \sum_{k=1}^{n} SNR_{srd}(k) \tag{8}$$

where the SNR_{sd} is the SNR on the direct branch and $SNR_{srd}(k)$ is the SNR on the kth indirect branch.

Moreover, the cooperating sequence is different from the one relay case. Two options are offered for multiple relays. First, all relays will send the received message from the source to the destination sequentially, which means that the more the relays used the more time slot lost. Second, all relays send the information back to the destination at the same time slot needed, which requires the destination to receive multiple copies from multiple relays simultaneously. Although this is possible, it puts constraints on the

hardware because of the co-phase transmission requirement. Obviously, since just one slot time is wasted, the throughput gain must increase as the relay number increases in this case.

3.5.2 Multiple Relays with Simultaneous Reception Simulation

In this case, we simulate the multiple relays' situation with simultaneous receptions. All relays send back the received message from the source to the destination simultaneously. We use the following set of parameters in this simulation.

Channel bandwidth: 5 MHZ

Bit Error Rate: 10^{-3}

Distance from the source to destination: d

Inter-relay distance: d/10 (d is the distance between the source and the destination)

Cooperative method: one slot time loss

Modulation levels: BPSK, 4QAM, 8QAM, 16QAM, 32QAM, 64QAM, 128QAM and 256QAM

Relay gain: 1

Number of samples: 8400000

Transmission power: fixed power per user

Link property: asymmetric network

Path-loss exponent: 4

Simulation Results

Figure 3-17 shows the throughput of the cooperative communication system with different number of relays. The BER results versus the SNR of each system will also be

shown in Figure 3-18. This simulation considers the number of relays from one to six. Besides, the one relay curve and classical communication curve shown in this figure are derived from the previous simulation. Hence, the BER versus SNR curves for these two cases are not shown.

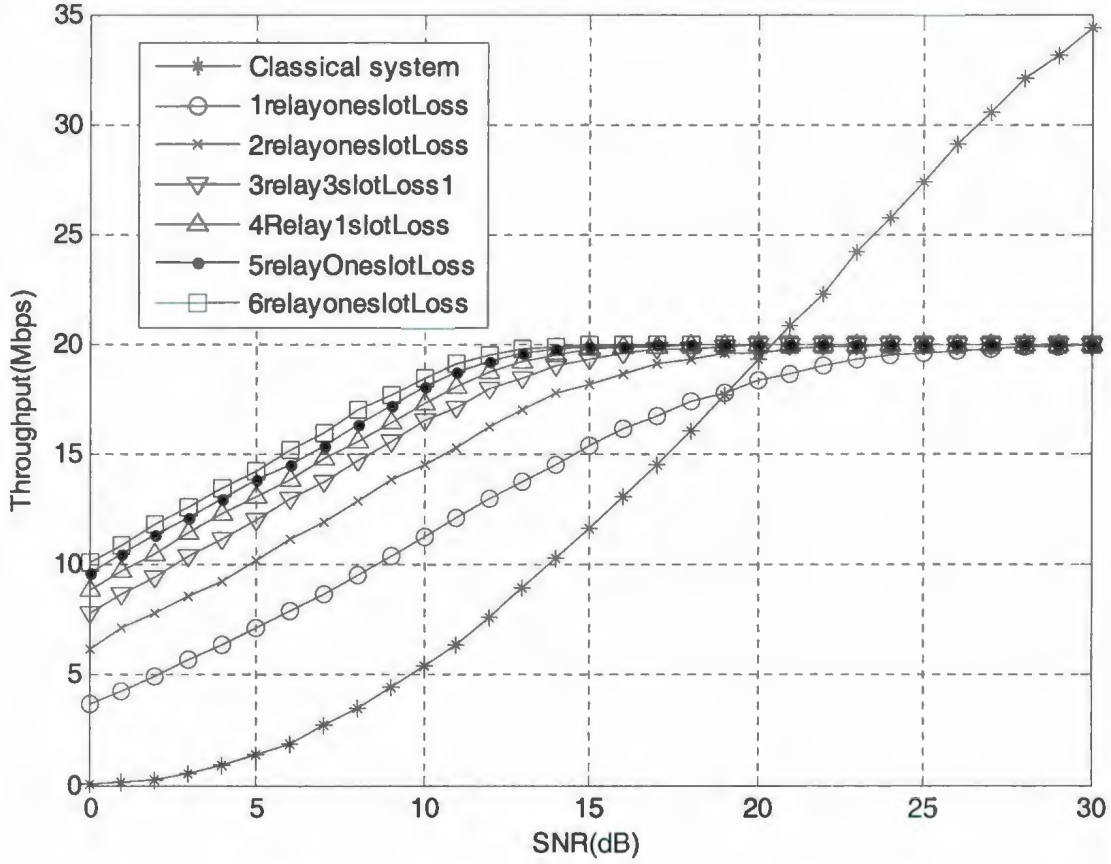

Figure 3-17 Throughput comparisons with multiple relays and one slot loss

As expected before, the throughput gain is continuously increasing if all relays send the received message to the destination simultaneously. However, the throughput does not increase too much when the number of relays is larger than three.

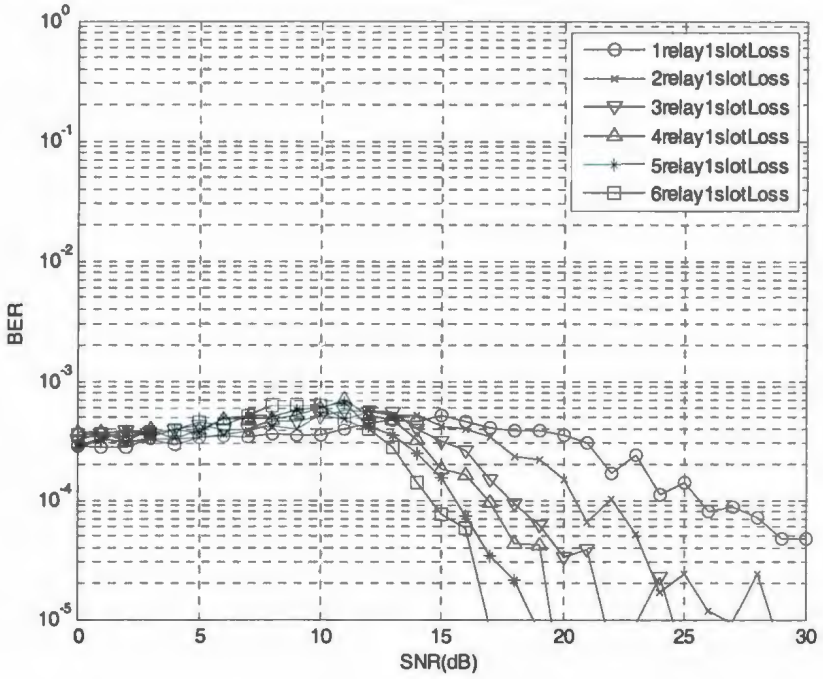

Figure 3-18 BER Performance of with multiple relays and one slot loss

3.5.3 Multiple Relay Simulation with Sequential Reception Simulation

In this case, the sequential cooperating method is used in cooperative communication systems with multiple relays. We use the following set of parameters in this simulation.

Channel bandwidth: 5 MHZ

Bit Error Rate: 10^{-3}

Distance from the source to destination: d

Inter-relay distance: d/10

Cooperating method: time slot loss = relay number

Modulation levels: BPSK, 4QAM, 8QAM, 16QAM, 32QAM, 64QAM, 128QAM and 256QAM

Number of samples: 8400000

Relay gain: 1

Transmission power: fixed power per user

Link property: asymmetric network

Path loss exponent: 4

Simulation Results

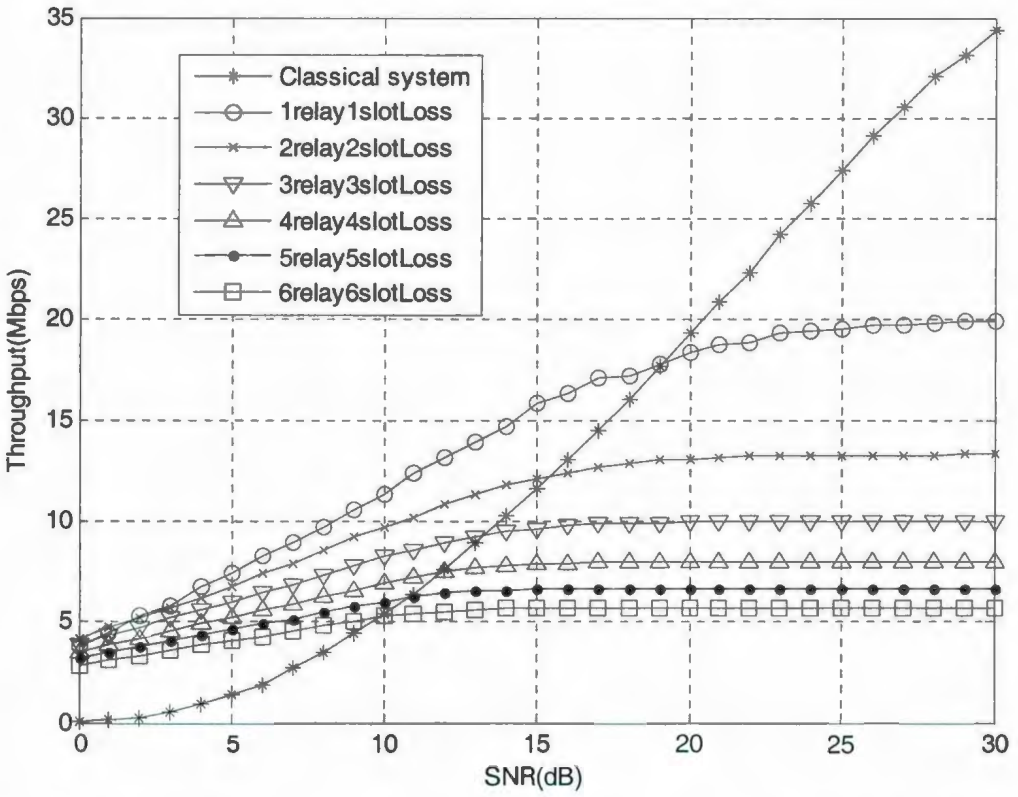

Figure 3-19 Throughput comparisons with multiple relays and multiple time slot loss

From the above throughput results in Figure 3-19, it is clear that the use of multiple relays reduces the throughput gain when sequential reception is adopted. For example, two thirds of time resources are lost in the two-relay case due to two slot relaying of each transmission; however, the increase in SNR is just 3 dB compared to one relay case, which has half time resource loss. It is impossible for this 3dB increase in SNR to compensate for almost 17% (66.7%-50%) time loss. As a result, for this case, the

optimum number of relay is one. In addition, the BER results are shown in Figure 3-20. Obviously, the target BER 10^{-3} is satisfied in all cases.

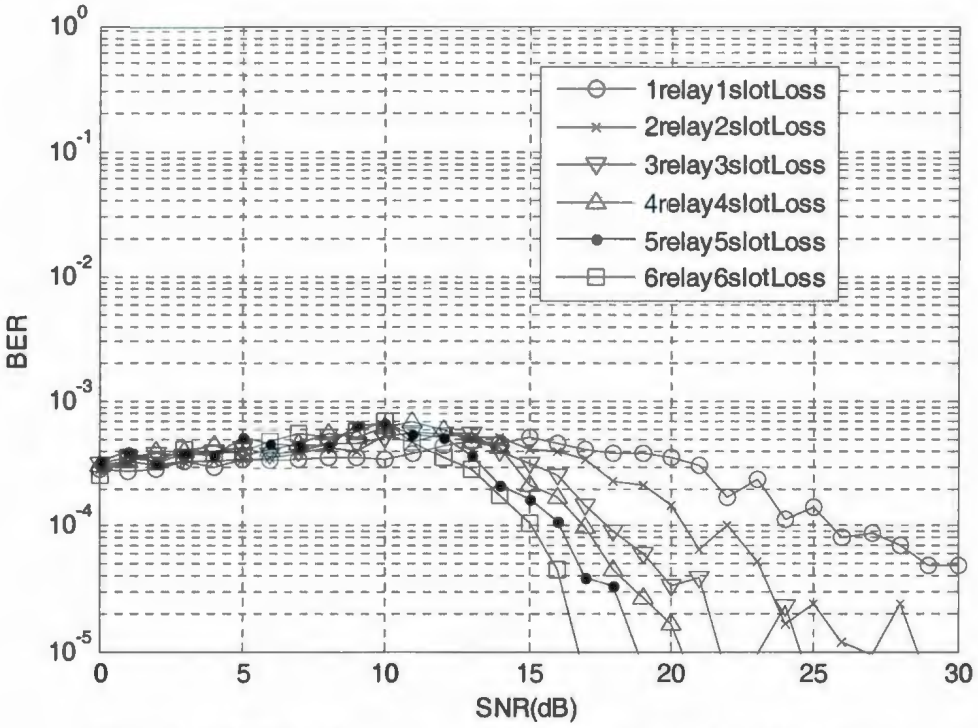

Figure 3-20 BER Performance with multiple relays and multiple time slot loss

Chapter 4

Cooperative Diversity Networks using Adaptive Modulation under Imperfect CSI

Cooperative diversity networks using adaptive modulation under Perfect CSI is capable of offering remarkable throughput gain, as shown in Chapter 3. However, this extraordinary enhancement on the throughput of cooperative diversity networks is based on the assumption that the CSI is perfectly known by all the terminals.

In the real world, there is no such means that can provide the terminals with perfect CSI. However, the estimation techniques can obtain the CSI with a certain degree of accuracy. In previous chapter (Equation (2.17)), the channel coefficients are used to generate the branch weights for MRC. Therefore, the error in channel coefficients will cause the error in branch weights in MRC. As a result, the total received signal at the output of MRC is affected by the branch weights error in both the amplitude and phase. Eventually, the error in channel coefficients will degrade the performance of the cooperative diversity network. An interesting question is how much throughput gain can be still maintained by the cooperative diversity network under imperfect CSI condition compared to that under perfect CSI condition.

In this chapter, we first introduce the mechanism of channel estimation and several channel estimators. After that, these channel estimators are applied to the cooperative diversity network and the simulation results are given. A general estimation error model

is given to generalize the various estimation techniques. Then, this general error model is used to simulate the cooperative diversity network in different relay gain cases. Furthermore, the analytical results are presented to prove the simulation results in each relay gain case.

4.1 Channel Estimation

In wireless communication, the channel estimation is essential to estimate the amplitude and the phase of the time-variant wireless channel. The coherent reception and the weighted combining of multiple received signals are based on the knowledge of CSI. The pilot aided estimation scheme is adopted in this thesis to estimate the channel coefficients. Just as its name indicates, a pilot sequence of symbols, which is known by the transmitter and receiver in advance, is transmitted from the transmitter to the receiver through the wireless channel. By doing this, the received pilot sequence at the receiver will carry the current CSI. Eventually, this CSI is extracted by using some channel estimators.

The transmission of each pilot symbol can be modeled by the following equation:

$$r_i = h_i s_i + n_i, \tag{4.1}$$

where s_i is the ith transmitted pilot symbol, h_i is the fading coefficient of this pilot symbol, n_i is the AWGN noise and r_i the ith received pilot symbol.

Suppose a pilot sequence length of 4 is used, the transmission of whole pilot sequence can be expressed by the following matrix,

$$\begin{bmatrix} r_1 \\ r_2 \\ r_3 \\ r_4 \end{bmatrix} = \begin{bmatrix} h_1 & 0 & 0 & 0 \\ 0 & h_2 & 0 & 0 \\ 0 & 0 & h_3 & 0 \\ 0 & 0 & 0 & h_4 \end{bmatrix} \begin{bmatrix} s_1 \\ s_2 \\ s_3 \\ s_4 \end{bmatrix} + \begin{bmatrix} n_1 \\ n_2 \\ n_3 \\ n_4 \end{bmatrix}. \tag{4.2}$$

Another equivalent matrix representation can be written as following:

$$\begin{bmatrix} r_1 \\ r_2 \\ r_3 \\ r_4 \end{bmatrix} = \begin{bmatrix} s_1 & 0 & 0 & 0 \\ 0 & s_2 & 0 & 0 \\ 0 & 0 & s_3 & 0 \\ 0 & 0 & 0 & s_4 \end{bmatrix} \begin{bmatrix} h_1 \\ h_2 \\ h_3 \\ h_4 \end{bmatrix} + \begin{bmatrix} n_1 \\ n_2 \\ n_3 \\ n_4 \end{bmatrix}. \tag{4.3}$$

This representation highlights the relationship among these parameters since our purpose using estimation technique is to estimate the unknown parameter h_i based on r_i and s_i known by receiver. By using vector notation, r_i, s_i, h_i and n_i matrix can be denoted as R, S, H and N, respectively. Therefore, the vector expression of pilot aided estimation model is derived as

$$R = SH + N. \tag{4.4}$$

4.2 Channel Estimators

4.2.1 Minimum Variance Unbiased (MVU) Estimator [17]

If the observed data has the model as

$$R = SH + N, \tag{4.5}$$

where R is an $N \times 1$ vector of observations, S is a known $N \times P$ observation matrix (with $N > P$) and rank P, H is a $P \times 1$ vector of parameters to be estimated, and N is an $N \times 1$ noise vector with PDF $N(0, \sigma^2 I)$, then the MVU estimator is

$$\hat{H} = (S^T S)^{-1} S^T R, \tag{4.6}$$

where $\hat{H}$ is the estimated vector of H.

4.2.2 Minimum Mean Square Error (MMSE) Estimator

Bayesian Linear Model [17]

$$R = SH + N, \tag{4.7}$$

where H is a P×1 random vector with prior PDF $N(\mu_H, C_H)$, and N is an $N \times 1$ noise vector with PDF $N(0, C_N)$ and independent of H. Then, this model is called the Bayesian general linear model. It differs from the classical general linear model in that H is modeled as a random variable with a Gaussian prior PDF.

The mean of Posterior PDF for the Bayesian General Linear Model is [17]

$$E(H \mid R) = \mu_H + C_H S^T (SC_H S^T + C_N)^{-1}(R - S\mu_H), \tag{4.8}$$

and covariance [17]

$$C_{H|R} = C_H - C_H S^T (SC_H S^T + C_N)^{-1} SC_H, \tag{4.9}$$

Assume the random variables with prior PDF

$$H \sim N(0, \sigma_\theta^2 I)$$

The following parameters can be rewritten like following: [17]

$u_H = 0$, $\quad C_H = \sigma_H^2 I$, $\quad C_N = \sigma^2 I$

Then, equation (4.8) and (4.9) can be simplified, the MMSE estimator can be written as following: [17]

$$\hat{H} = E(H \mid R) = \sigma_H^2 S^T (S\sigma_H^2 S^T + \sigma^2 I)^{-1} R, \tag{4.10}$$

$$C_{\theta|x} = \sigma_\theta^2 I - \sigma_\theta^2 H^T (H\sigma_\theta^2 H^T + \sigma^2 I)^{-1} H\sigma_\theta^2. \tag{4.11}$$

4.2.3 Correlation Estimator [10]

A known pilot sequence with K symbols is sent out from the transmitter to the receiver

one by one. Let's assume the fading coefficient h never change in the whole pilot sequence transmission. At the reception of each pilot symbol, the receiver uses the conjugate of the same pilot symbol to multiply the received pilot symbol which experiences fading and noise in the wireless channel. This can be shown in the equation as follows:

$$(hs_i + n_i) \times s_i^* = |s_i|^2 h + s_i^* n_i, \tag{4.12}$$

After the successful reception of the whole pilot sequence at the receiver, the estimated channel fading coefficient can be obtained by adding up the whole received pilot sequence and then normalized the symbol power. The resultant correlation estimator is given by [10]

$$\hat{H} = \frac{1}{\sigma_s^2}\left[\sum_{i=1}^{K} \frac{|s_i|^2 h}{K} + \sum_{k=1}^{K} \frac{s_i^* n_i}{K}\right] \tag{4.13}$$

where σ_s^2 is the average transmitted signal power and $\hat{H}$ is the estimated channel fading coefficient h.

4.3 Channel Estimation in Cooperative Diversity Networks

4.3.1 Distribution of Channel Estimators

As shown in Figure 4-1, two channel estimators are used in the cooperative diversity network to estimate the channel information. One estimator is used by the relay terminal to measure the fading coefficient h_2 of the source-to-relay link. The other estimator is used by the destination terminal to measure the fading coefficient h_1 of the-source-to-

destination link and the fading coefficient h_3 from the relay-to-destination link.

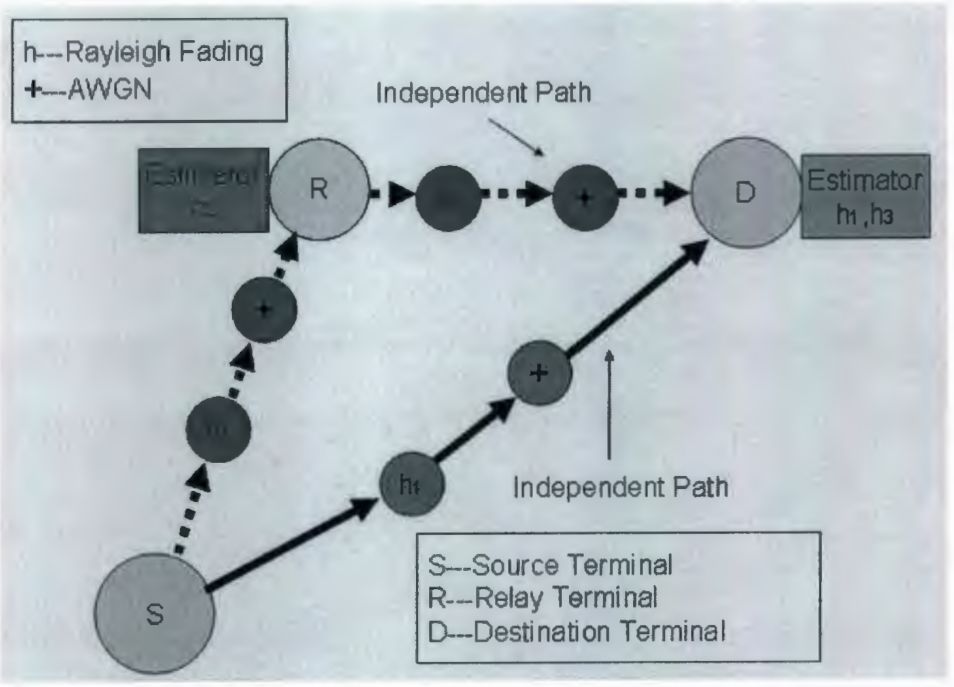

Figure 4-1 The distribution of channel estimators

4.3.2 Estimation Algorithm

The channel coefficients of the cooperative diversity network using single relay can be implemented by using the following steps. The source terminal first sends out the pilot sequence. The relay and the destination terminals estimate the channel coefficients h_2 and h_3. Then, the relay sends out another pilot sequence to destination terminal in order to estimate channel effects h_3. Next, the relay sends the measured h_2 to the destination terminal. After that, the destination terminal has all estimated channel coefficients. The total SNR can be predicted based on these estimated channel coefficients. Finally, this estimated total SNR is sent back to the source terminal to assist the source terminal in choosing a proper modulation scheme.

Estimated SNR calculation at the Destination Terminal

Branch weights of MRC can be calculated based on the estimated channel coefficients in the following two equations:

$$\beta_D = \frac{\hat{h}_1^*}{N}, \tag{4.14}$$

$$\beta_I = \frac{\alpha \hat{h}_2^* \hat{h}_3^*}{(1+\alpha^2 \left|\hat{h}_3\right|^2)N}, \tag{4.15}$$

where $\hat{h}_1^*$, $\hat{h}_2^*$ and $\hat{h}_3^*$ are the conjugates of $\hat{h}_1$, $\hat{h}_2$ and $\hat{h}_3$, respectively, N is the noise power and α is the amplifying gain.

The estimated received signal can be written as the following equation:

$$R_{combined} = \left(\beta_D \hat{h}_1 + \beta_I \alpha \hat{h}_3 \hat{h}_2\right) s + (\beta_D n_1 + \alpha \hat{h}_3 \beta_I n_2 + \beta_I n_3), \tag{4.16}$$

The estimated SNR can be obtained by following equation

$$SNR\_est = \frac{\left|\left(\beta_D \hat{h}_1 + \beta_I \alpha \hat{h}_3 \hat{h}_2\right)\left(\beta_D \hat{h}_1 + \beta_I \alpha \hat{h}_3 \hat{h}_2\right)^*\right| E}{\left|\left(\beta_D \beta_D^* + \left(\beta_I \alpha \hat{h}_3\right)\left(\beta_I \alpha \hat{h}_3\right)^* + \beta_I \beta_I^*\right)\right| N}. \tag{4.17}$$

4.3.3 Adaptive Modulation Thresholds in Imperfect CSI

In the perfect CSI case, a decision look up table is used to determine the proper modulation scheme. However, results from this table cannot be applied to the imperfect CSI case anymore since BER in this case will exceed the target BER. In the perfect CSI case, the target BER is determined only by the AWGN due to the coherent detection; however, the incoherent detection in the imperfect CSI case will cause the phase error in conjunction with the AWGN. A simple means to achieve the target BER is to add SNR

margin to compensate the extra phase error caused by the incoherent detection. We have found experimentally that a 3dB SNR margin is adequate to guarantee 10^{-3} BER. Table 4-1 shows the minimum SNR for all kinds of modulation levels to guarantee 10^{-3} BER under imperfect CSI condition.

Table 4-1 Adaptive Threshold for BER (10^{-3}) under imperfect CSI

Modulation Scheme	Minimal(Es/No)(dB)	Modulation Scheme	Minimal(Es/No)(dB)
BPSK	9.781	32QAM	22.73
4QAM	12.79	64QAM	25.53
8QAM	17.37	128QAM	28.57
16QAM	19.52	256QAM	31.37

4.4 Fixed Relay Gain Case

4.4.1 Simulation of Fixed Relay Gain Case

With the knowledge of various channel estimators and new modulation thresholds, the cooperative diversity network under imperfect CSI is investigated in simulation under different estimation techniques. Subsequently, the throughput and BER performance of cooperative diversity networks under imperfect CSI are given to show the performance change of cooperative diversity networks from the perfect CSI case to the imperfect CSI case.

The set of parameters used in the simulations is listed as follows:

Channel bandwidth: 5 MHZ

Bit Error Rate: 10^{-3}

Modulation levels: BPSK, 4QAM, 8QAM, 16QAM, 32QAM, 64QAM

Relay gain: 1

Number of samples: 600000

Transmission power: fixed power per user

Link property: asymmetric network

Path-loss exponent: 4

Estimation technique: MVU, MMSE, CE

Modulation scheme in estimation: BPSK

Number of training symbols: 4

Simulation Results

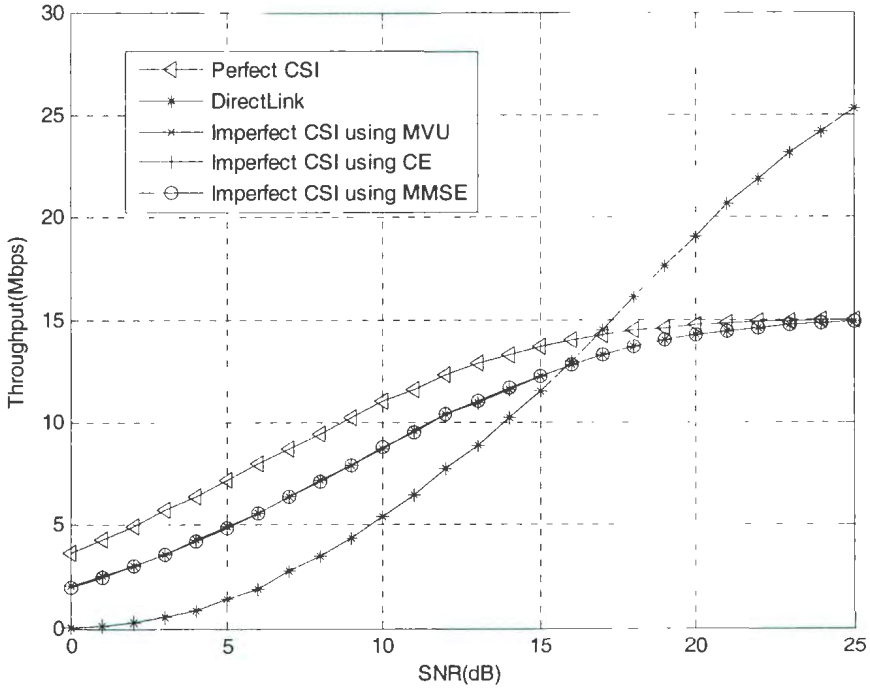

Figure 4-2 Throughput performance with imperfect CSI using MVUE, MMSE and CE

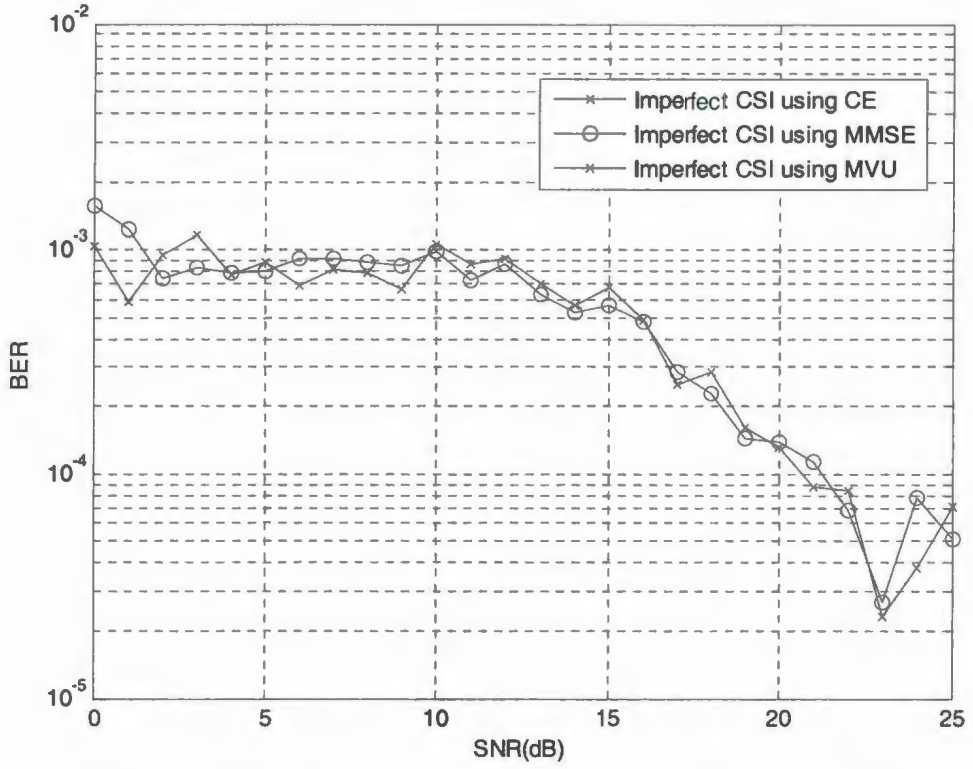

Figure 4-3 BER performance with imperfect CSI using MVUE, MMSE and CE

In Figure 4-2, the throughputs of the cooperative diversity network using MVU, MMSE and CE estimators are shown respectively. In addition, the throughputs of the cooperative diversity network under perfect CSI and the direct transmission system are also given to provide a reference for comparison. As seen from Figure 4-2, all throughput curves using channel estimator are between the throughput curve of perfect CSI and the throughput curve of direct transmission. The relationship between the throughput curves from the various channel estimators and the throughput curve from the perfect CSI demonstrates the throughput performance degradation due to the imperfect CSI condition. For example, the throughput at 10 dB decreases from 11.5 Mbps in the perfect CSI case to 9 Mbps in the imperfect CSI case. Nevertheless, the relationship between the throughput curves

from various channel estimators and the throughput curve from the direct transmission shows the existence of great throughput gain in cooperative diversity network under imperfect CSI compared with the direct transmission system. For instance, at the same 10dB, the throughput of cooperative diversity networks in imperfect case is 9Mbps while the throughput of direct transmission system is only 5 Mbps.

Figure 4-3 shows the BER performance of the cooperative diversity network using MVU, MMSE and CE estimators. As shown in the figure, the target BER 10^{-3} is almost achieved in each estimation method.

The overlap of throughput curves from different estimation techniques can be observed from the Figure 4-2. It is likely that the throughput performance of cooperative diversity network under imperfect CSI is independent of the estimation technique. The explanation of the overlap problem is illustrated in the following part.

4.4.2 General Model of Channel Estimator

In the previous part, three different estimation techniques are applied to the cooperative diversity networks under imperfect CSI. It is interesting that these throughput results from different estimation techniques are very close to each other. This can be explained by the Gaussian estimation error theory [9]. The separate transmission of pilot and signal in time will result in the Gaussian error in the weighting factor regardless of the estimation method, if the transmission is over the Raleigh fading channel. Moreover, this point can be verified by following equations from the correlation estimation technique discussed before.

The estimated channel coefficient can be modeled as the sum of its true value and the

estimation error. The following equation offers the relationship between the true and estimated channel coefficients.

$$\hat{h} = h + e, \tag{4.18}$$

To find the distribution of e, the signal to estimation noise ratio can be computed using Equation (4.13) as follows.

$$\gamma(\hat{h}) = \frac{\left(\frac{1}{K}\sum_{i=1}^{K}|s_i|^2\right)^2 h^H h}{\left\langle \left(\frac{1}{K}\sum_{i=1}^{K} s_i^* n_i\right)^2 \right\rangle}, \tag{4.19}$$

Further simplification can result in following form [10]

$$\gamma(\hat{h}) = \frac{K\sigma_s^2 h^H h}{N\sigma_n^2} = \frac{h^H h}{(\sigma_n^2/K\sigma_s^2)N}, \tag{4.20}$$

where σ_n^2 is the noise power and H is the transposition operator.

As seen from equation (4.20), the estimation noise can be modeled by a scaled version of the AWGN noise. Therefore, estimation error e is a spatially white Gaussian random variable with variance $\sigma_n^2/K\sigma_s^2$. Hence, this general estimation model can be treated as a general estimation technique to generalize the previous different estimation techniques.

4.4.3 Simulation of Cooperative Diversity Networks using GM

In this case, the GM method is used in cooperative diversity networks to estimate the fading parameters. We use the following set of parameters in this simulation.

Channel bandwidth: 5 MHZ

Bit Error Rate: 10^{-3}

Modulation levels: BPSK, 4QAM, 8QAM, 16QAM, 32QAM, 64QAM

Relay gain: 1

Transmission Power: fixed power per user

Number of samples: 600000

Link property: asymmetric network

Path-loss exponent: 4

Estimation technique: General Model

Modulation level in estimation: BPSK

Number of training symbols: 4

Simulation Results

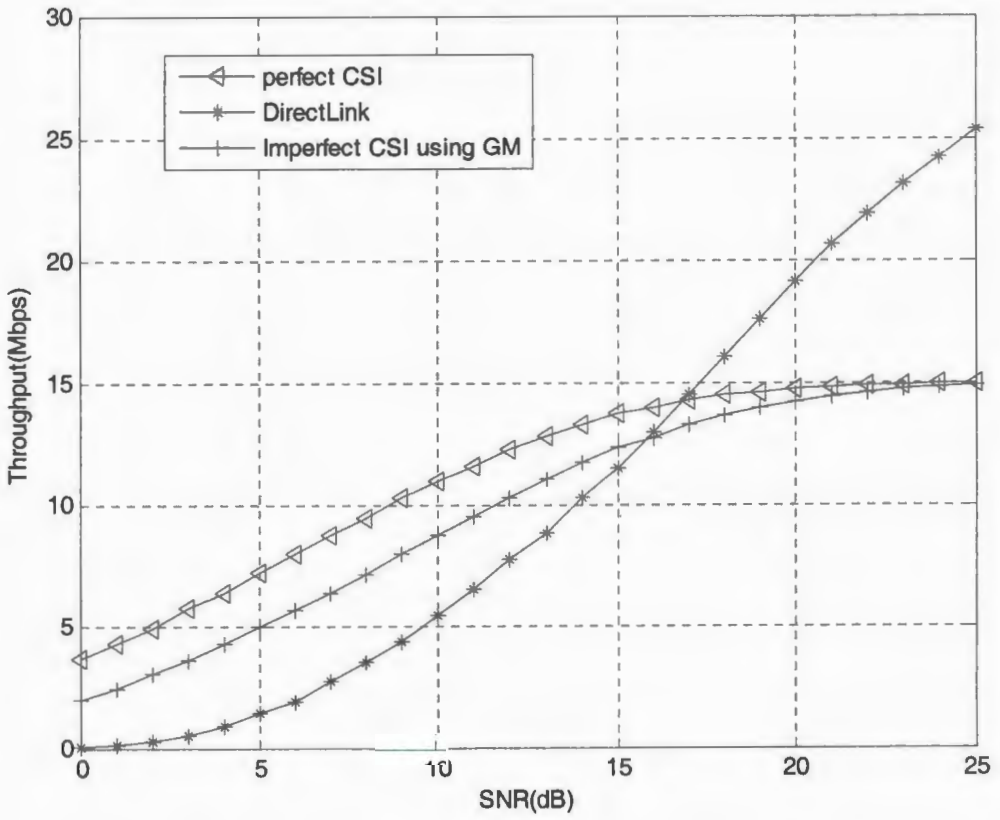

Figure 4-4 Throughput performance with imperfect CSI using GM

In Figure 4-4, the throughput of the cooperative diversity network using GM method is

shown as well as the throughput results from the perfect CSI and direct transmission system. The results show that the throughput curve from the GM method situates at the same location as the throughput curves from other estimation techniques. For example, the throughput from GM method at 10 dB is 9 Mbps, which is equal to the throughputs from other estimation techniques at 10 dB. Besides, as shown in Figure 4-5, the targeted BER 10^{-3} is satisfied. Therefore, this GM method is a good generalization of different estimation techniques.

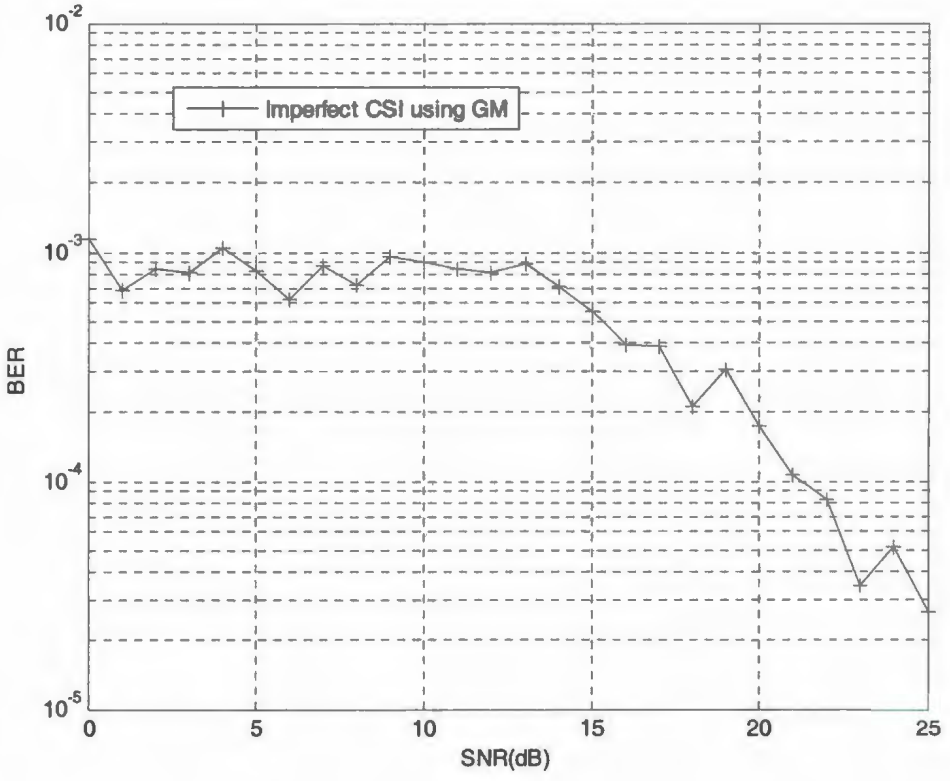

Figure 4-5 BER performance with imperfect CSI using GM

4.4.4 Analytical Evaluation of Fixed Relay Gain

The simulation results of the cooperative diversity network with fixed relay gain under

the imperfect CSI are presented to show the influence of the channel estimation on the throughput performance. The verification of these simulation results requires analytical calculation. In this part, an analytical method is proposed to verify the simulation results.

Basics

The problem of channel estimation errors has been studied extensively in classical diversity system (e.g. space and frequency diversity). However, most of these results cannot be applied to the cooperative diversity network. One reason for this is that the channel fading on the direct and indirect branches in the cooperative diversity network are not identical. The other reason is that the noise power on the direct and indirect branches are also different. In classical diversity system, the results are derived based on the identical channel fading and the equal noise power on each branch. Nevertheless, a model given in [10], [22] and analyzes the CSI estimation error and its influence on the performance even for non-identical channels in classical diversity system.

In [10], the author found the PDF of normalized total SNR under imperfect CSI conditioned on the total SNR under perfect CSI at the output of the MRC. Moreover, this model did not make any specific assumption on the noise power and the channel models. Therefore, it is general enough to be extended to fit the cooperative diversity network.

PDF of the total SNR under imperfect CSI

The PDF of normalized total SNR under imperfect CSI conditioned on the total SNR under perfect CSI at the output of MRC is given by[10]

$$f_{\rho|\gamma_0}(\rho \mid \gamma_0) = (N-1)e^{-\frac{\gamma_0}{s}}(1-\rho)^{N-2}\,{}_1F_1(N,1;\frac{\rho\gamma_0}{s}), \tag{4.21}$$

where γ_0 is the total SNR under imperfect CSI, γ is the total SNR under perfect CSI,

$\rho = \gamma/\gamma_0$ is the normalized total SNR under imperfect CSI, N is the number of branches, s is equal to $\sigma_n^2/K\sigma_s^2$ and F is the non-central F-distribution.

It is shown that Equation (4.21) can be simplified to the summation form [22]

$$f_{\rho|\gamma_0}(\rho|\gamma_0) = (N-1)e^{\frac{-(1-\rho)\gamma_0}{s}}(1-\rho)^{N-2} \times \sum_{k=0}^{N-1}\binom{N-1}{k}\frac{\left(\frac{\rho\gamma_0}{s}\right)^k}{k!}, \tag{4.22}$$

In this thesis, the cooperative diversity network with single relay is mainly discussed. Hence, N should be equal to 2 in single relay case. Equation (4.22) can be further simplified to the following form.

$$f_{\rho|\gamma_0}(\rho|\gamma_0) = e^{\frac{-(1-\rho)\gamma_0}{s}}(1+\frac{\rho\gamma_0}{s}), \tag{4.23}$$

The PDF of total SNR under the imperfect CSI can be derived by using following transformations.

$$\begin{aligned} f_\gamma(\gamma) &= \int_\gamma^\infty f_{\gamma,\gamma_0}(\gamma,x)dx \\ &= \int_\gamma^\infty f_{\gamma|\gamma_0}(\gamma|x)f_{\gamma_0}(x)dx \\ &= \int_\gamma^\infty \frac{1}{x} f_{\rho|\gamma_0}(\frac{\gamma}{x}|x)f_{\gamma_0}(x)dx. \end{aligned} \tag{4.24}$$

From equation (4.23), the conditional PDF inside integral can be expressed as

$$f_{\rho|\gamma_0}(\frac{\gamma}{x}|x) = \exp(-(\frac{x}{s}-\frac{\gamma}{s}))\left[1+\frac{\gamma}{s}\right], \tag{4.25}$$

$f_{\gamma_0}(x)$ is the PDF of the total SNR under perfect CSI, which has already been obtained in Chapter 3.

We solve this integration in Equation (4.24) numerically because the PDF of the total

SNR under perfect CSI is provided in numerical form. Then, this PDF derived from Equation (4.24) can be used to determine the throughput of cooperative diversity networks under imperfect CSI by using the throughput calculation method given in Equations (3.18) and (3.19).

Analytical Results

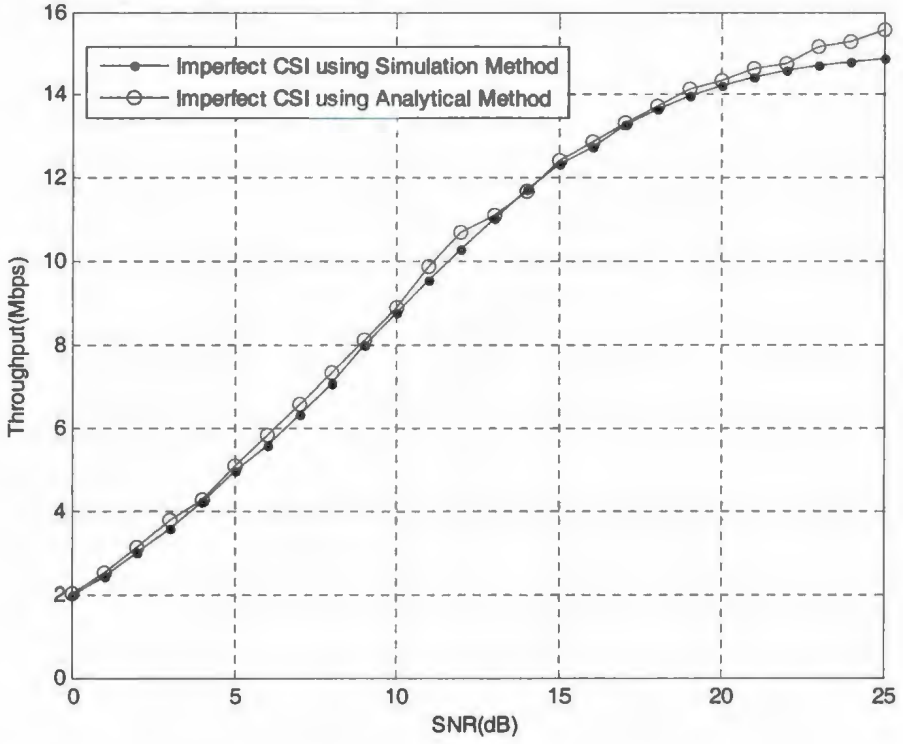

Figure 4-6 Analytical throughput with imperfect CSI

In Figure 4-6, the analytical throughput curve of cooperative diversity networks under imperfect CSI is given as well as the throughput curve from the simulation. As shown in Figure 4-16, the analytical throughput results are very close to the throughput results obtained from the simulation. This verifies the correctness and accuracy of the simulation results.

4.4.5 Simulation of Large Number Pilot Symbols

The number of pilot symbols used in channel estimator is related to the channel estimation error. A larger number of pilot symbols results in smaller channel estimation error. In the previous simulation, we investigated the throughput performance of cooperative diversity network, which use 4 pilot symbols to do the channel estimation. In this case, 8 pilot symbols are used in cooperative diversity network using adaptive modulation. The set of parameters used in the simulations is listed as follows:

Channel bandwidth: 5 MHZ

Bit Error Rate: 10^{-3}

Modulation levels: BPSK, 4QAM, 8QAM, 16QAM, 32QAM, 64QAM

Relay gain: 1

Number of samples: 600000

Transmission Power: fixed power per user

Link property: asymmetric network

Path-loss exponent: 4

Estimation technique: General Model

Modulation level in estimation: BPSK

Number of pilot symbols: 8

Simulation Results

In Figure 4-7, the throughput results of cooperative diversity network using 8 pilot symbols are given as well as the results from the 4 pilot symbols simulation. It is clear that the throughput loss due to channel estimation errors in 8 pilot symbols is much less than that in 4 pilot symbols. Therefore, increasing the number of pilot symbols is able to

decrease the throughput loss due to the channel estimation error. The targeted BER 10-3 is satisfied as shown in Figure 4-8,

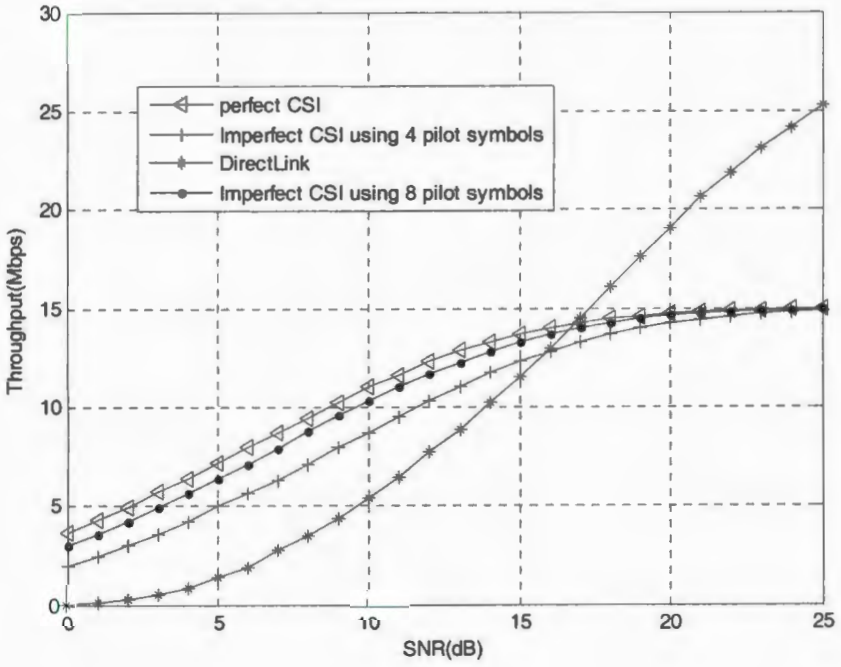

Figure 4-7 Throughput of cooperative diversity network using 8 pilot symbols

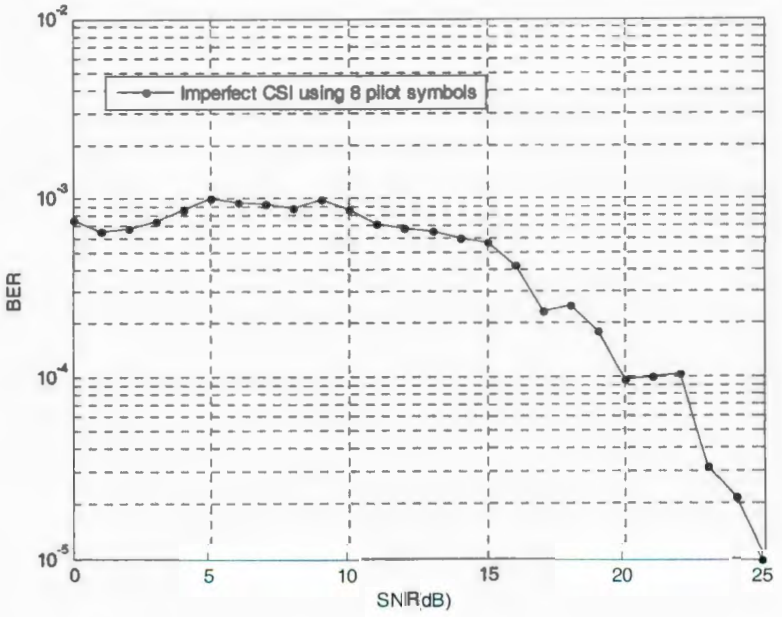

Figure 4-8 Throughput of cooperative diversity network using 8 pilot symbols

4.5 Variable Relay Gain

In this section, the cooperative diversity network with variable relay gain is investigated under imperfect CSI. All the simulations in this section are based on the GM estimation method. As shown in Chapter 3, two types of changeable gain are commonly used in the variable relay gain situation. One of them is set to $1/|h_2|$, which is called as variable relay gain I case. The other one is set to $\sqrt{\frac{E}{N+E|h_2|^2}}$, which is called as variable relay gain II case. The variable gain I case is first investigated in simulation; then the analytical evaluation is given to verify the simulation results. Second, the variable gain II case is studied similarly in simulation and analytical evaluation.

4.5.1 Variable Relay Gain Case I Simulation

In this case, the cooperative diversity network under imperfect CSI with variable gain I is simulated. The GM method is used to estimate the fading parameters. We use the following set of parameters in this simulation.

Channel bandwidth: 5 MHZ

Bit Error Rate: 10^{-3}

Number of samples: 600000

Modulation levels: BPSK, 4QAM, 8QAM, 16QAM, 32QAM, 64QAM

Relay gain: the reciprocal of the fading between source and relay

Transmission Power: fixed power per user

Link property: asymmetric network

Path-loss exponent: 4

Estimation technique: General Model

Modulation level in estimation: BPSK

Number of training symbols: 4

Simulation Results

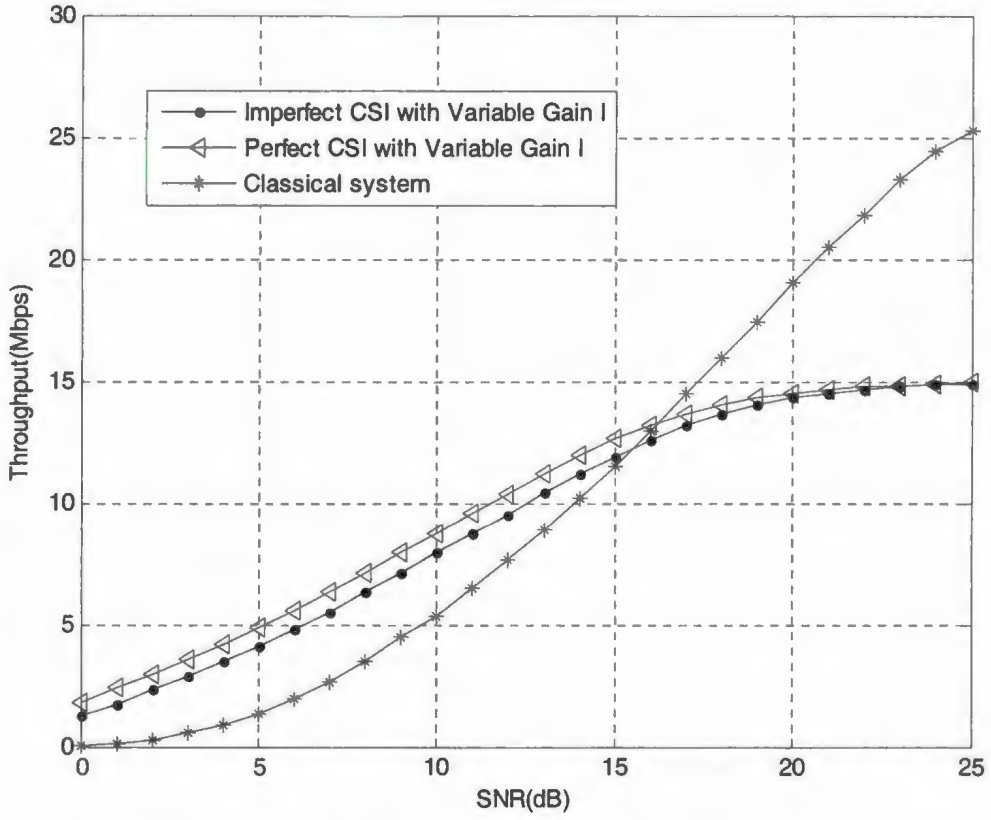

Figure 4-9 Throughput performance with variable relay gain I under imperfect CSI

In Figure 4-9, the throughput results of the cooperative diversity network with variable gain I are given in both perfect and imperfect CSI conditions. The throughput loss due to channel estimation error is observed in this figure. For example, the throughput decreases from 8.7 Mbps in perfect CSI case to 7.9 Mbps in imperfect CSI at 10 dB. However, a great throughput gain still exists compared with the direct transmission system. It is clear that the throughput loss in variable gain I case is less than the fixed gain case. The

targeted BER 10^{-3} is satisfied as shown in Figure 4-10.

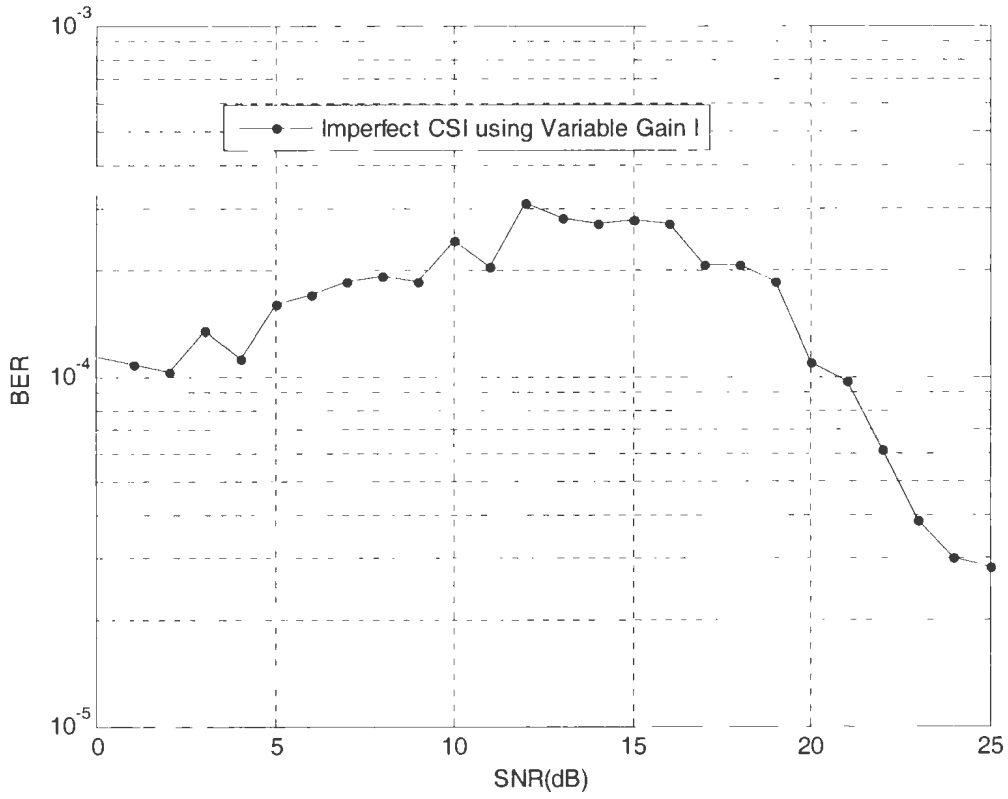

Figure 4-10 BER performance with variable relay gain I under imperfect CSI

4.5.2 Analytical Evaluation of Variable Relay Gain case I

Since the conditional PDF of normalized SNR is independent of the relay gain, it is still used in finding the PDF of the received SNR under imperfect CSI. However, the PDF of the received SNR under perfect CSI is changed due to the different relay gain. In Chapter 2, the PDF of the total SNR with variable gain II is derived under perfect CSI. Hence, the analytical PDF expression of the total SNR under imperfect CSI can be obtained by solving Equation (4.24) numerically.

Finally, the analytical throughput is derived based on the PDF of the total SNR under

imperfect CSI. The analytical throughput results are shown in Figure 4-9.

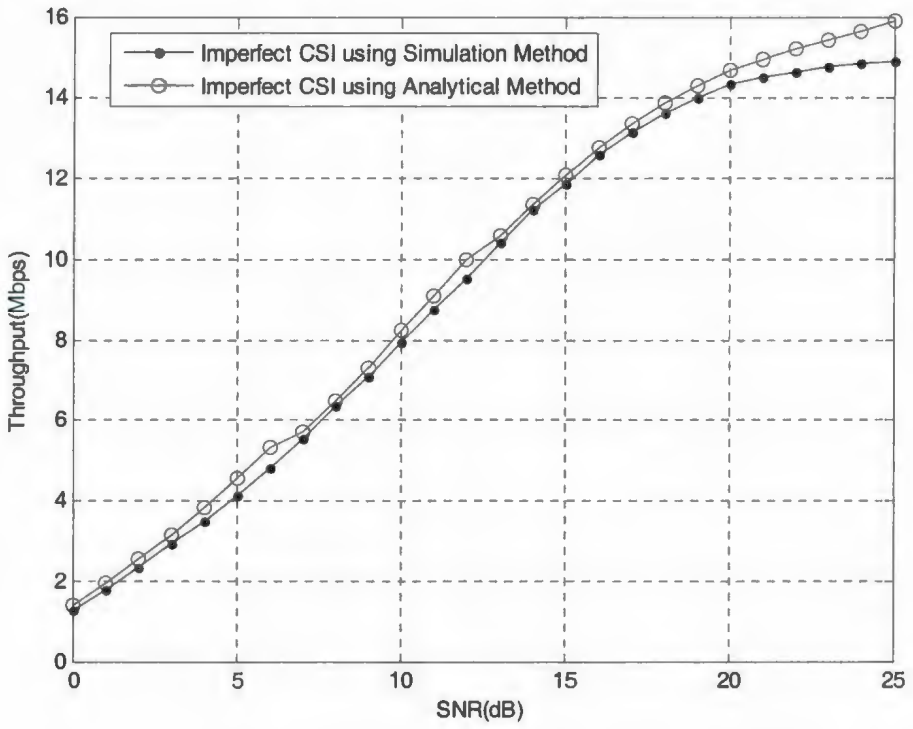

Figure 4-11 Analytical throughput with variable gain I under imperfect CSI

As shown from Figure 4-11, the throughput results from the simulation are very close to the derived analytical throughput in the range from 0 dB to 20 dB. After 20 dB, the difference gradually becomes large. In fact, this difference is caused by the insufficient integration precision. Hence, the throughput verify from the simulation is verified to be correct.

4.5.3 Simulation of Variable Relay Gain Case II

In this case, the cooperative diversity network under imperfect CSI with constant average power is simulated. As mentioned before, the GM method can generalize the estimation methods in the cooperative communication system to estimate the fading

parameters. We use the following set of parameters in this simulation.

Channel bandwidth: 5 MHZ

Bit Error Rate: 10^{-3}

Modulation levels: BPSK, 4QAM, 8QAM, 16QAM, 32QAM, 64QAM

Relay gain: $\sqrt{\frac{E}{N + Eh_2^{\ 2}}}$

Number of samples: 600000

Transmission Power: fixed power per user

Link property: asymmetric network

Path-loss exponent: 4

Estimation technique: General Model

Modulation level in estimation: BPSK

Number of training symbols: 4

Simulation Results

Figure 4-12 shows results of the throughput of the cooperative diversity network under imperfect CSI with variable gain II. Compared with the throughput of the cooperative diversity network under the perfect CSI, certain amount of throughput loss can be observed. For example, the throughput at 10 dB decreases from 8Mbps in perfect CSI case to7Mpbs in imperfect CSI case. However, the throughput loss in variable gain I case due to the imperfect CSI is less than the case with fixed relay gain. Figure 4-13 shows that the target BER 10^{-3} is achieved in the simulation.

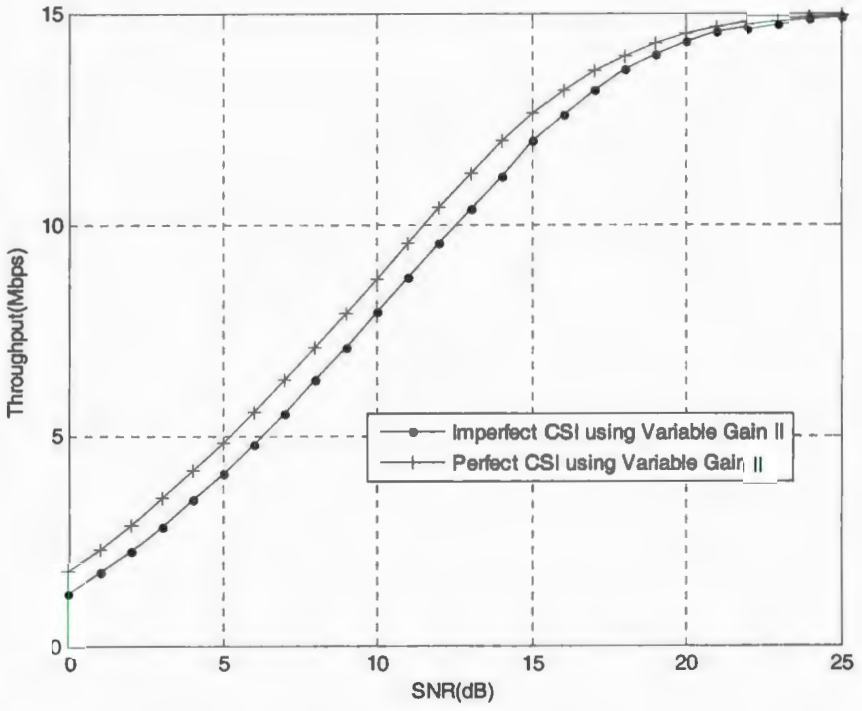

Figure 4-12 Throughput performance with variable relay gain II

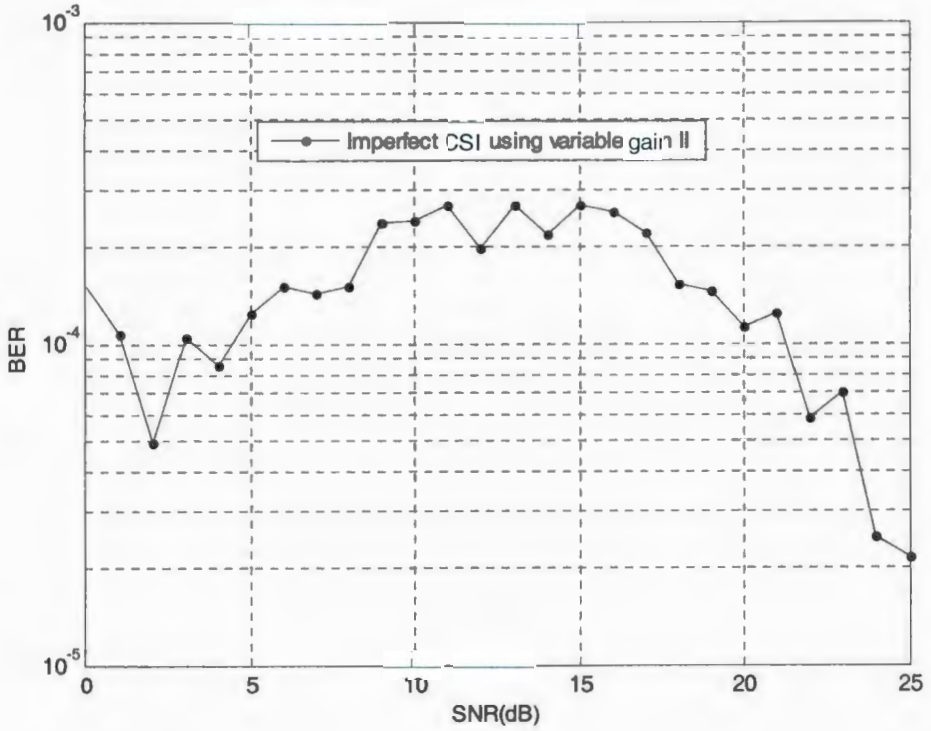

Figure 4-13 BER performance with variable relay gain II

4.5.4 Analytical Evaluation of Variable Relay Gain case II

Since the conditional PDF of normalized SNR given in Equation (4.23) is independent of the relay gain, it can be still used to find the PDF of the total SNR under imperfect CSI. However, the PDF of the total SNR under perfect CSI is changed due to the different relay gain. In Chapter 2, the PDF closed-form expression of the total SNR under perfect CSI is derived. Hence, a PDF closed-form expression of the total SNR under imperfect CSI can be obtained through following steps. The PDF of the total SNR under perfect CSI is given by

$$f(\gamma_t) = \frac{1}{\bar{\gamma}\bar{\gamma}_1} \exp(-\frac{\gamma_t}{\bar{\gamma}_1}) \left[\frac{1-\exp(-\gamma_t(1/\bar{\gamma}-1/\bar{\gamma}_1))}{(1/\bar{\gamma}-1/\bar{\gamma}_1)} \right], \tag{4.26}$$

This equation can be simplified by using the following substitutions

$a = (1/\bar{\gamma}-1/\bar{\gamma}_1), b = \bar{\gamma}\bar{\gamma}_1, c = 1/\bar{\gamma}_1$

$$f_{\gamma_t}(\gamma_t) = \frac{1}{b}\exp(-c\gamma_t)\left[\frac{1-\exp(-\gamma_t a)}{a}\right], \tag{4.27}$$

The PDF of the total SNR under imperfect CSI can be found as follows:

$$\begin{aligned}
f_\gamma(\gamma) &= \int_\gamma^\infty \frac{1}{x} f_{\rho|\gamma_0}(\frac{\gamma}{x}\,|\,x) f_{\gamma_t}(x)dx \\
&= \int_\gamma^\infty \frac{1}{x}\exp(-(\frac{x}{s}-\frac{\gamma}{s}))\left[1+\frac{\gamma}{s}\right]\frac{1}{b}\exp(-cx)\left[\frac{1-\exp(-ax)}{a}\right]dx \\
&= \frac{\left[1+\frac{\gamma}{s}\right]}{ab}\exp(\frac{\gamma}{s})\int_\gamma^\infty \frac{1}{x}[1-\exp(-ax)]\exp(-(c+d)x)dx, d = 1/s \\
&= \frac{\left[1+\frac{\gamma}{s}\right]}{ab}\exp(\frac{\gamma}{s})\left[\int_\gamma^\infty x^{-1}\exp(-(c+d)x)dx - \int_\gamma^\infty x^{-1}\exp(-(a+c+d)x)dx\right],
\end{aligned} \tag{4.28}$$

The following integration can be used to find the solution for above integral

$$\int x^{-1}\exp(-fx)dx = Ei(-fx) = -[-Ei(-fx)] = -E_1(fx), \tag{4.29}$$

where $Ei(x)$ is the exponential integral, which is defined by $E_1(x)=-Ei(-x)$.

Therefore, two integrals inside the PDF function can be solved as follows

$$\int_{\gamma}^{\infty} x^{-1}\exp(-(c+d)x)dx = \left[-E_1[(c+d)x]\right]_{\gamma}^{\infty} = E_1[(c+d)\gamma], \tag{4.30}$$

$$\int_{\gamma}^{\infty} x^{-1}\exp(-(a+c+d)x)dx = \left[-E_1[(a+c+d)x]\right]_{\gamma}^{\infty} = E_1[(a+c+d)\gamma], \tag{4.31}$$

Then, substitute the above results into the PDF function

$$\begin{aligned}
&= \frac{\left[1+\frac{\gamma}{s}\right]}{ab}\exp(\frac{\gamma}{s})\bullet\left[\int_{\gamma}^{\infty} x^{-1}\exp(-(c+d)x)dx - \int_{\gamma}^{\infty} x^{-1}\exp(-(a+c+d)x)dx\right] \\
&= \frac{\left[1+\frac{\gamma}{s}\right]}{ab}\exp(\frac{\gamma}{s})\bullet\left[E_1[(c+d)\gamma] - E_1[(a+c+d)\gamma]\right] \\
&= \frac{\left[1+\frac{\gamma}{s}\right]}{(1/\bar{\gamma}-1/\bar{\gamma}_1)\bar{\gamma}\bar{\gamma}_1}\exp(\frac{\gamma}{s})\bullet\left[E_1[(1/\bar{\gamma}_1+1/s)\gamma] - E_1[((1/\bar{\gamma}-1/\bar{\gamma}_1)+1/\bar{\gamma}_1+1/s)\gamma]\right]
\end{aligned} \tag{4.32}$$

Analytical Results

The PDF closed-form expression of the total SNR with variable gain II is found in Equation (4.32). Then, this PDF can be used to determine the throughput of cooperative diversity networks under imperfect CSI by using the throughput calculation method given by Equations (3.18) and (3.19).

As shown from Figure 4-12, the analytical throughput results are slightly higher than the simulation throughput. However, the distance between these two curves shrinks as the SNR increases. Actually, this difference is caused by the approximate PDF of the indirect

branch since this approximation is accurate only when the SNR is fairly large. Hence, the analytical throughput can be used as an upper bound.

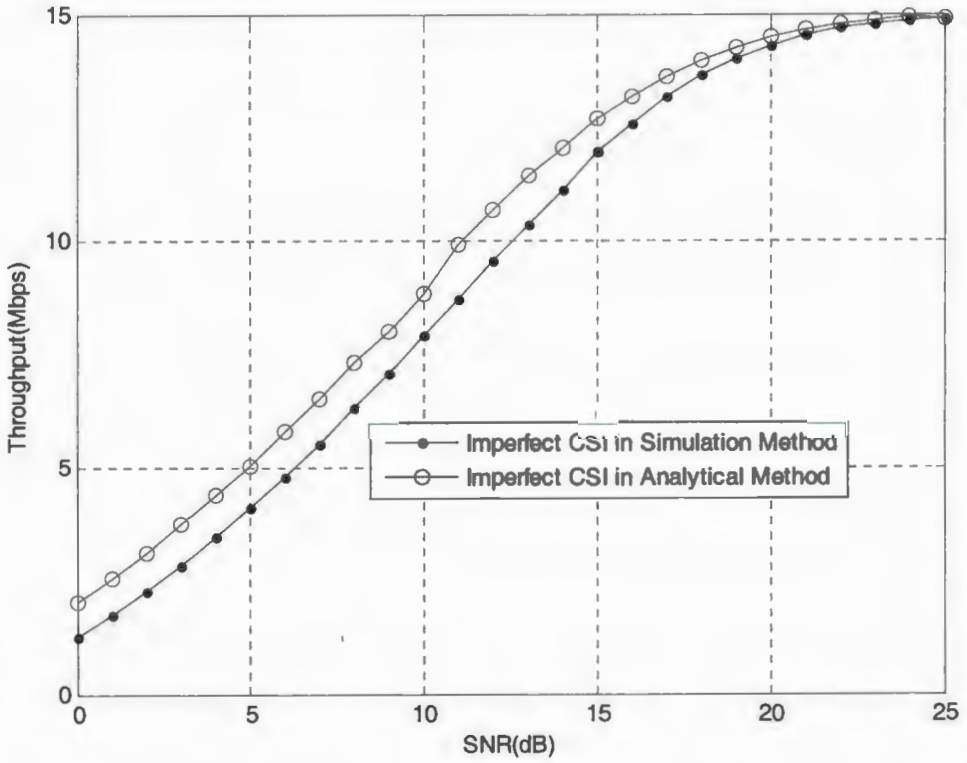

Figure 4-14 Analytical throughput with variable gain II under imperfect CSI

Chapter 5

BER Analysis of Cooperative Diversity Networks using Fixed Modulation

In Chapter 2, we have already discussed the cooperative diversity networks using fixed modulation in simulation briefly. As a result, the BER curve is given for fixed BPSK modulation scheme. However, all these work are restricted on the simulation of variable relay gain case in the cooperative diversity network under perfect CSI only. In this section, the cooperative diversity network using BPSK modulation is studied in fixed relay gain case and variable relay gain case, respectively. For each case, the perfect CSI and imperfect CSI conditions are considered. Moreover, the analytical evaluation is provided to verify the simulation results.

In cooperative diversity networks using fixed modulation, the obtained diversity gain is used to improve the received SNR at the destination node. Therefore, the BER performance should be examined. In this section, we investigate the BER performance of cooperative diversity networks under perfect and imperfect CSI conditions. In addition, the BER performance of direct transmission system is also given to show the superiority of cooperative diversity networks. The GM method is used in all simulations related to imperfect CSI.

5.1 BER Performance in Simulation

Figure 5-1 and 5-2 show the BER performance of cooperative diversity network in both fixed and variable relay gains, respectively. As seen from Figure 5-1 and 5-2, the BER performance of cooperative diversity networks in perfect and imperfect CSI conditions performs much better than that of the classical direct transmission system. Moreover, the BER of imperfect CSI case is worse than that of perfect CSI case due to the channel estimation error.

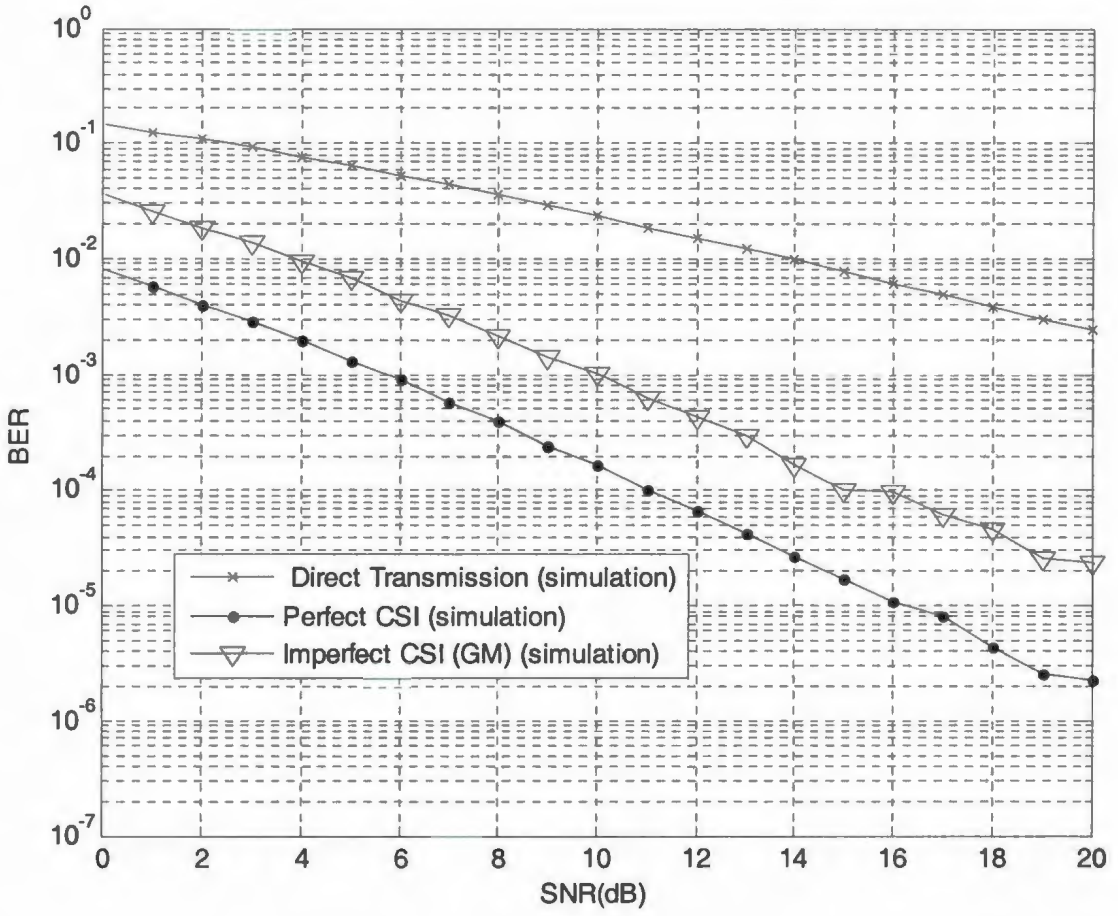

Figure 5-1 BER performance of fixed gain case in simulation

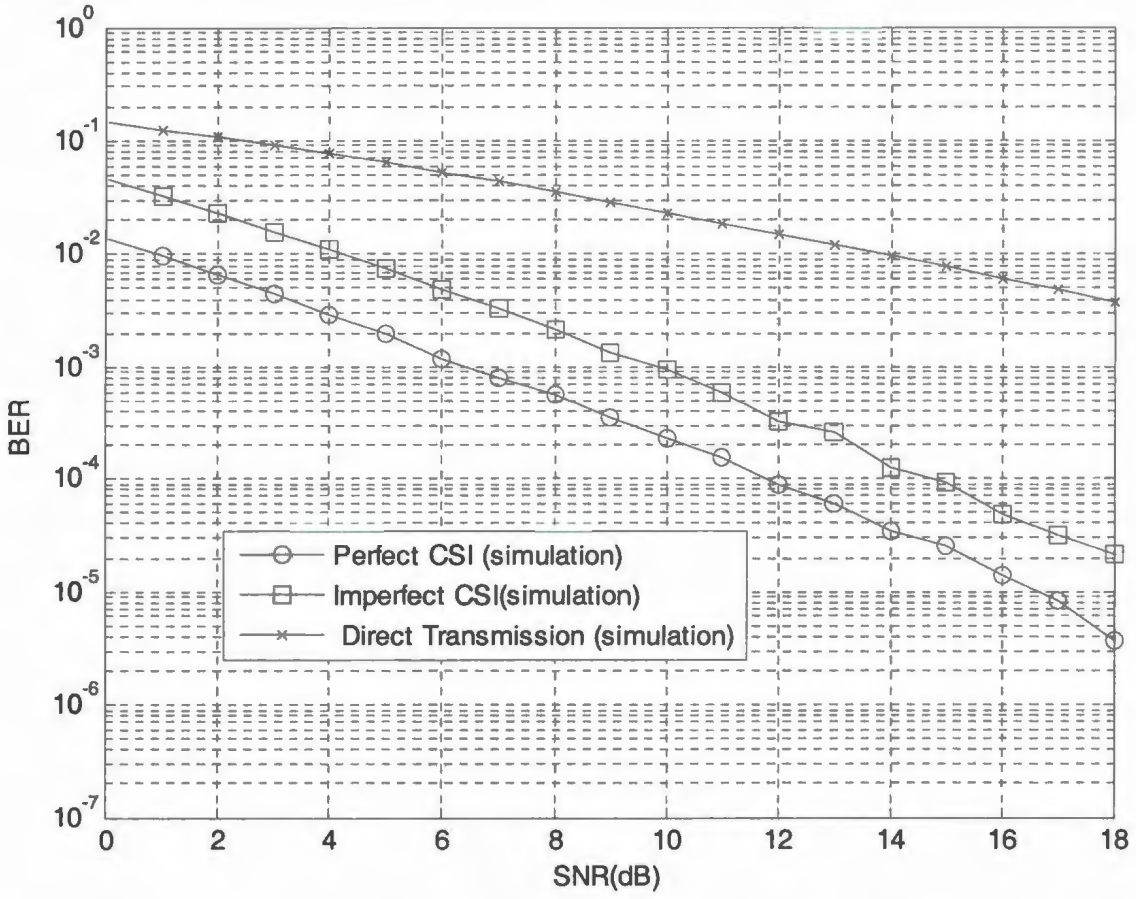

Figure 5-2 BER performance of variable gain case in simulation

5.2 Analytical Evaluation of BER Performance

The BER performance can be calculated as follows:

$$P_e = \int_0^\infty P_{e|\gamma} f_\gamma(\gamma) d\gamma, \tag{5.1}$$

where $P_{e|\gamma}$ is the probability density function of error conditioned on SNR γ and $f_\gamma(\gamma)$ is the PDF of the total SNR. The PDF of error conditioned on SNR for cooperative diversity network under perfect CSI in BPSK modulation can be expressed as follows:

$$P_{e|\gamma} = Q(\sqrt{2\gamma}), \tag{5.2}$$

where Q is the normalized form of cumulative distribution function and γ is the SNR.

In Chapter 3, the PDF of the total SNR in cooperative diversity network under perfect CSI is found in both fixed and variable relay gain. Therefore, Equation (5.1) can be solved numerically. The analytical BER performance of perfect CSI case is given in Figure 5-3 and 5-4, individually.

The PDF of error conditioned on SNR for imperfect CSI in BPSK modulation is completely different since the imperfect CSI cause the phase error. The conditional BER of BPSK is given in [21] as follows:

$$P_e(\gamma,\theta) = \frac{1}{2} erfc(\sqrt{\gamma}\cos\theta), \tag{5.3}$$

where erfc(z) is the complementary error function and θ is the Gaussian distributed phase error. The PDF of Gaussian distributed phase error

$$P(\theta) = \exp(-\theta^2 / 2\alpha^{-1}) / \sqrt{2\pi\alpha^{-1}}, \tag{5.4}$$

where α is the loop SNR and α is proportional to γ. The PDF of error function conditioned SNR for imperfect CSI case can be found by using following integration.

$$P_{e|\gamma} = \int_{-\pi}^{\pi} P_e(\gamma,\theta) P(\theta) d\theta. \tag{5.5}$$

The PDF of the total SNR in cooperative diversity networks under imperfect CSI using fixed relay gain is derived in Chapter 4. Therefore, Equation (5.1), (5.3), (5.4) and (5.5) can be used to find the BER of cooperative diversity networks using BPSK modulation under imperfect CSI. The analytical BER performance of imperfect CSI case is given in Figure 5-3 and 5-4.

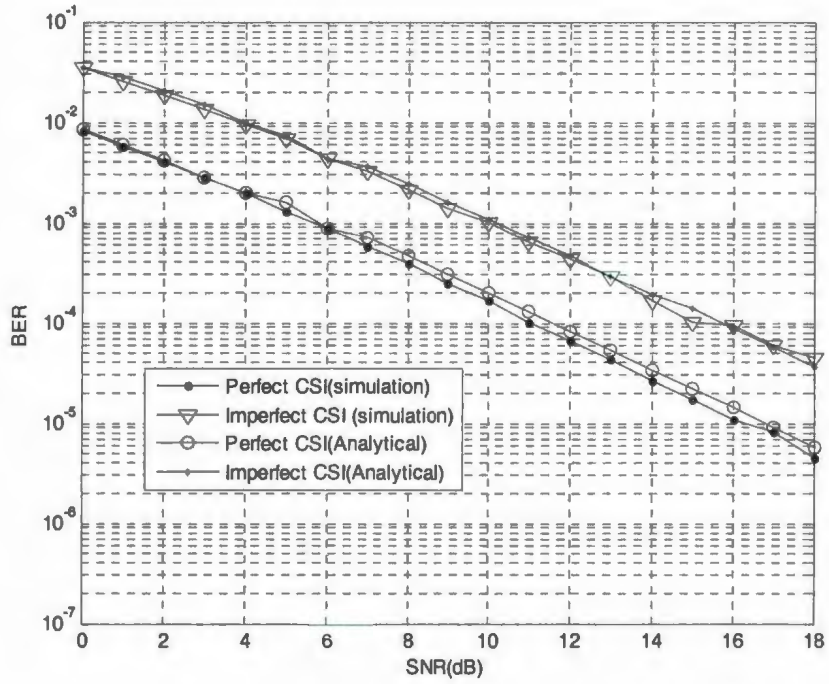

Figure 5-3 Analytical BER performance of fixed gain case

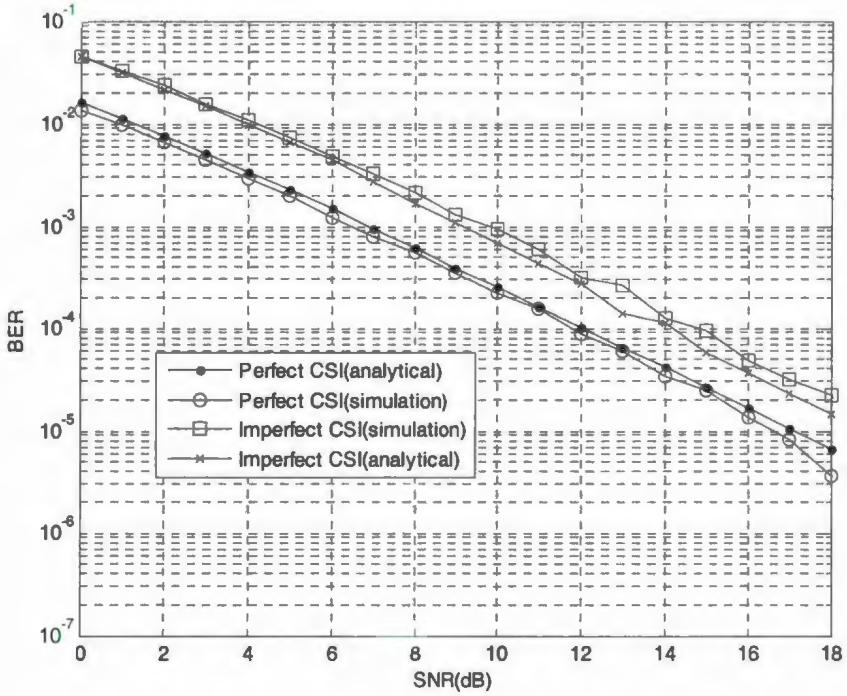

Figure 5-4 Analytical BER performance of variable gain case

As shown in Figure 5-3, the analytical BER performances in perfect and imperfect CSI are very close to the BER performance from the simulation in fixed relay gain. Similarly, Figure 5-4 shows that the analytical BER performances in perfect and imperfect CSI are close to the simulation results as well. Therefore, all the simulation results are verified by the analytical results.

Chapter 6

Conclusions

This thesis investigated the performance of cooperative diversity networks using adaptive modulation over Rayleigh fading channel with perfect and imperfect CSI.

The thesis starts with the simulation of the simple classical communication system over the AWGN channel. This simple system is then modified to work over the Rayleigh fading channel. Finally, a cooperative diversity network system is set up based on the simple system over the Raleigh fading system. By doing this, not only is a cooperative diversity network system generated, but also a classical direct communication system, which is used to provide the reference. In this part, some interesting results regarding the SNR enhancement of cooperative diversity networks are given. The results show that the cooperative diversity network using BPSK modulation over Rayleigh fading channel under perfect CSI condition can achieve much better BER performance than the classical system. The imperfect CSI condition of cooperative diversity networks results in large BER performance degradation. However, the BER performance in imperfect CSI is still superior to that of the classical system.

A cooperative diversity networks system using adaptive modulation over the Raleigh fading channel is set up and the throughput performance and BER performance are investigated based on the perfect CSI assumption. We have investigated the benefits of using adaptive modulation in cooperative diversity networks to compensate for the resource loss due to relaying. Results show that the cooperative diversity network using

adaptive modulation not only compensates for the resource loss but also provides significant throughput gain compared with the classical communication system. Next, we investigated the multiple-relay case. We showed that multiple relays can not provide further throughput gain unless the co-phase transmission is used. Moreover, an analytical approach is presented to verify the results from the simulation in one relay case. The PDFs of the total SNR of cooperative diversity network in fixed and variable relay gain are found analytically under perfect CSI condition.

Since the perfect CSI assumption is not practical in the real world, the cooperative diversity network using adaptive modulation over the Rayleigh fading channel under the imperfect CSI is investigated to provide a more realistic model. In this part, various estimation techniques are applied to the cooperative diversity networks to replace the perfect CSI assumption. Results show that the throughput gain degrades greatly in cooperative diversity networks with fixed and variable relay gain. However, a considerable throughput gain still exists. The throughput loss can be reduced by increasing the number of pilot symbols in channel estimator. Besides, the throughput loss in variable relay gain due to imperfect CSI is less than that of the fixed relay gain.

An analytical approach is also found for the imperfect CSI case. The PDFs of the total SNR of cooperative diversity network in fixed and variable relay gain under imperfect is found analytically under imperfect CSI condition. The results show that the simulation results conform to the analytical results in fixed and variable relay gain cases.

Therefore, the cooperative diversity network using adaptive modulation over the Rayleigh fading channel is able to provide significant throughput gain in both perfect and imperfect CSI situations.

Besides, the BER performance of cooperative diversity networks using fixed (BPSK) modulation is found to be able to provide better BER performance than the classical direct transmission system in both perfect and imperfect CSI cases. Based on the PDFs of the total SNR in cooperative diversity networks, an analytical approach is proposed to verify the simulation results in each case. Results show that the simulation results conform to the analytical results in fixed and variable relay gain cases.

In this thesis, the cooperative diversity network with single-relay under adaptive modulation has been studied in simulation and analytical evaluation. However, the multiple-relay case of the cooperative diversity network using adaptive modulation is only evaluated in simulation for the perfect CSI only. Therefore, one direction of our future work is to simulate the cooperative diversity network with multiple-relay using adaptive modulation under imperfect CSI. Meanwhile, the analytical work of cooperative diversity networks with multiple-relay under perfect and imperfect CSI should be investigated.

Some additional work can also be carried out in the BER performance of cooperative diversity networks using other fixed modulation schemes since we only studied the BER performance of cooperative diversity networks using BPSK modulation scheme.

References

[1] Theodore S. Rappaport, Wireless Communications Principles and Practices, Second Edition, Prentice Hall Communications Engineering and Emerging Technologies Series, 2001

[2] A. Nosratinia, T. E. Hunter and A. Hedayat, "Cooperative Communication in Wireless Networks," *IEEE Communication Magazine*, vol. 42, no.10, pp. 74-84, Oct. 2004.

[3] J. N. Laneman, D. N.C. Tse, and G. W. Wornell, "Cooperative Diversity in Wireless Networks: Efficient Protocols and Outage Behavior," *IEEE Transactions on Information Theory*, vol. 50, no. 12, pp. 3062-3080, Dec. 2004.

[4] A. Sendonaris, E. Erkip, and B. Aazhang, "User cooperation diversity part I: system description," *IEEE Trans. Commun.*, vol. 51, pp. 1927-1938, Nov. 2003.

[5] E. Armanious, D. D.Falconer, and H. Yanikomeroglu, "Adaptive Modulation, Adaptive Coding, and Power Control for Fixed Cellular Broadband Wireless Systems: some new insights," in *Proc. IEEE Wireless Communications and Networking Conference (WCNC)*, vol. 1, pp. 238-242, March 2003.

[6] Md. R. Islam and W. Hamouda, "Performance of cooperative ad-hoc networks in rayleigh fading channels," in *Proc. of IEEE Vehicular Technology Conference (VTC)*, pp. 1-4, Sept. 2006.

[7] P. Rost and G. Fettweis, "A Cooperative Relaying Scheme Without The Need For Modulation With Increased Spectral Efficiency," in *Proc. of IEEE Vehicular Technology Conference (VTC)*, 2006, pp. 1-5, Sept. 2006

[8] H. S. Ryu, C. G. Kang and D. S. Kwon, "Transmission Protocol for Cooperative

MIMO with Full Rate: Design and Analysis," *Proc. of IEEE Vehicular Technology Conference (VTC)*, 2007, pp. 934-938, April 2007 .

[9] M. J. Gans, "The Effect of Gaussian Error in Maximal Ratio Combiners," *IEEE Transactions on Communication Technology*, vol. com-19, no. 4, pp. 492-500, Aug. 1971.

[10] S. Roy, and P. Fortier, "Maximal-Ratio Combining Architectures and Performance With Channel Estimation Based on a Training Sequence," *IEEE Transaction on Wireless Communication,* vol. 3, no. 4, pp. 1154-1164, July 2004.

[11] K. Balachandran, R. Kadaba, and S. Nanda, "Channel Quality Estimation and Rate Adaptation for Cellular Mobile Radio," *IEEE Journal on Selected Areas in Communications*, vol.17, no.7, pp. 1244-1256, July 1999.

[12] J. G. Proakis and M. Salehi, Communication Systems Engineering, Second Edition, 2004.

[13] M. O. Hasna and M.-S. Alouini, "Performance analysis of two-hop relayed transmissions over Rayleigh fading channels," *Proc. IEEE Vehicular Technology Conference (VTC)*, 2002, pp. 1992-1996.

[14] M. O. Hasna and M.-S Alouini, "A performance study of dual-hop transmissions with fixed gain relays, " *IEEE Trans on Wireless Communication*, vol. 3, no. 6, pp. 1963-1968, November 2004.

[15] S. Ikki and M. H. Ahmed, "Performance Analysis of Cooperative Diversity Wireless Networks over Nakagami-m Fading Channel, " *IEEE Communication Letters*, Vol. 11, No. 4, pp. 334-336, April 2007.

[16] H. Chen and M. H. Ahnmed, "Throughput Enhancement in Cooperative Diversity Wireless Networks using Adaptive Modulation," *Proc. IEEE Canadian Conference on Electrical and Computer Engineering* (*CCECE'08*), Niagara Falls, Canada, May 2008, pp.

527-530.

[17] S. M. Kay, Fundamentals of Statistical Signal Processing: Estimation Theory, Prentice-Hall signal processing series, 1993.

[18] A. Goldsmith, Wireless Communications, Cambridge University Press, 2005.

[19] I. S. Gradshteyn and I. M. Ryzhik, *Table of Integrals, Series and Products, Fifth Edition*. San Diego: Academic Press, 1994.

[20] A. Ribeiro, X. Cai, and G. B. Giannakis, "Symbol error probabilities for general cooperative links," *IEEE Trans. Wireless Commun.*, vol. 4, no. 3, pp. 1264-1273, 2005.

[21] C.M. Lo and W.H. Lam, "Error probability of binary phase shift keying in Nakagami-m fading channel with phase noise," *IEEE Electronics Letters*, vol. 36, no. 21, pp. 1773-1774, Oct. 2000.

[22] S. Roy, "The performance of maximal-ratio combiners in Nakagami fading with imperfect weight estimation," in Proc. 22nd Biennial Symposium on Communications, Kingston, pp. 389-391, June 2004.

[23] Paul A. Anghel and Mostafa Kaveh,"Exact Symbol Error Probability of a Cooperative Network in a Rayleigh-Fading Environment," *IEEE Transactions on Wireless Communications*, VOL.3, NO.5, September 2004.